Direct Measurement of the $^{14}O(\alpha,p)^{17}F$ Cross Section Using TexAT_v2

Ewha Womans University
Chaeyeon Park

Korea-China joint workshop for rare isotope physics

Motivation

Astrophysical Improtance

- Alternate break-out path from the hot CNO cycle to the rapid proton burning (rp-process).
- One of the most important (α,p) cross sections in Type I X-ray bursts that can produce a significant change (7%) in calculated luminosity.

R. Cyburt *et al.* (2016)

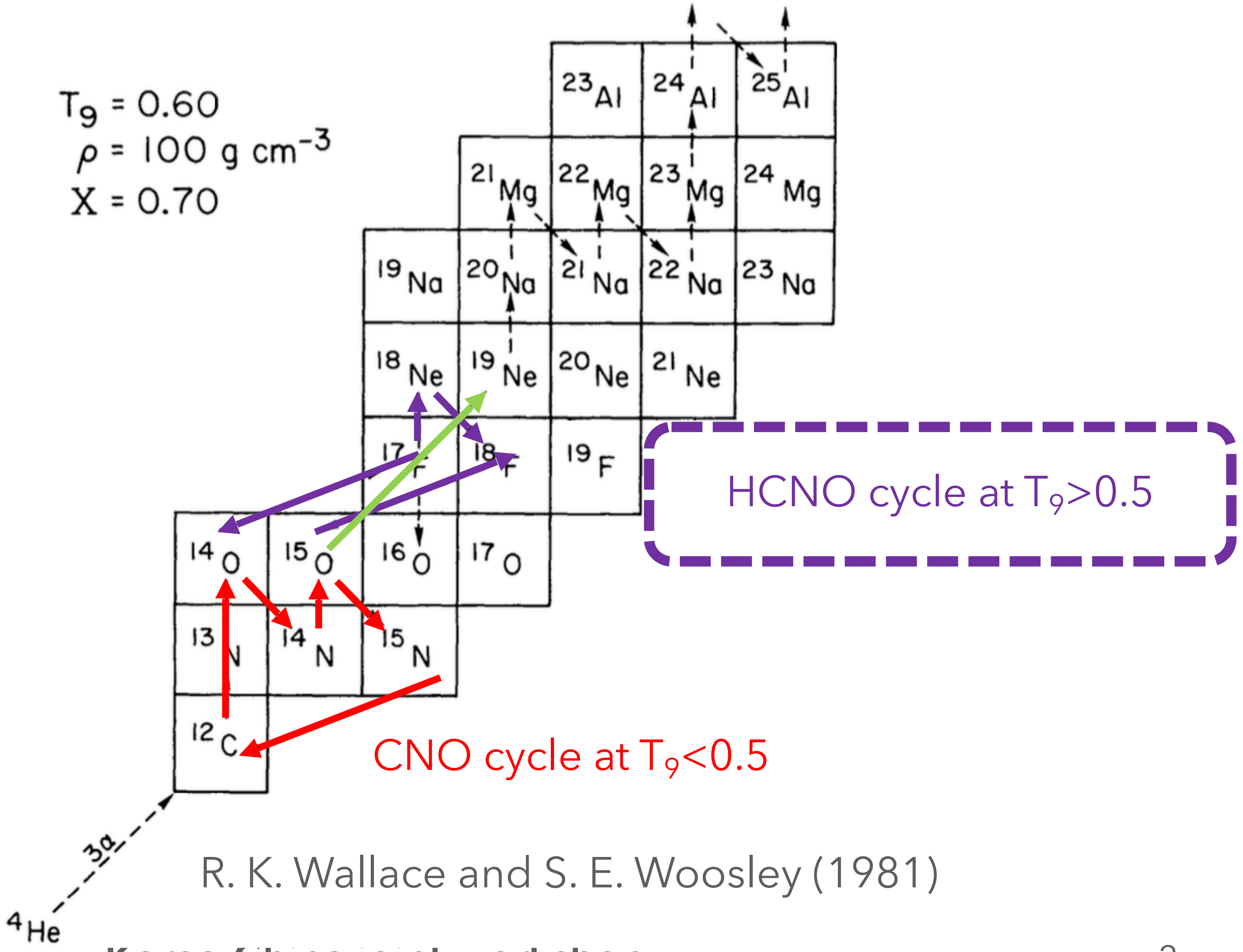

R. K. Wallace and S. E. Woosley (1981)

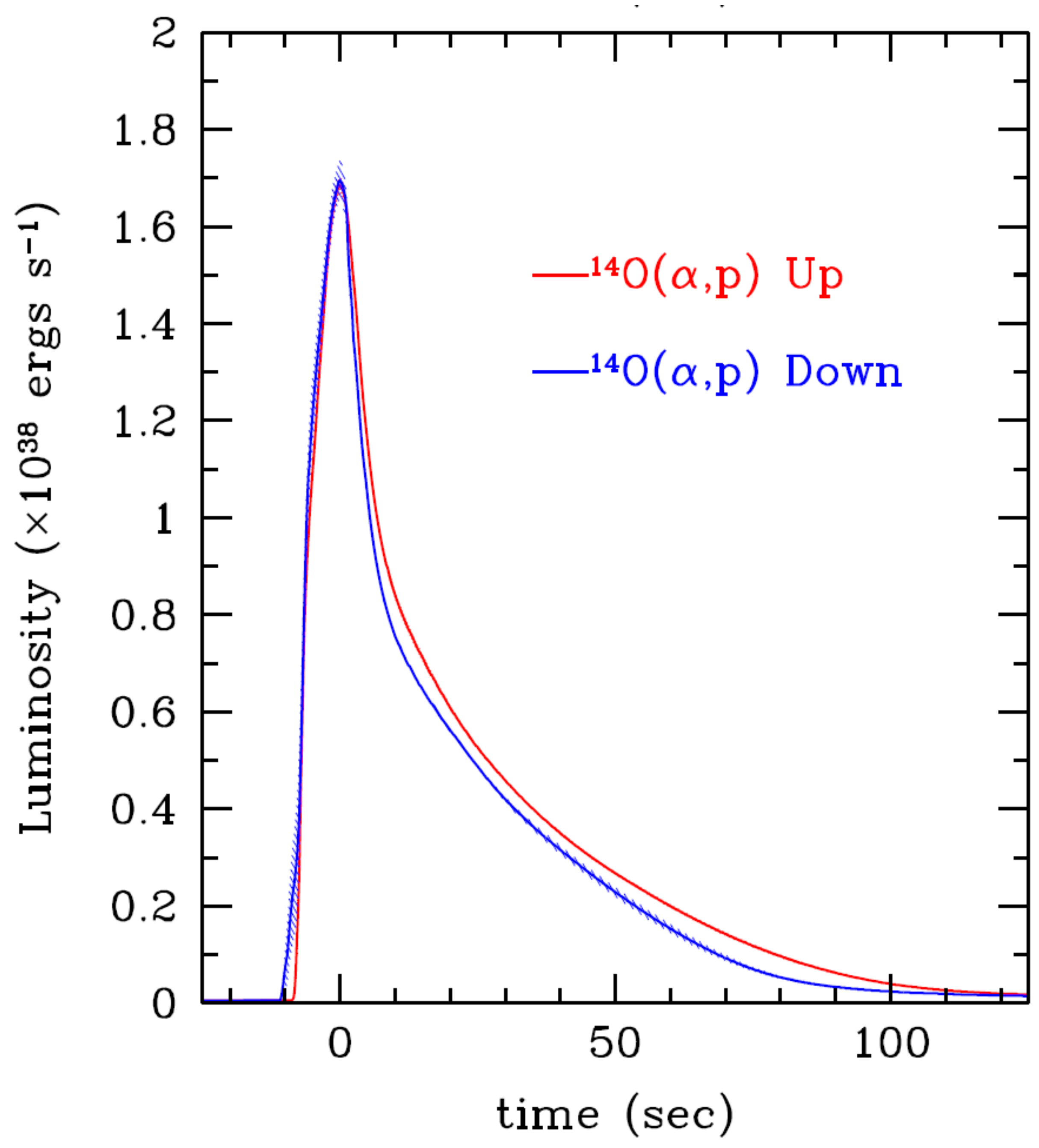

Motivation

Previous Studies

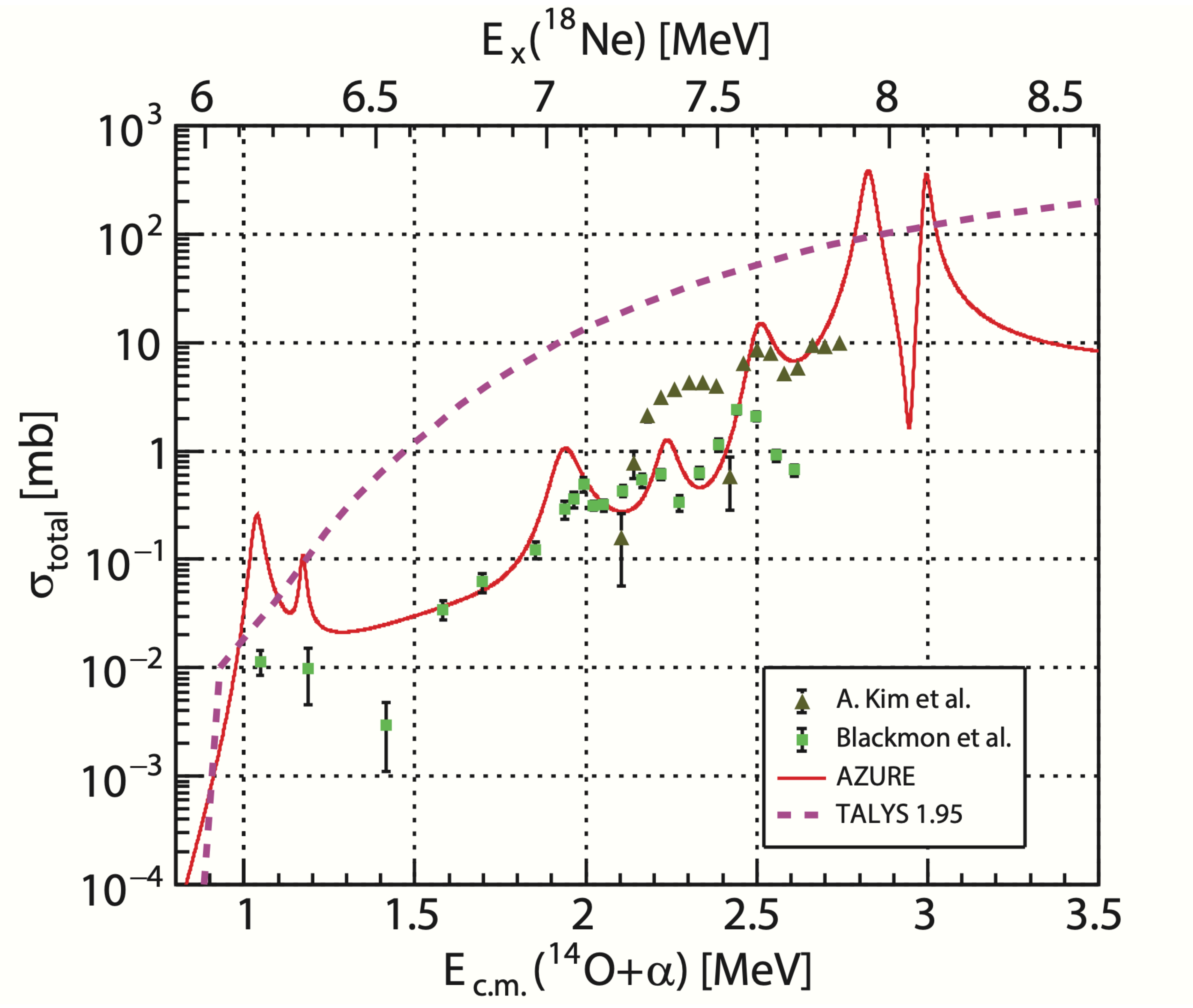

- A. Kim *et al.*
  → Direct measurement using Si telescopes
- Blackmon *et al.*
  → Time-reversal reaction: $^{1}H(^{17}F,\alpha)^{14}O$
- Hu *et al.* (AZURE parameter)
  → Indirect measurement of ^{17}F + p scattering

➡ **Large discrepancies in measured and calculated cross section**

Experimental Setup

CRIB
CNS Radio-Isotope Beam Separator

F0 target: H_2 gas (90K, 80 mm, ~500 Torr)

Primary beam: $^{14}N^{6+}$
- 8.40 MeV/u
- 3100 enA

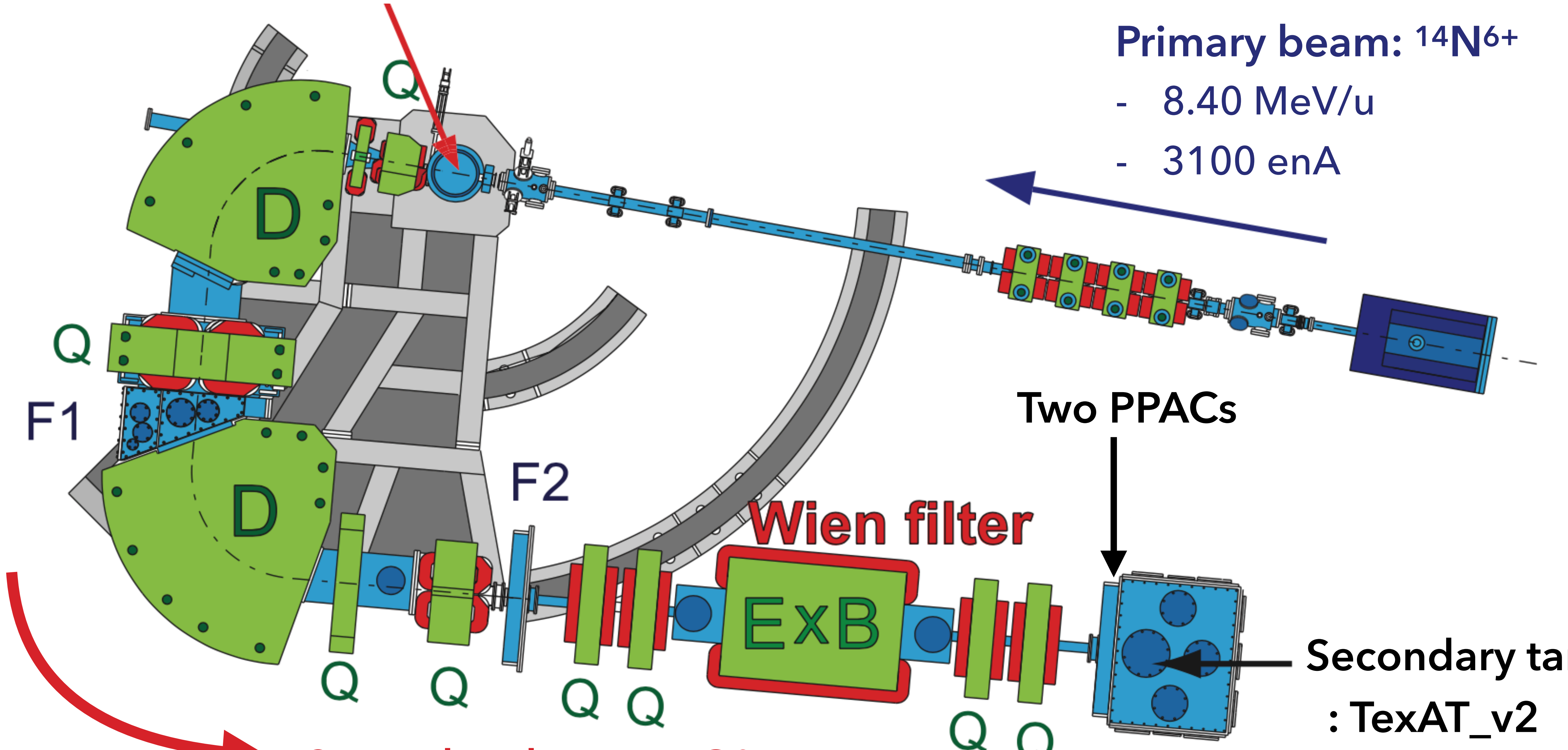

Secondary target / detector
: TexAT_v2
- He:CO_2 (90:10), 300 Torr

Secondary beam: $^{14}O^{8+}$
- 4.66 MeV/u
  → 3 MeV/u, 10^5 pps after thin scintillator

TexAT chamber

Texas Active Target TPC (TexAT)

- Consist of …
  - Field cage
  - Micromegas
  - GEM
  - Silicon detectors
  - CsI(Tl) + PIN diode

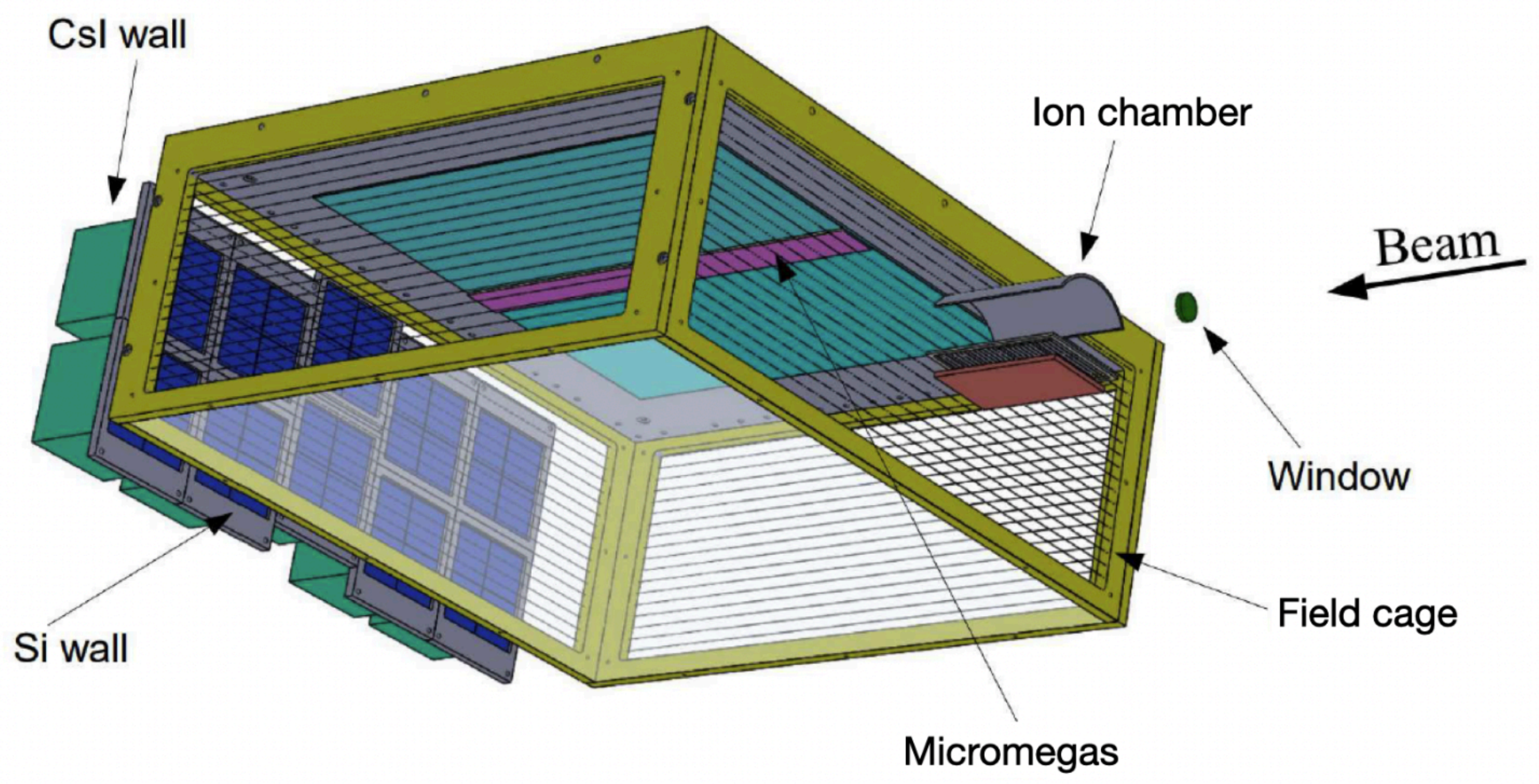

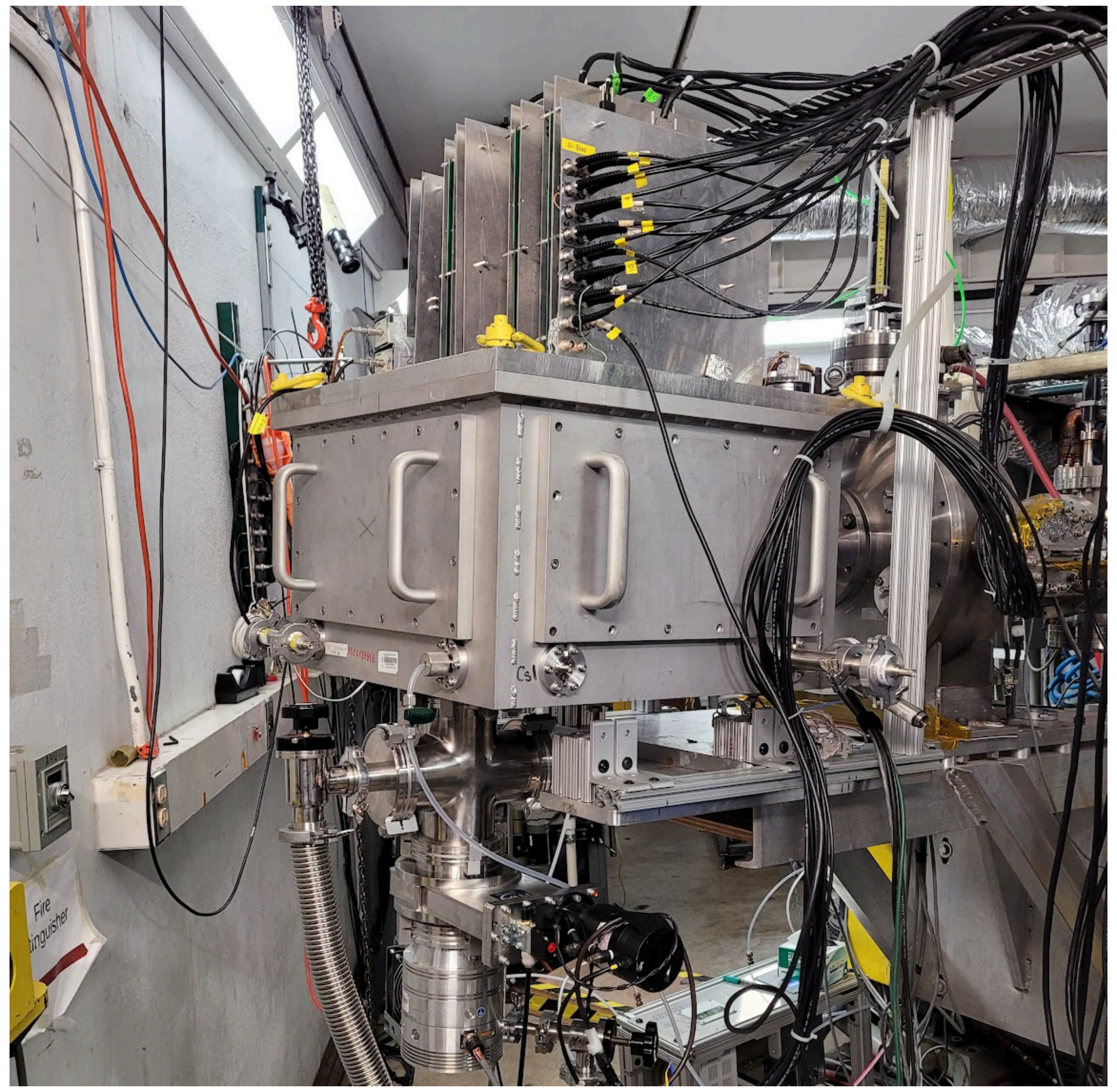

TexAT_v2 Upgrade

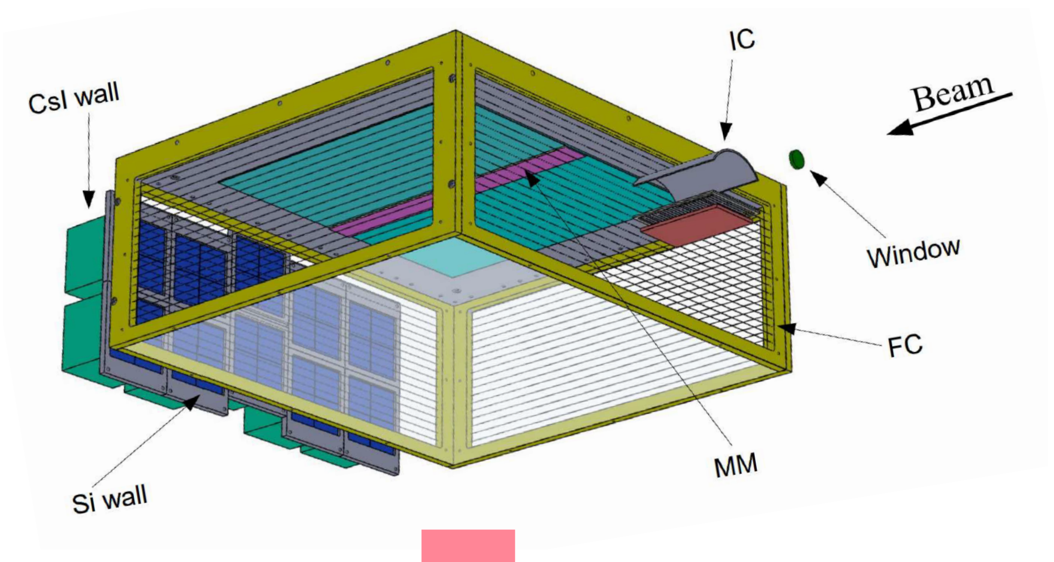

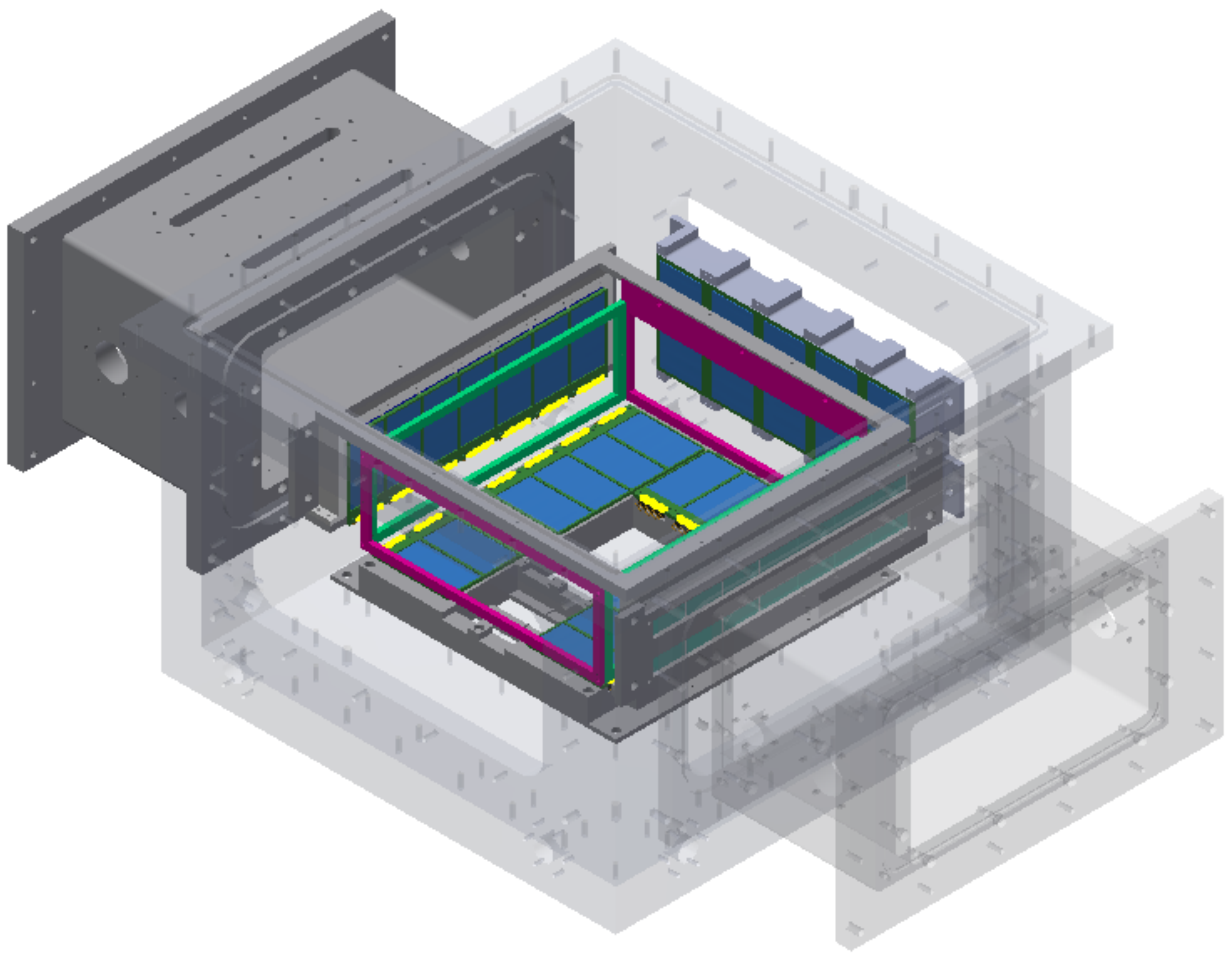

- **Goals**
  - Larger solid angle coverage
  - Higher energy and position resolution
  - Endure high beam intensity (~10^5 pps)

  → Measure low-energy protons!

- **Upgraded points**
  - New field cage: width optimization, gating grid
  - New detector arrays: X6, CsI(Tl) + SiPM
  - Beam monitor

TexAT_v2

New Field Cage

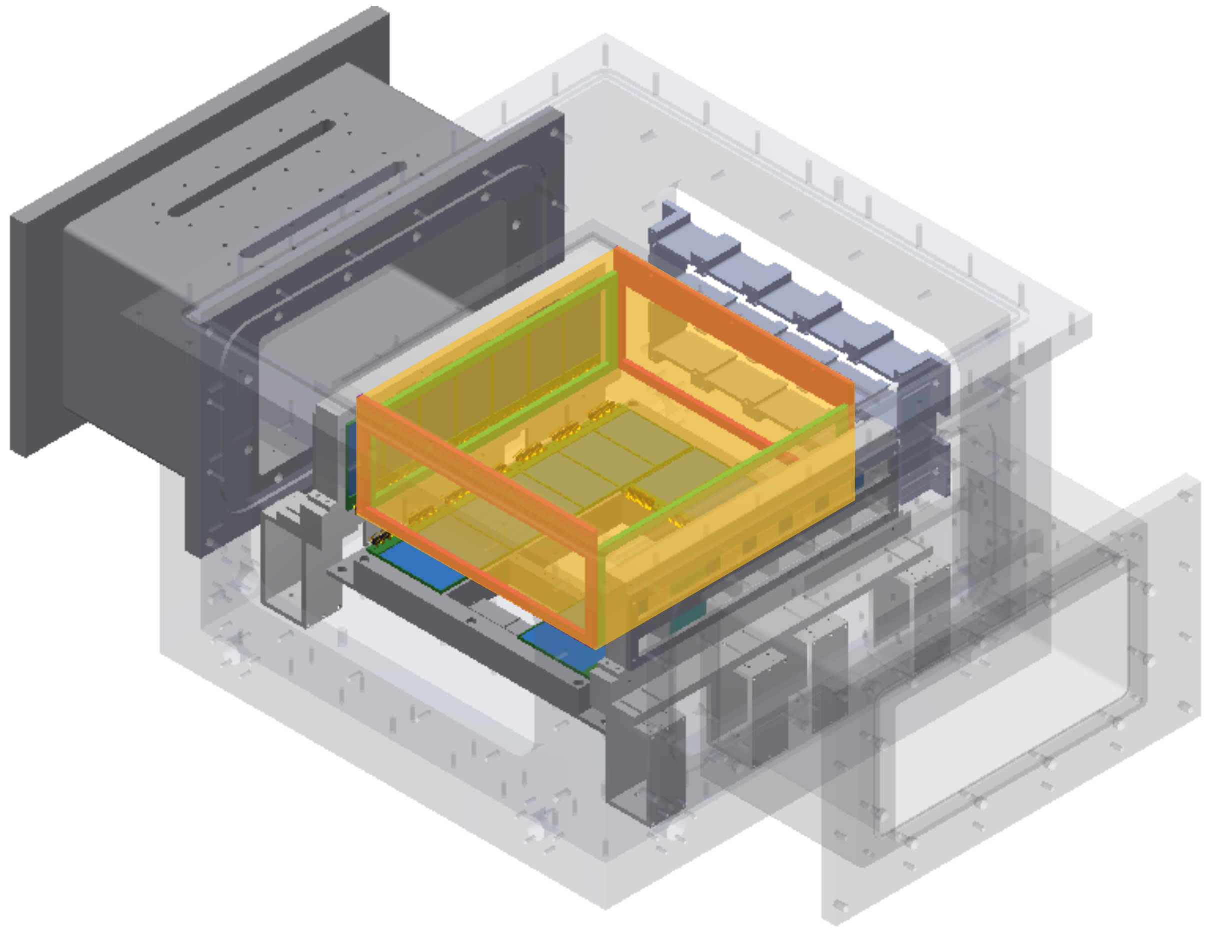

- Field cage made with PCB, 50μm gold-plated tungsten wire and 100MΩ resistors
- **Cathode modification**: Cu plate → Au-plated tungsten wires + PCB
- **Width optimization**: to bring the side X6 detectors closer to the reaction vertex
- **Gating grid**: to handle beam intensity ~10^5 pps

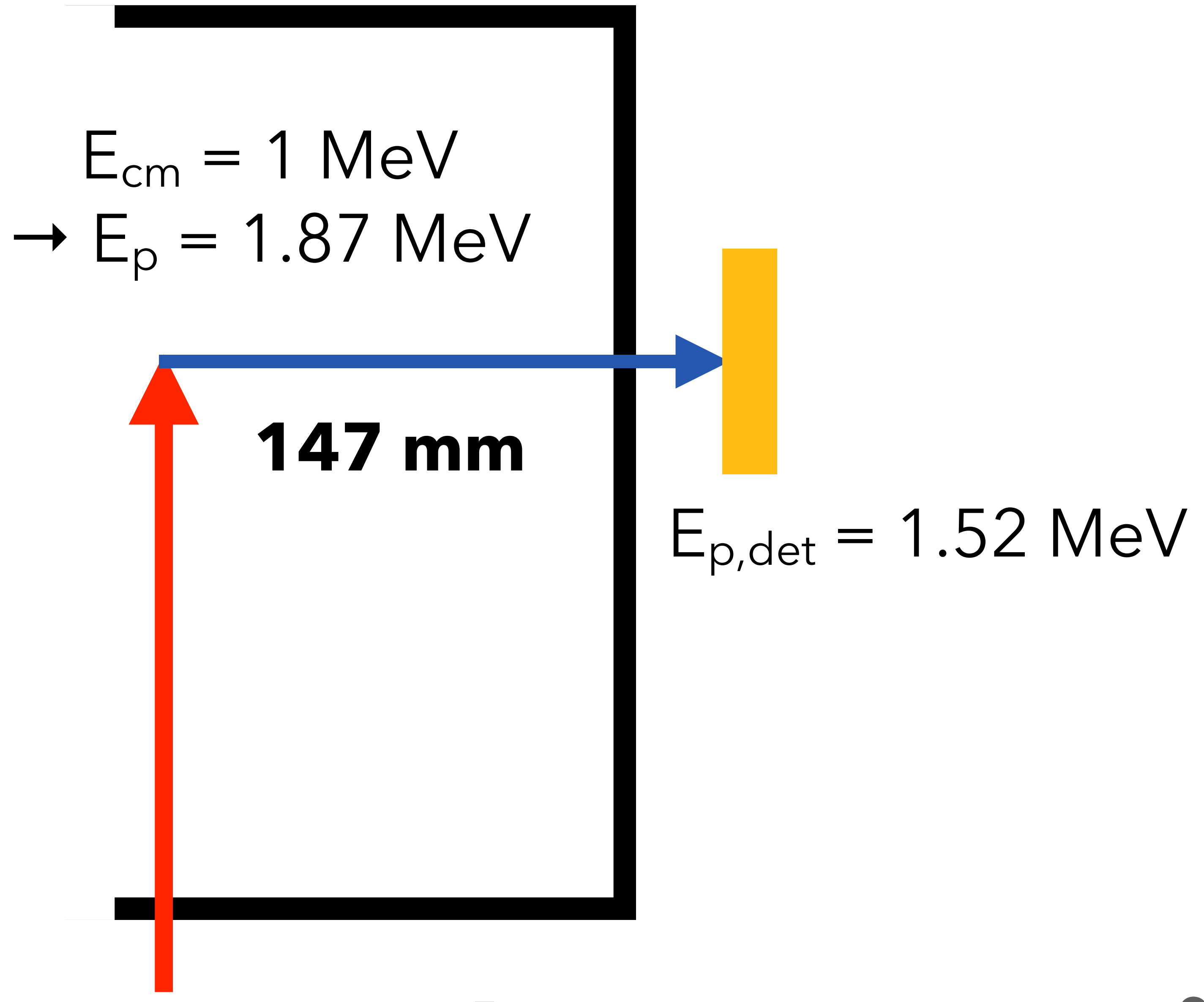

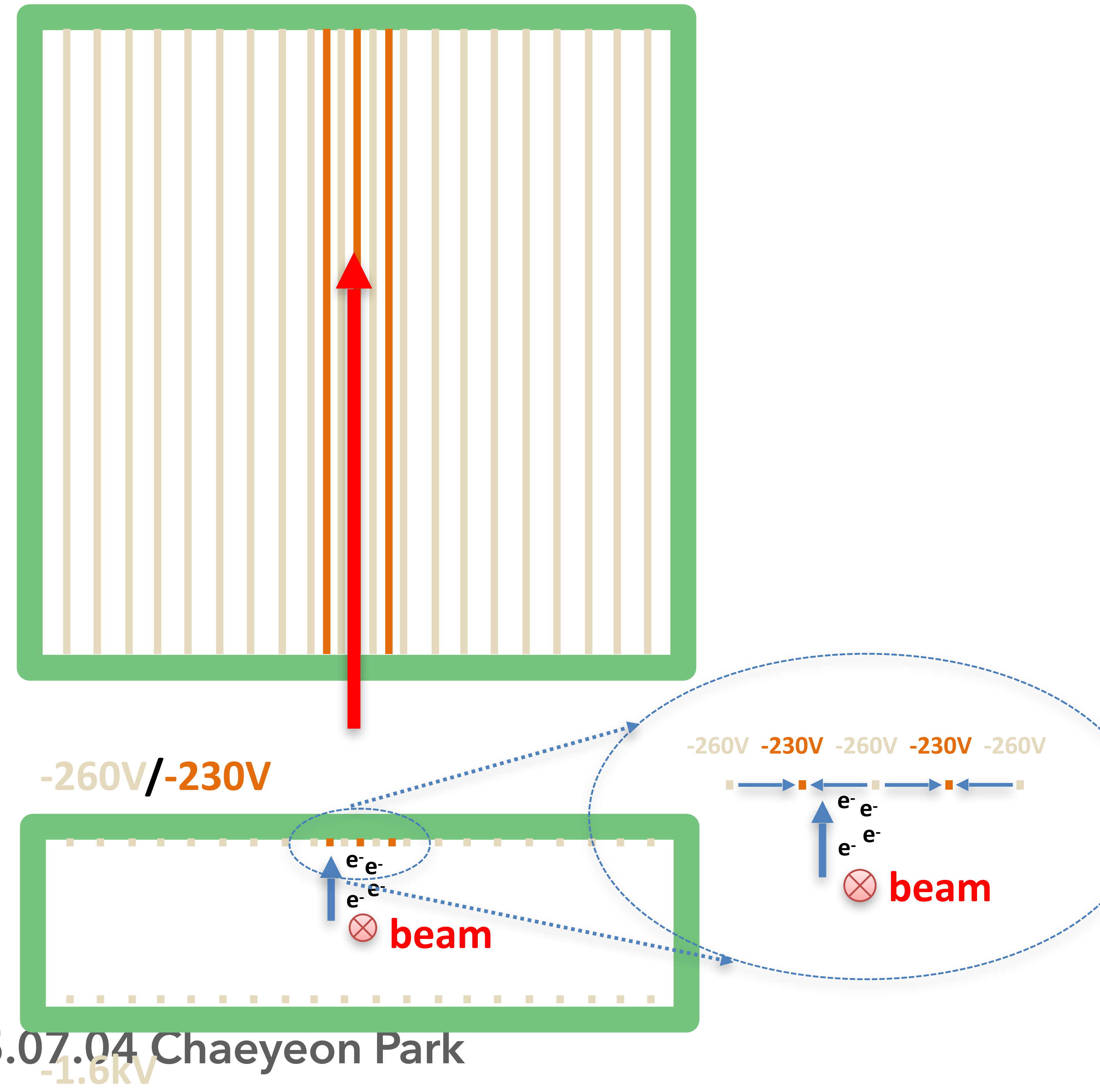

TexAT_v2

New Detector Arrays

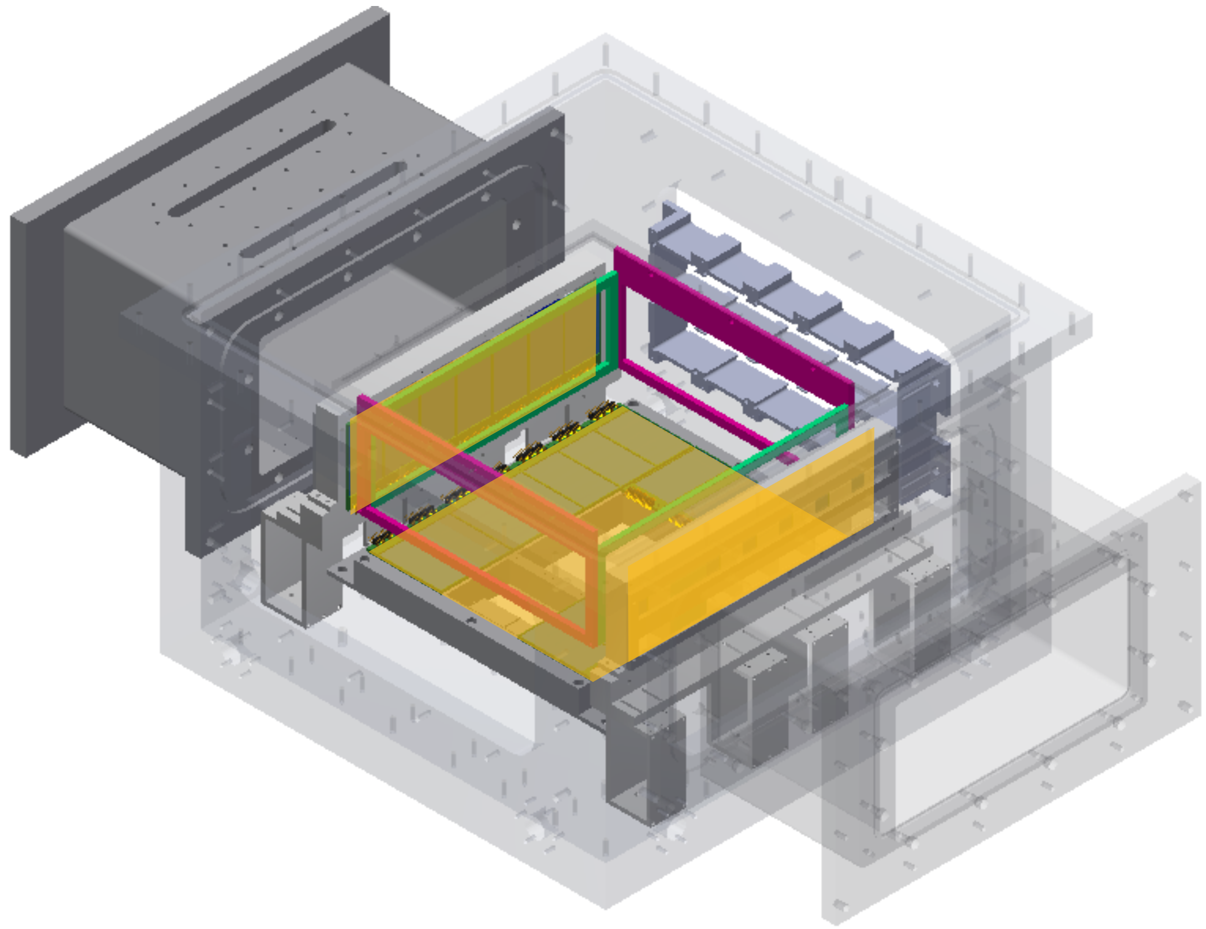

- **X6 silicon detector**
  improved position and energy resolution
  (< 1 mm position, ~1% energy resolution @ 5.5 MeV α particle)
- **CsI(Tl) + Silicon photomultiplier (SiPM)**
  enhanced energy resolution thatn CsI(Tl) + PIN diode
  (8% energy resolition @ 5.5 MeV α particle)

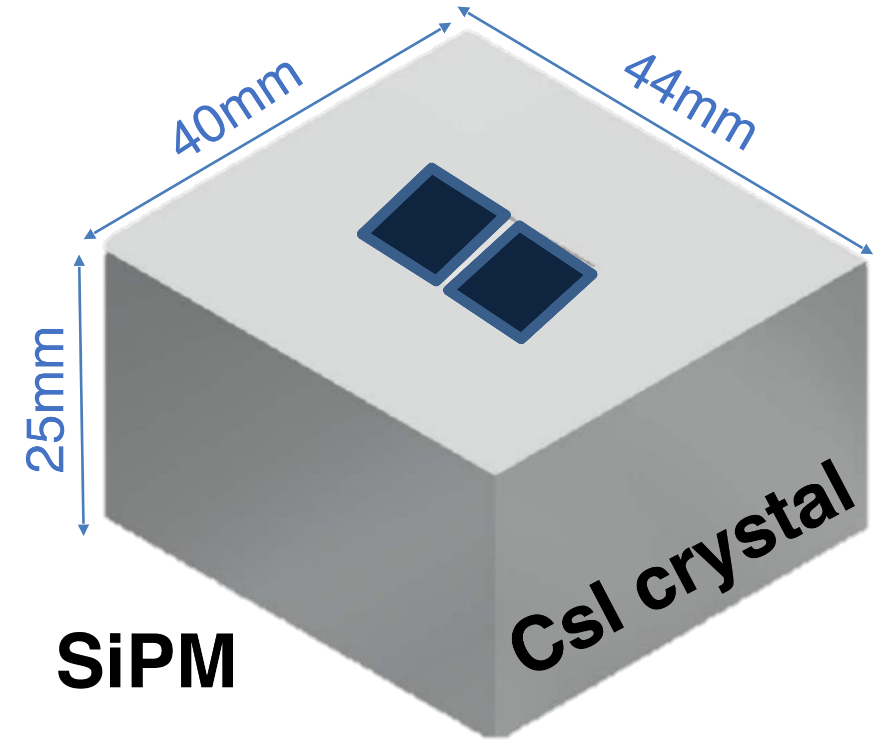

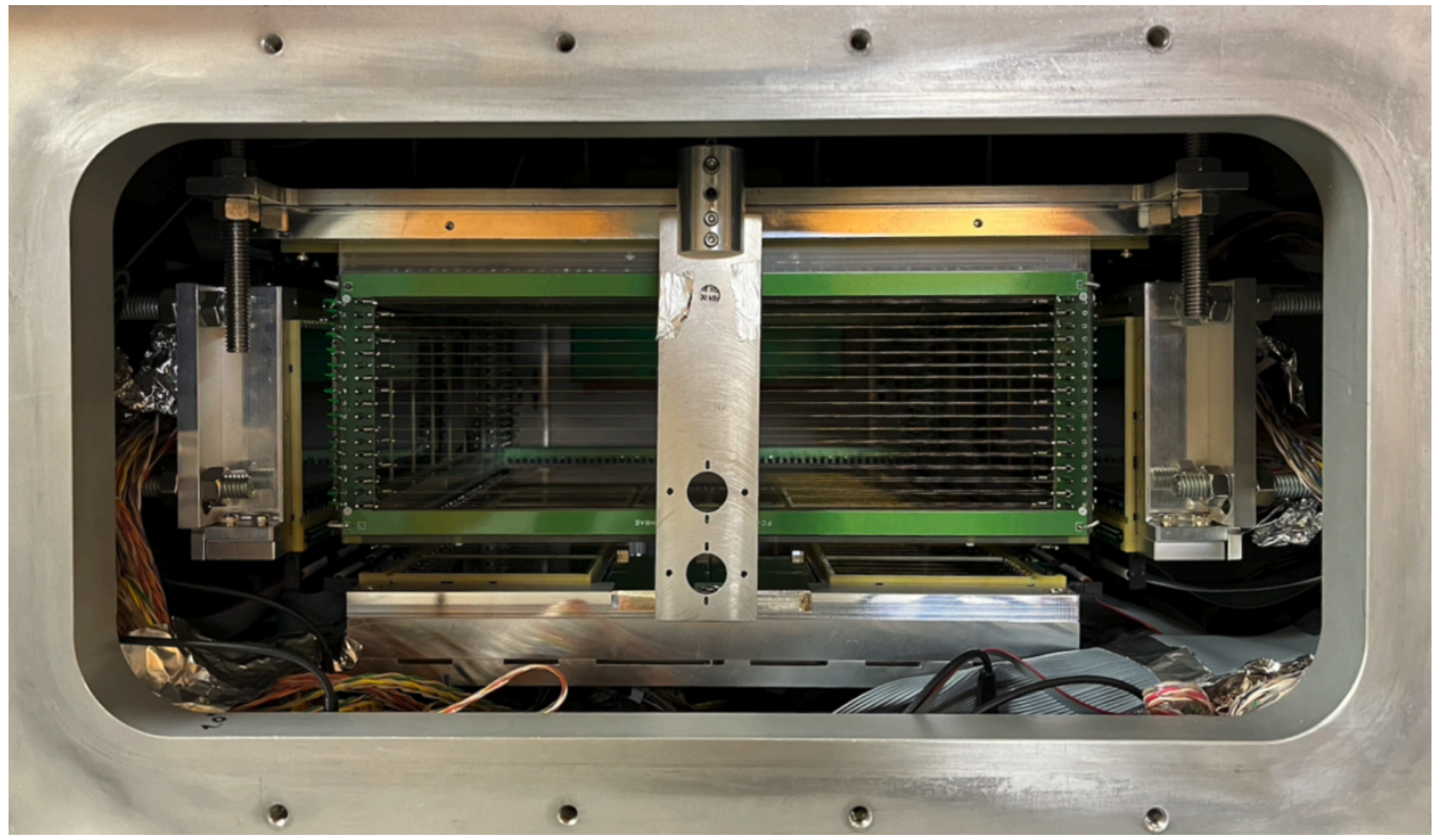

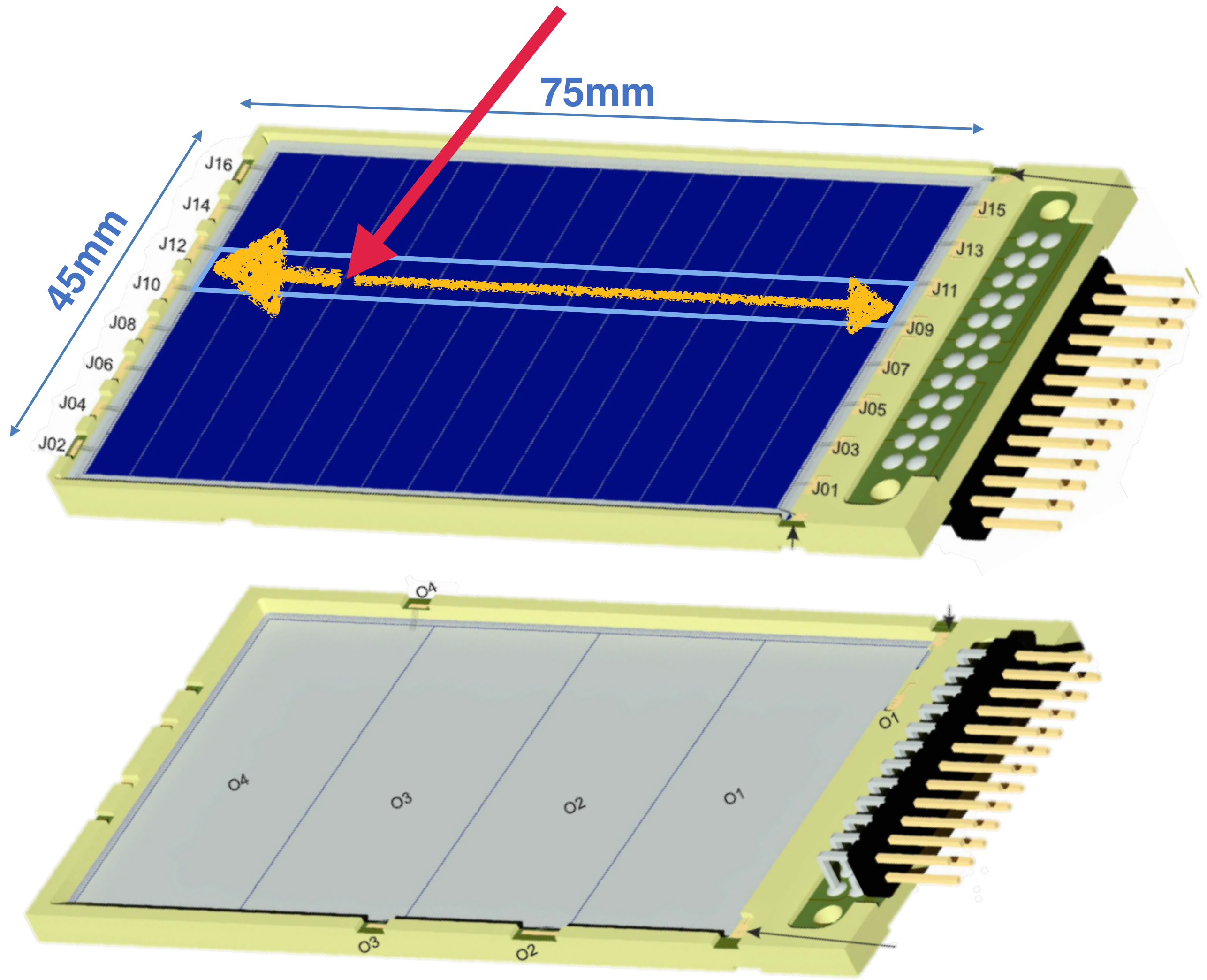

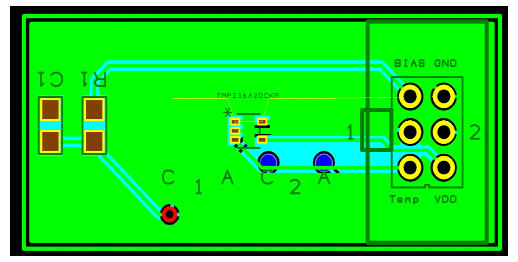

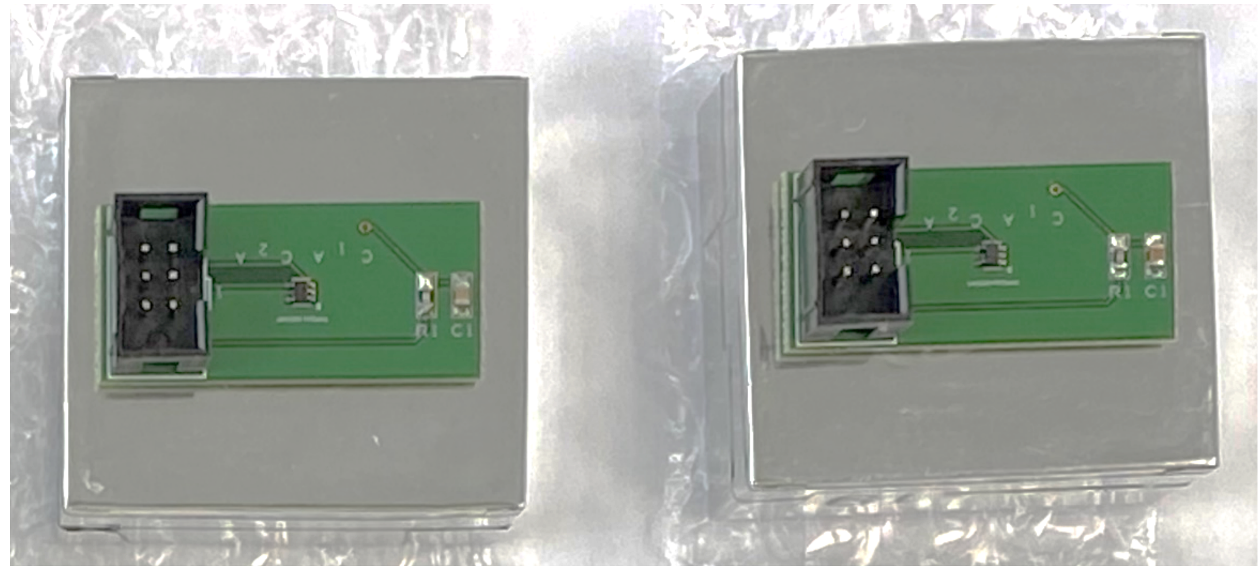

TexAT_v2

Beam Monitor

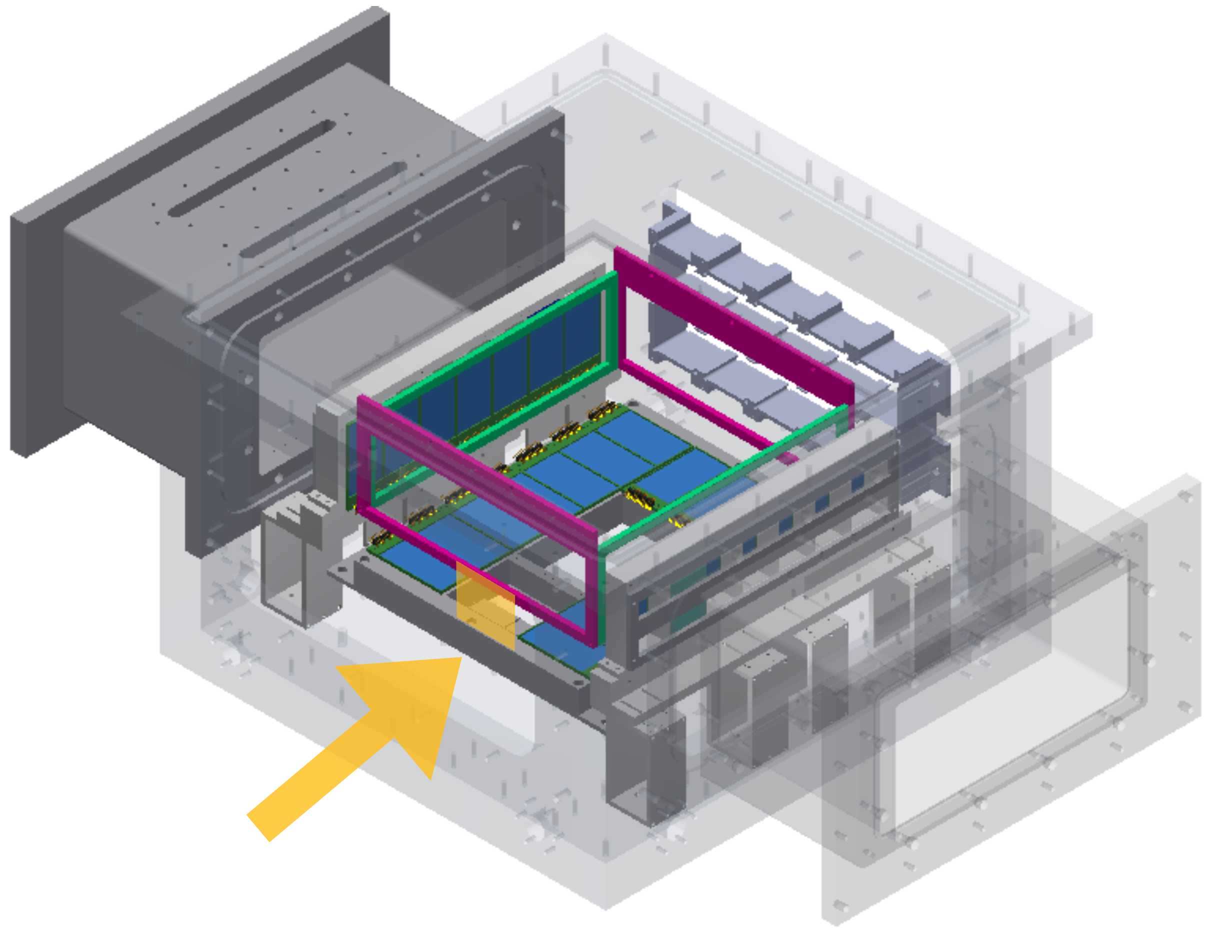

- 5μm scintillator foil + SiPM provides beam signals
- Reliable direct measurement of beam intensity up to 10^5 pps
- BM × Si trigger to reduce random backgrounds
  (80% dead ime → 20% dead time with 300 ns coincidence gate)

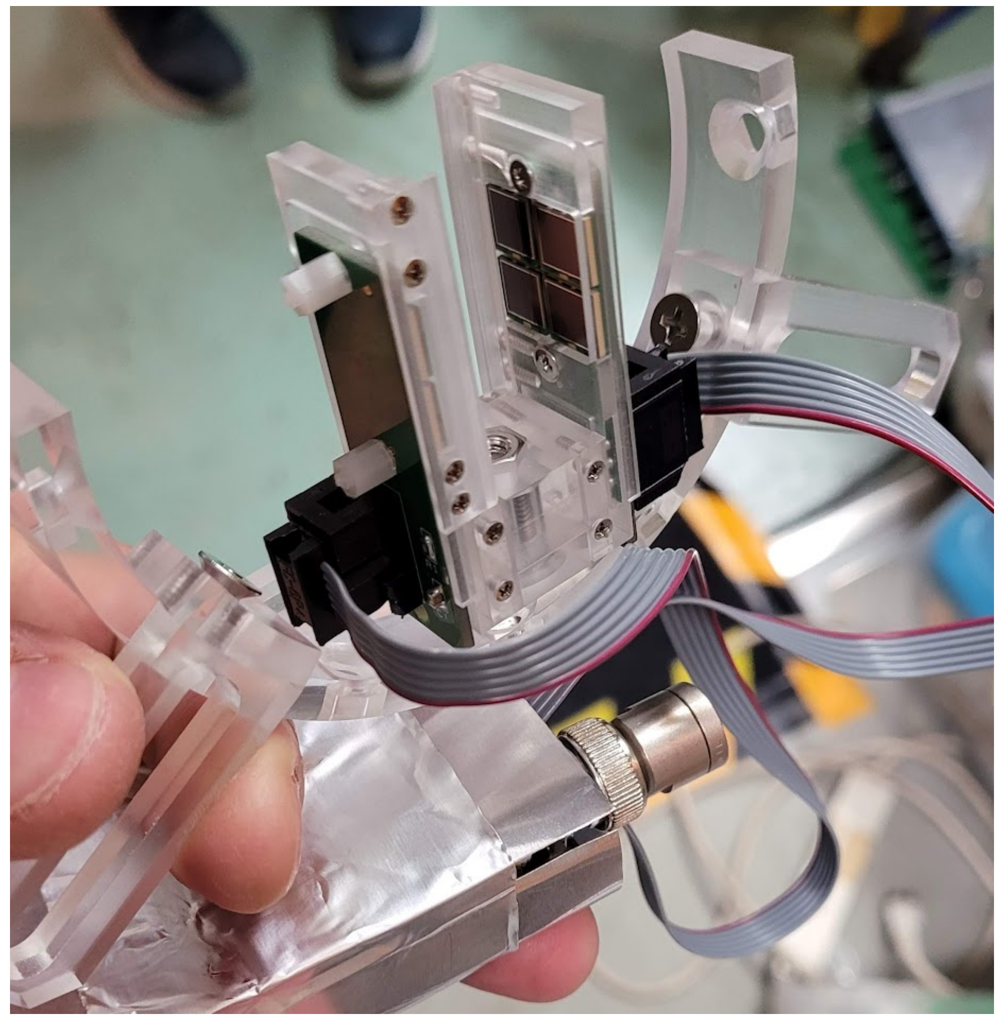

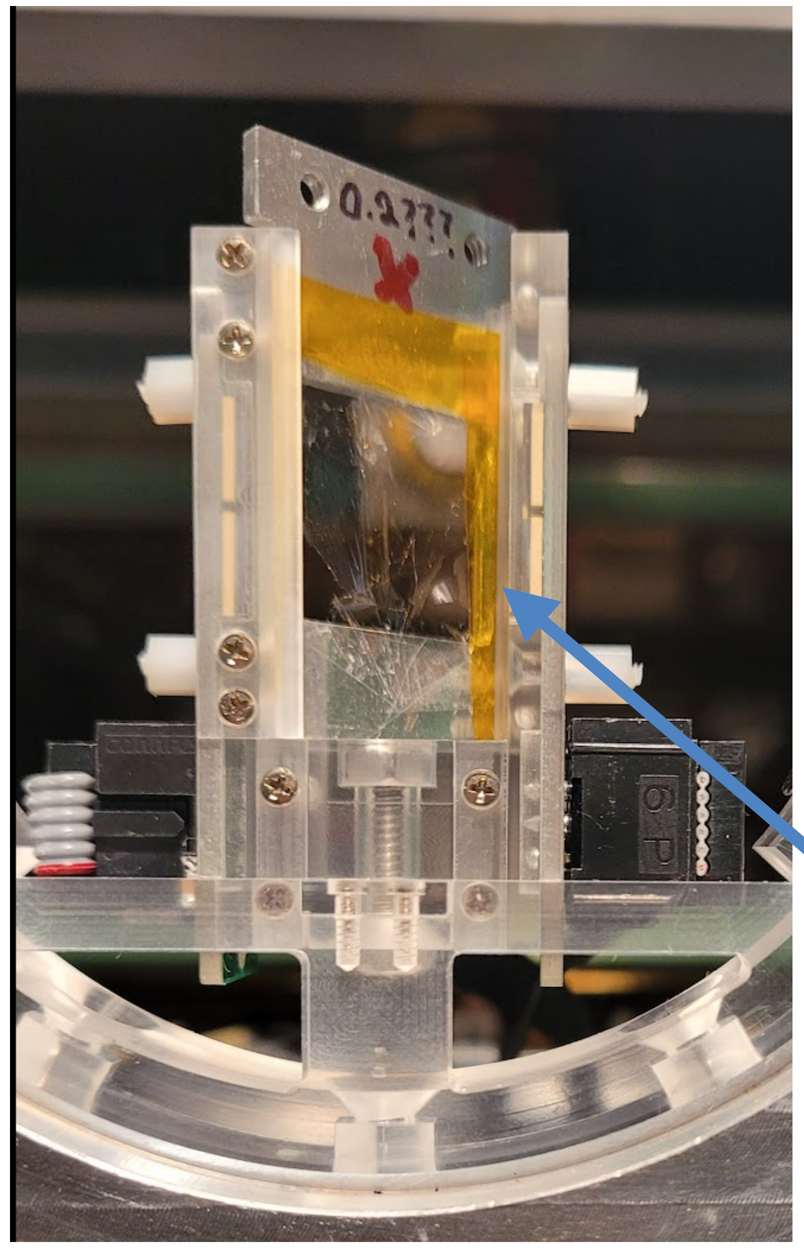

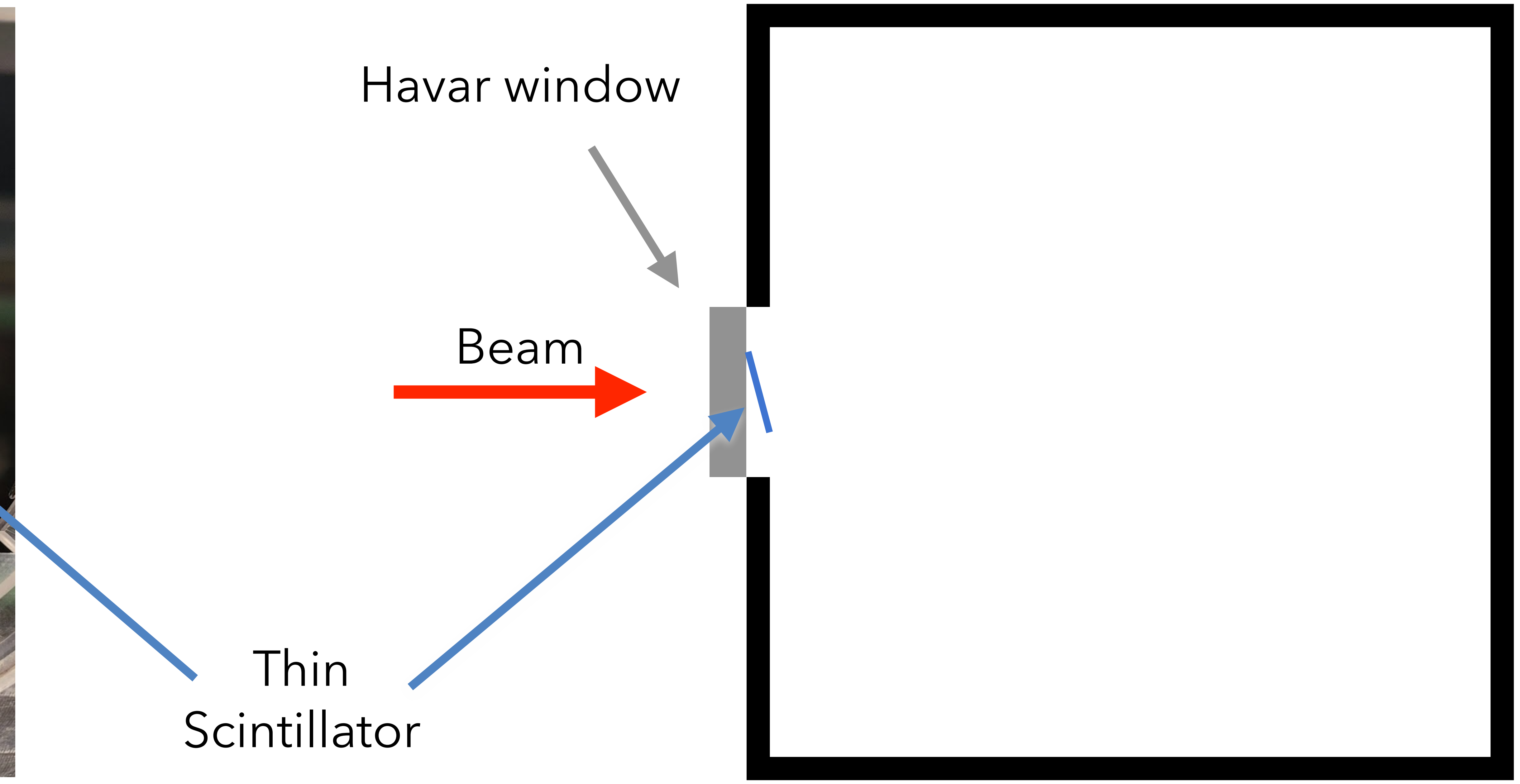

Experimental Setup

CRIB

CNS Radio-Isotope Beam Separator

F0 target: H_2 gas (90K, 80 mm, ~500 Torr)

Primary beam: $^{14}N^{6+}$
- 8.40 MeV/u
- 3100 enA

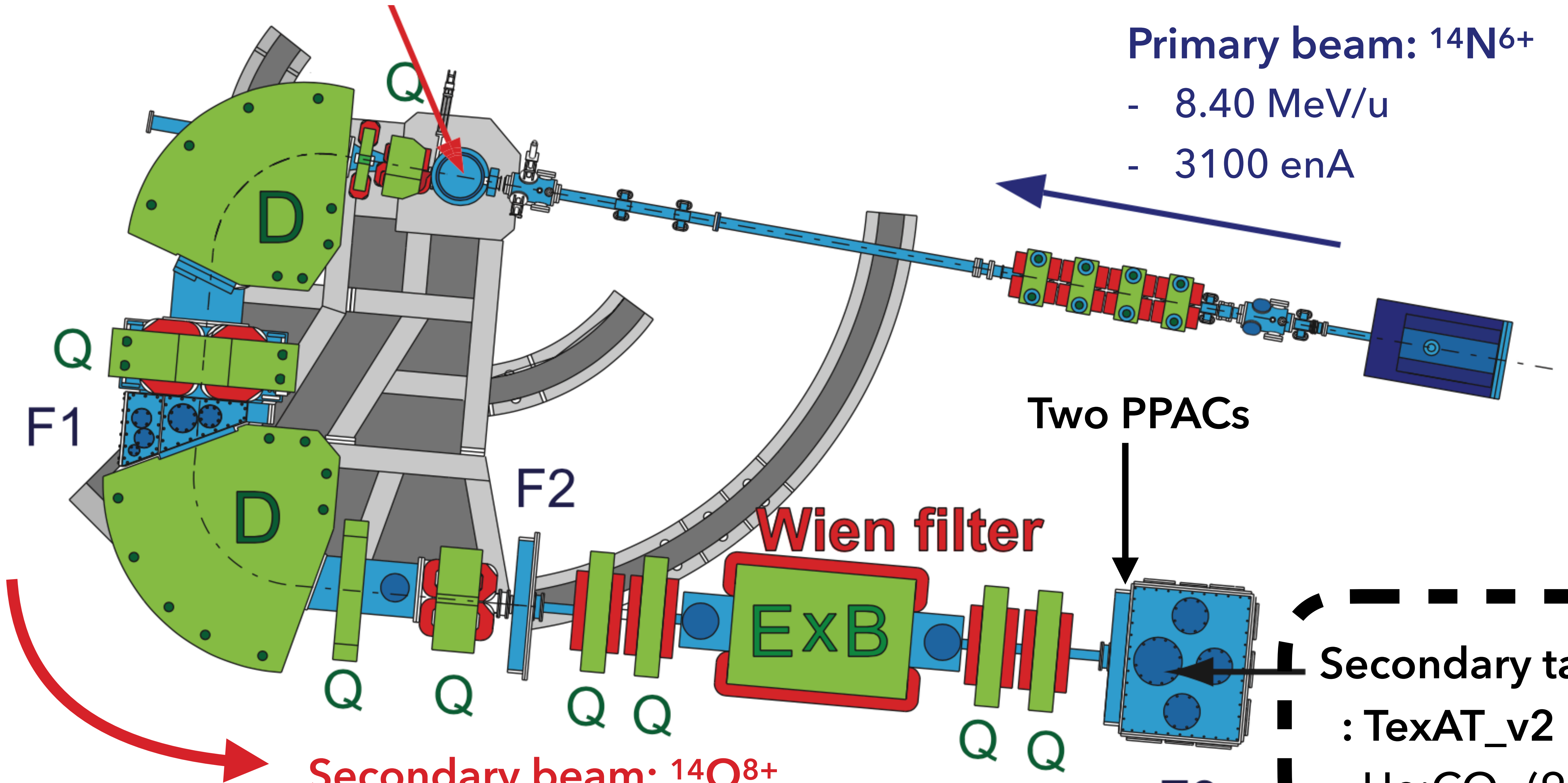

Secondary beam: $^{14}O^{8+}$
- 4.66 MeV/u

  → 3 MeV/u, 10^5 pps after thin scintillator

Secondary target / detector
: TexAT_v2
- He:CO_2 (90:10), 300 Torr

TexAT chamber

^{14}O Beam Production

F0 gas cell target: H_2 gas (90K, 80 mm, 500 Torr)

Primary Beam: $^{14}N^{6+}$
- 8.40 MeV / u
- 3100 enA

Double achromatic System

$$B\rho = \frac{p}{q}$$

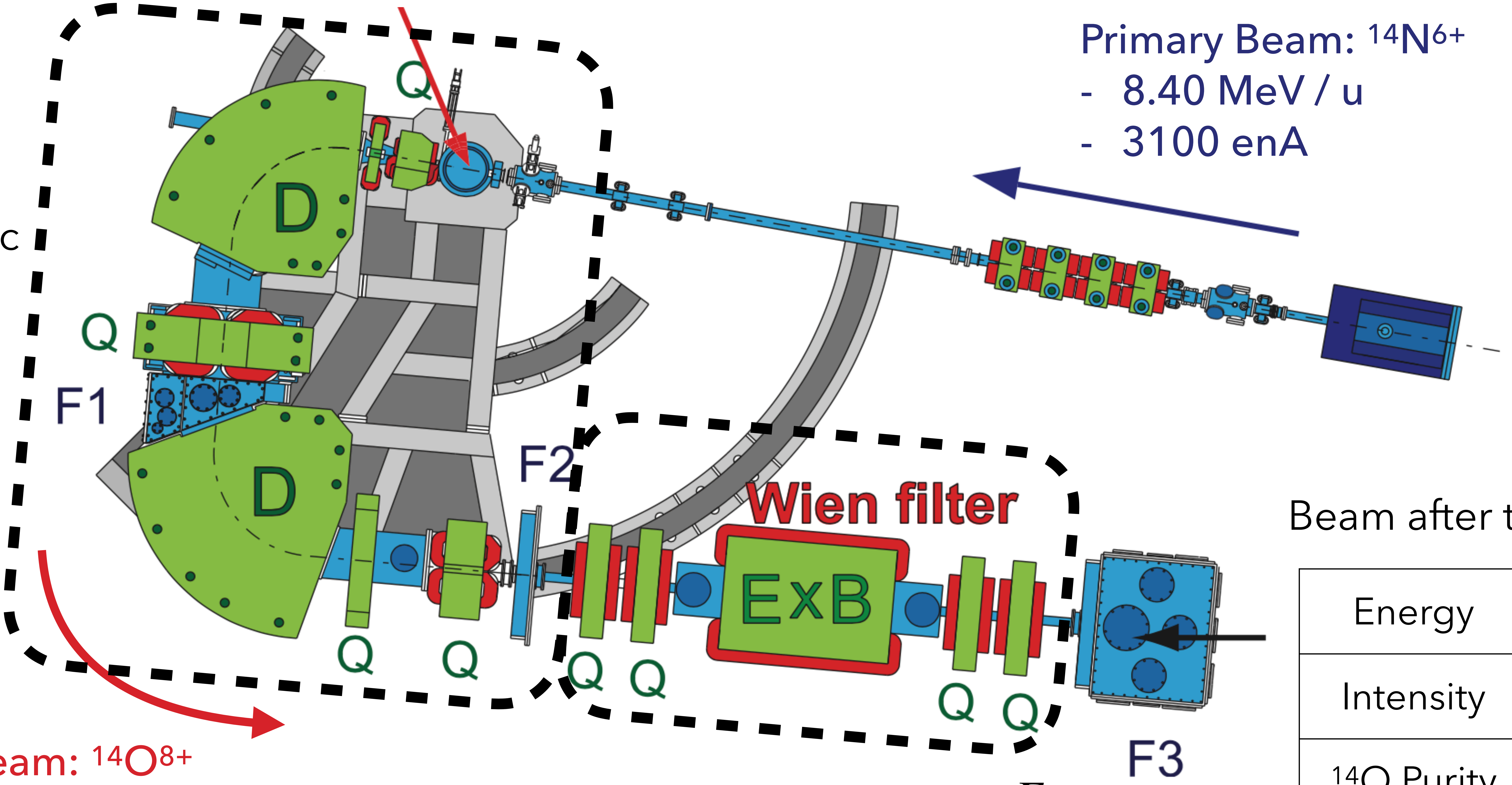

Secondary Beam: $^{14}O^{8+}$

Wien Filter System $v = \frac{E}{B}$

Beam after the beam monitor

Energy	39.112 MeV
Intensity	1.07×10^5 pps
^{14}O Purity	50 - 70%

^{14}O Beam Production

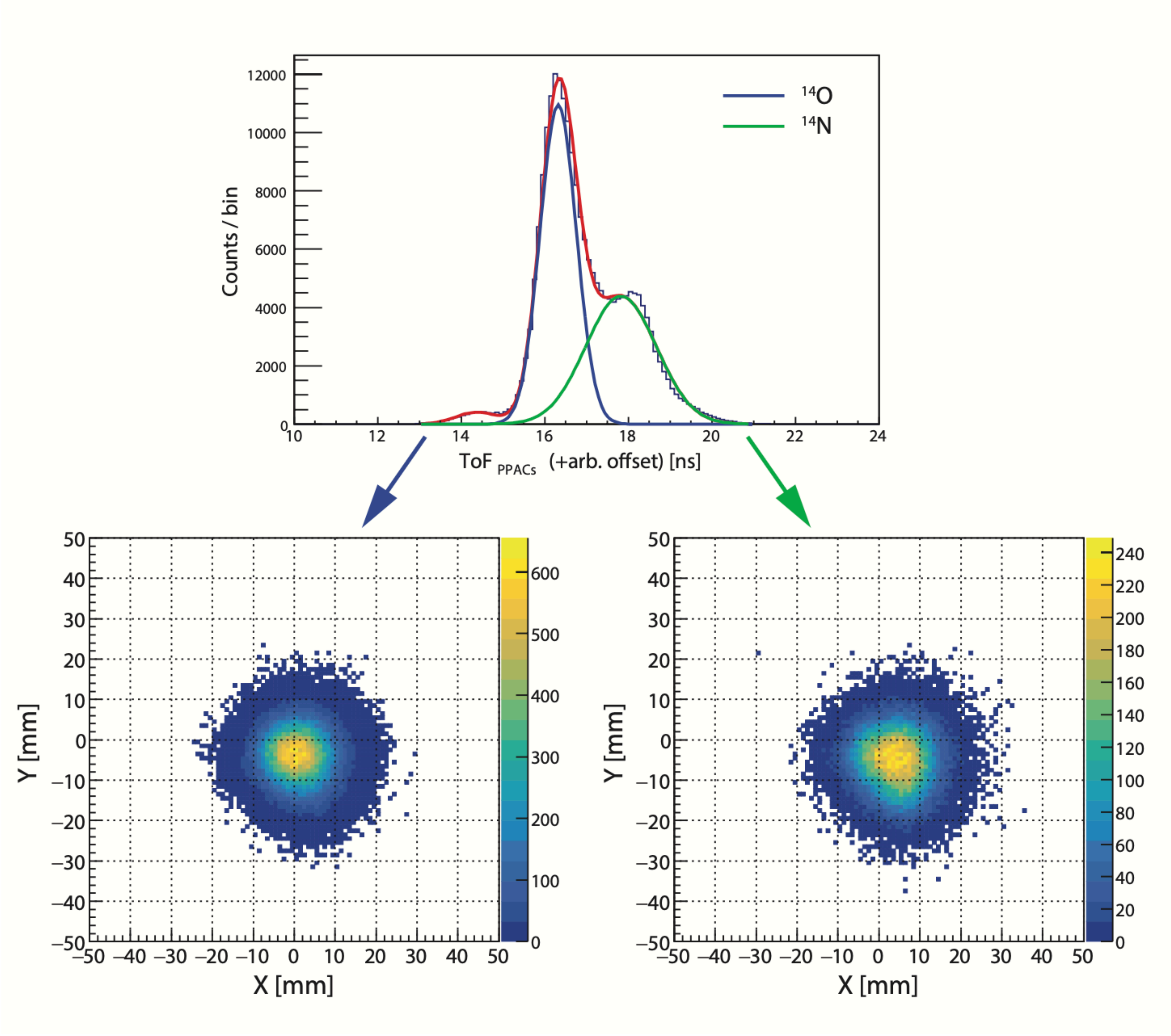

F3 focal plane PID (w. beam monitor gate)

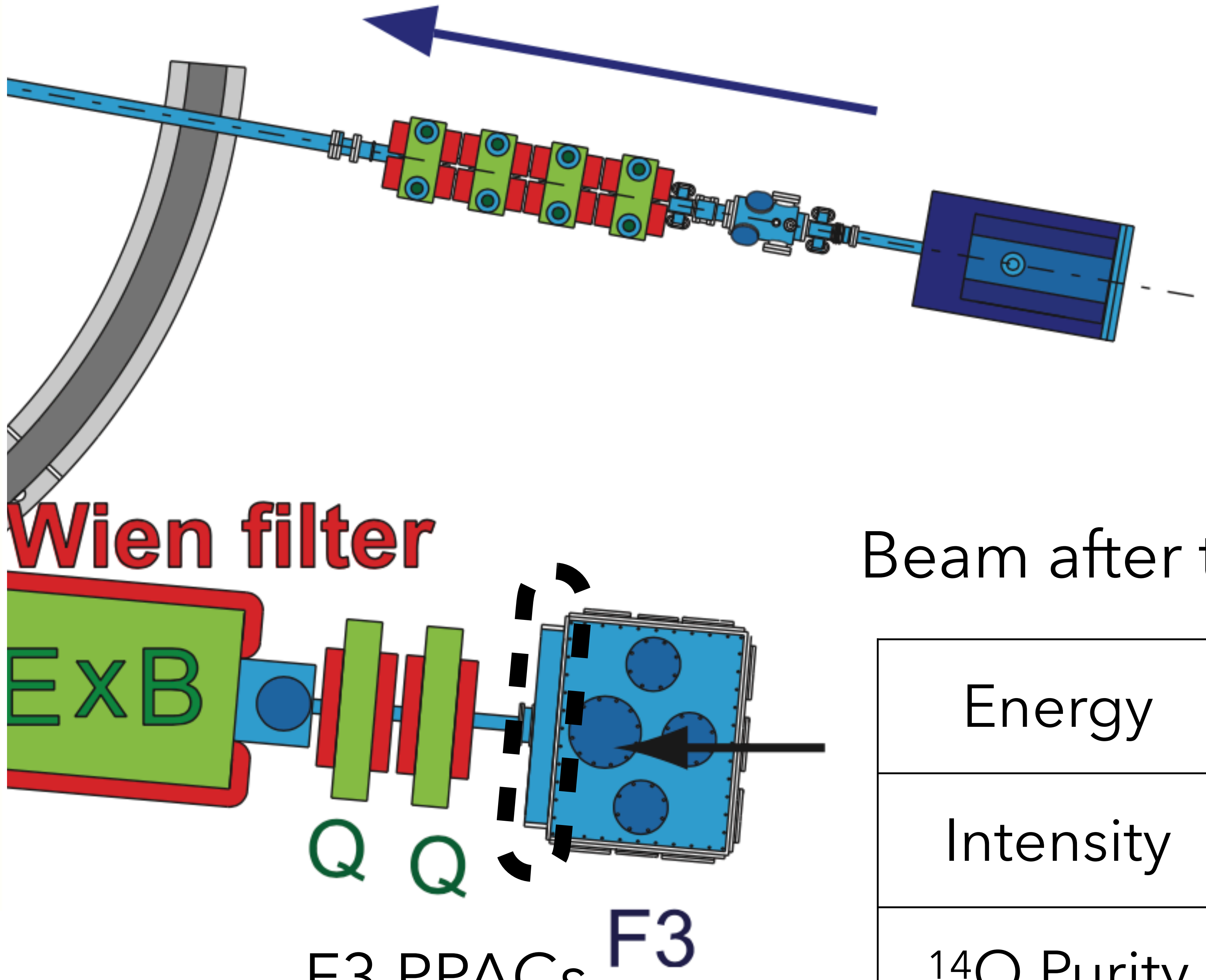

F3 PPACs

Beam after the beam monitor

Energy	39.112 MeV
Intensity	1.07×10^5 pps
^{14}O Purity	50 - 70%

LILAK: An Analysis Toolkit

Low and intermediate energy nuclear experiment analysis toolkit

- A workflow-based analysis structure with sequential data processing and a flexible toolkit of pre-defined methods.
- LILAK enables transparent data flow and ensures a reproducible, step-by-step analysis.

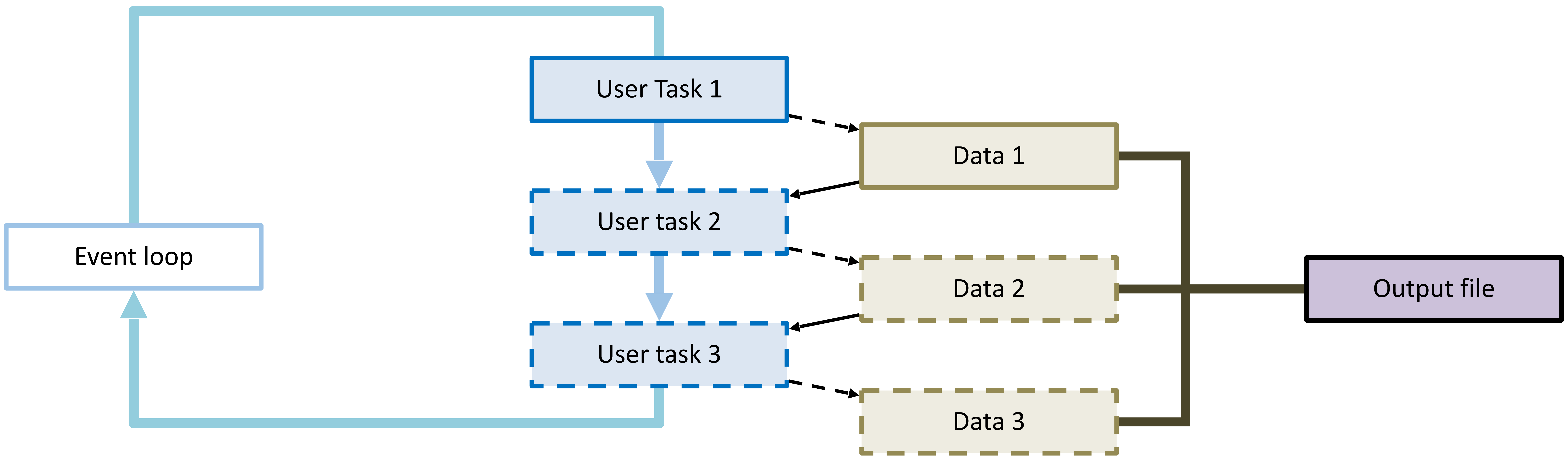

Pulse Shape Analysis

Pulse Extraction

⇩

Pulse Analysis

: Find and fit pulse signal from the given channel buffer using input pulse data by detector.

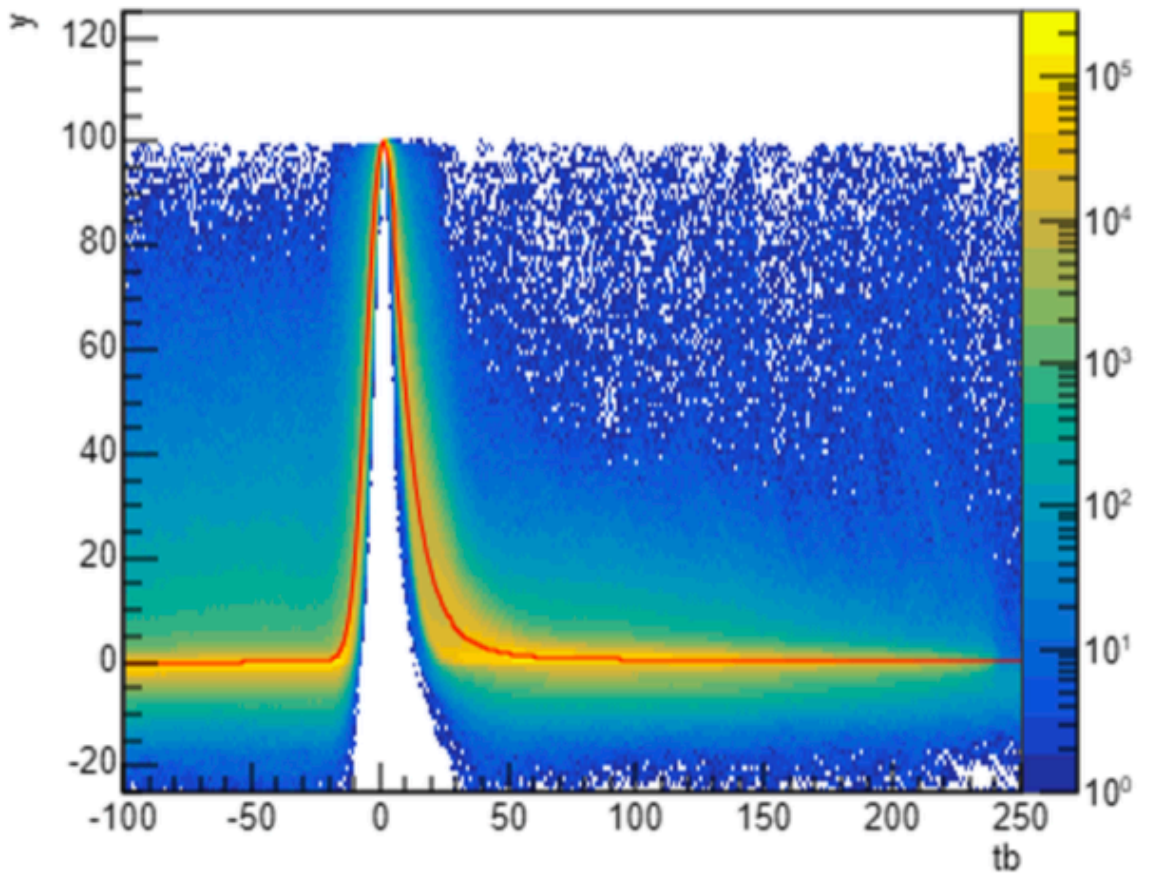

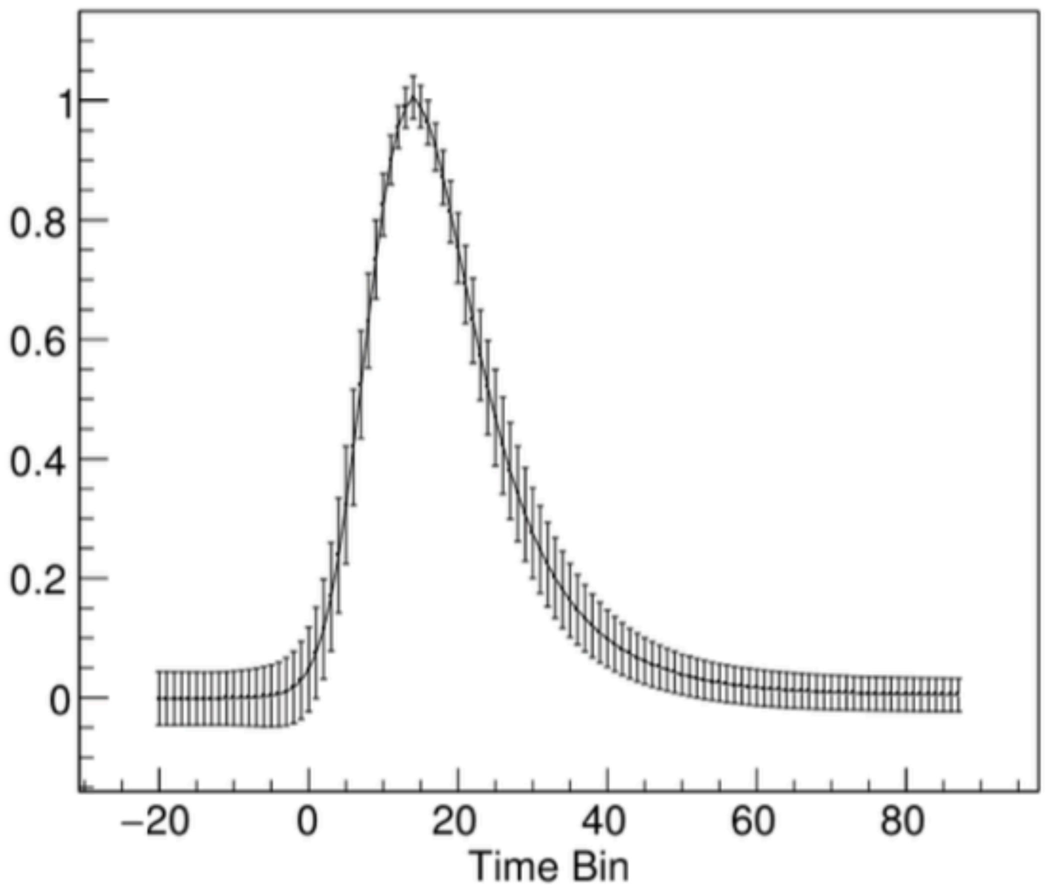

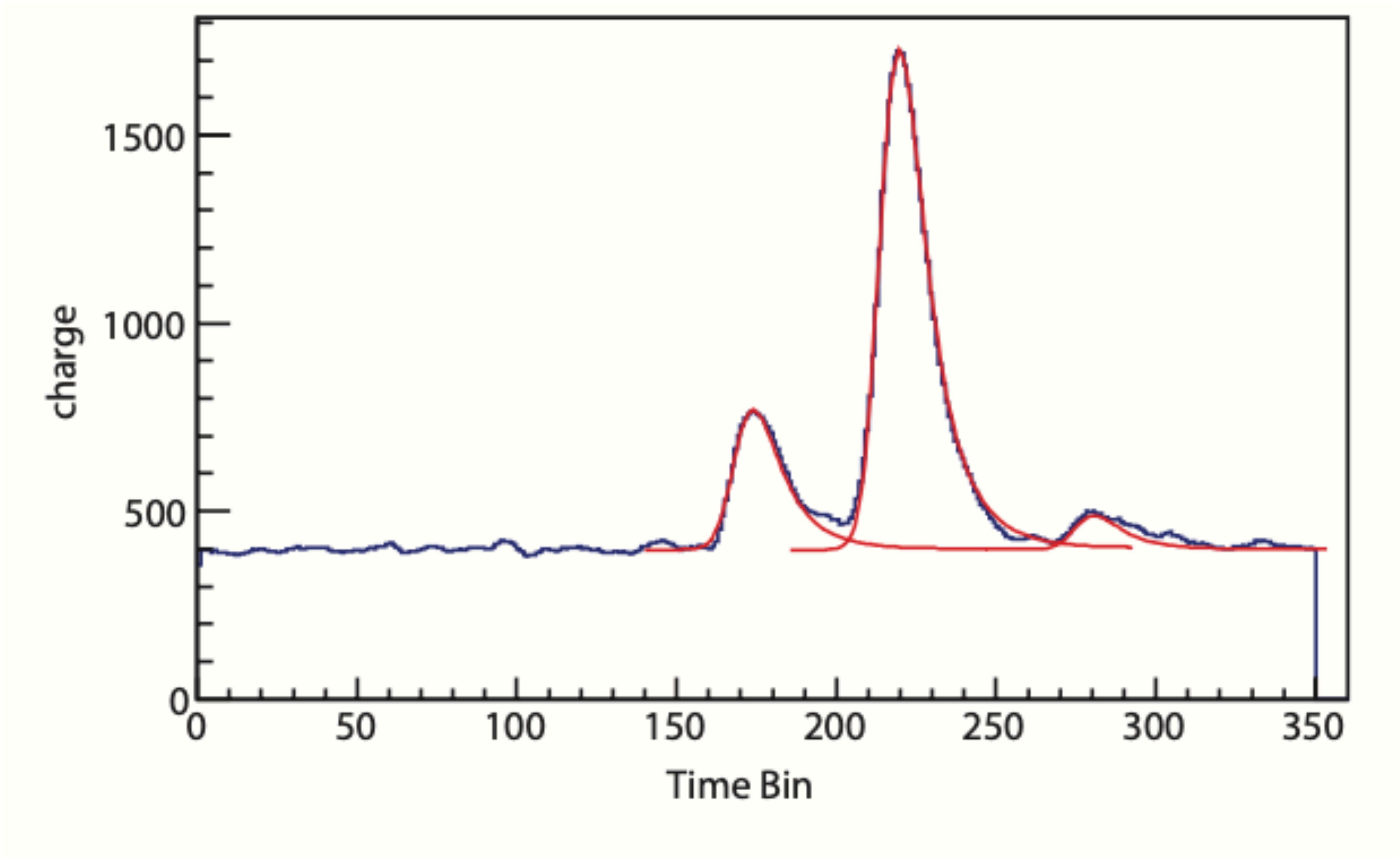

Particle Tracking

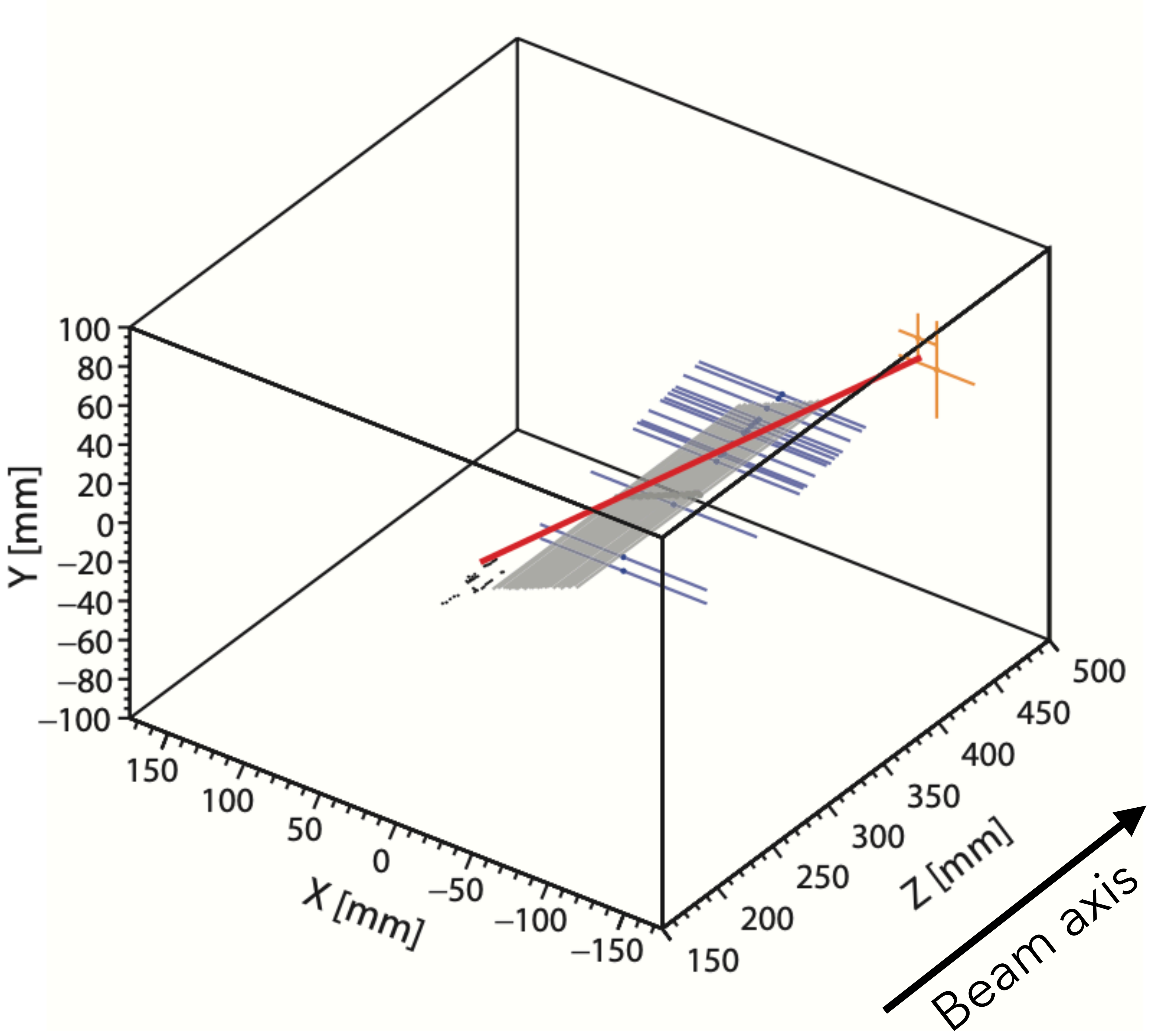

[mm]

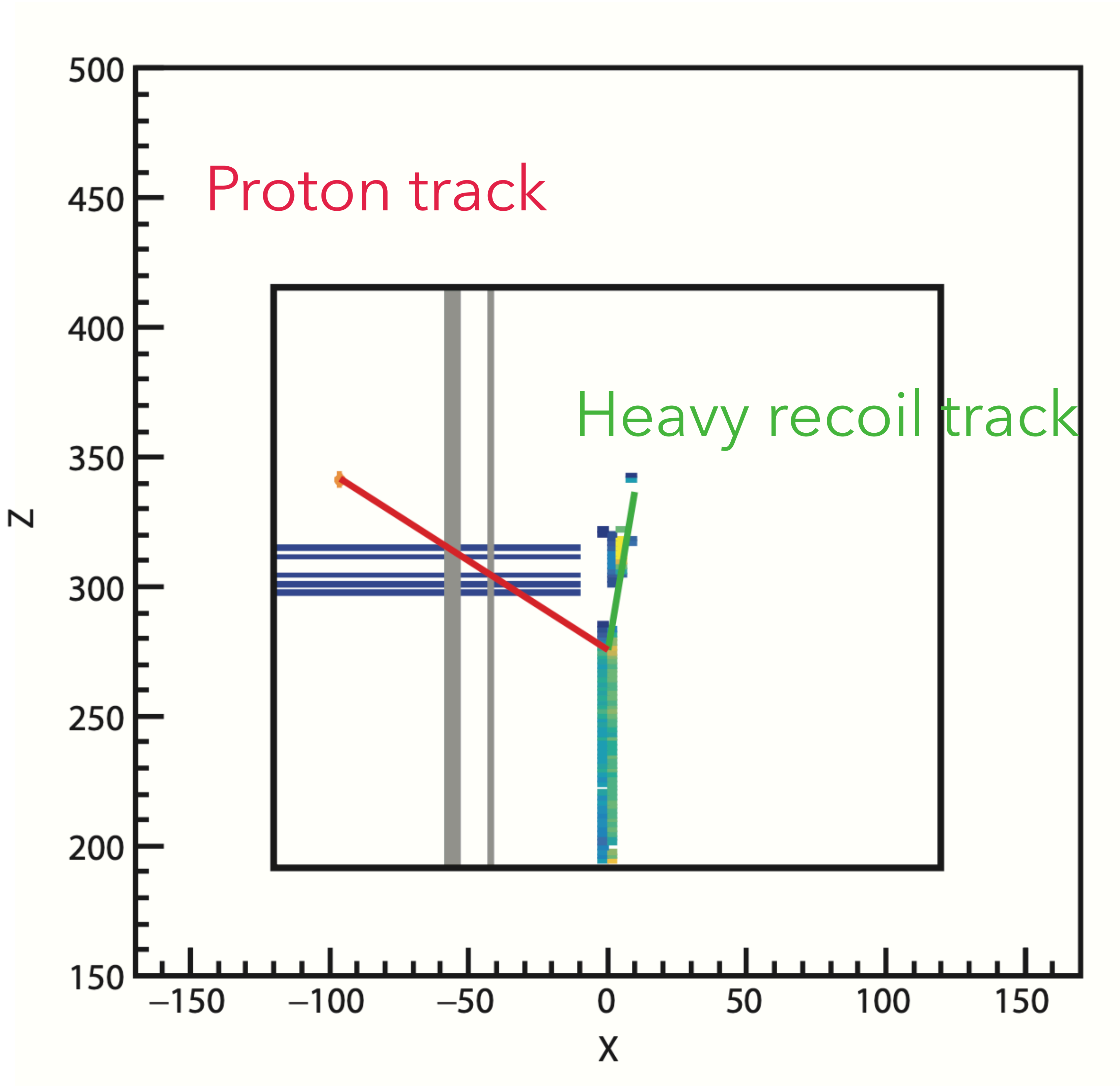

Reaction Identification

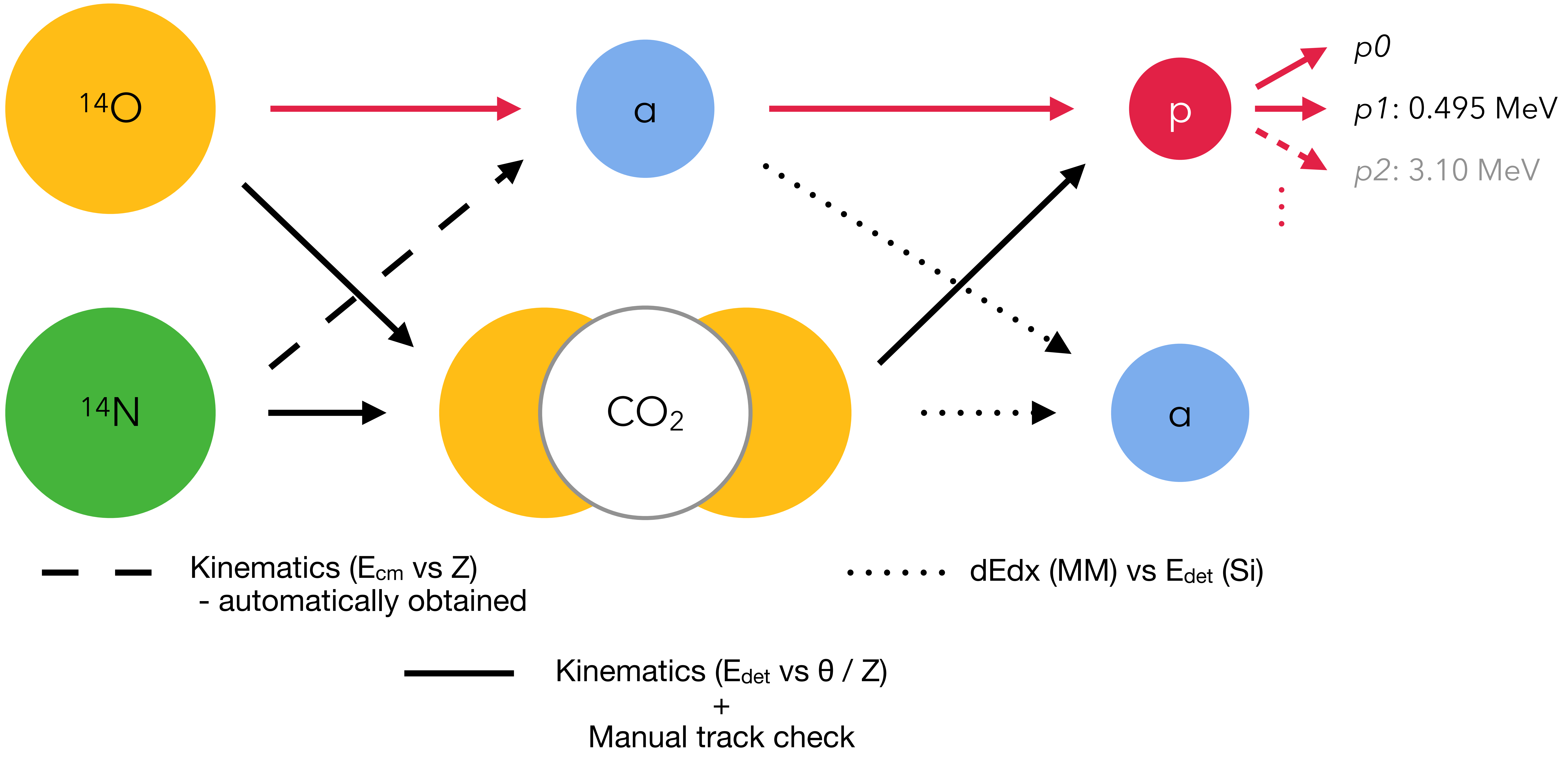

Reaction Identification

- Standard energy loss technique

dE/dx vs E_{det} → proton / alpha

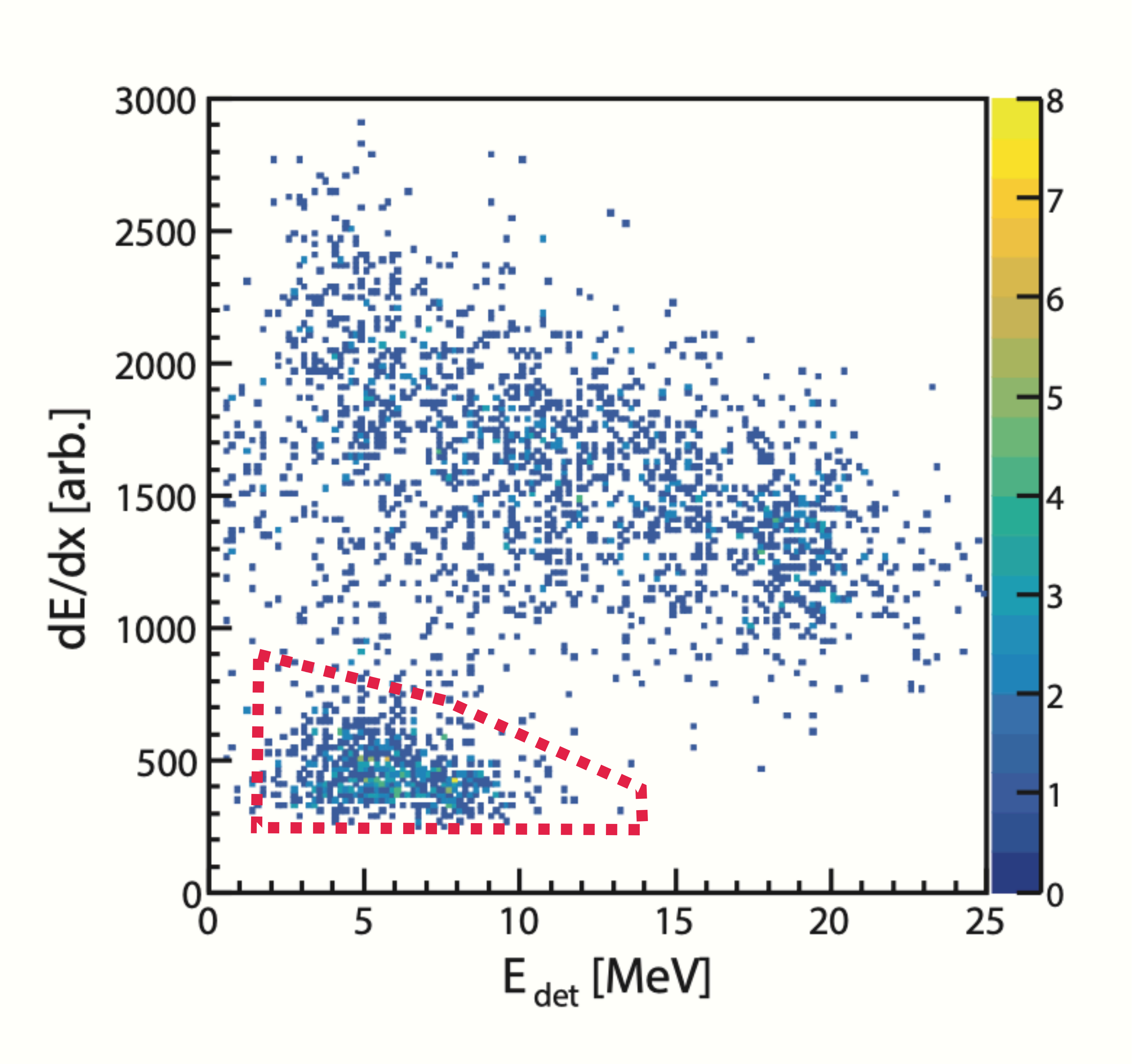

- Kinematics

Convensional TTIK analysis

: assume *p0*

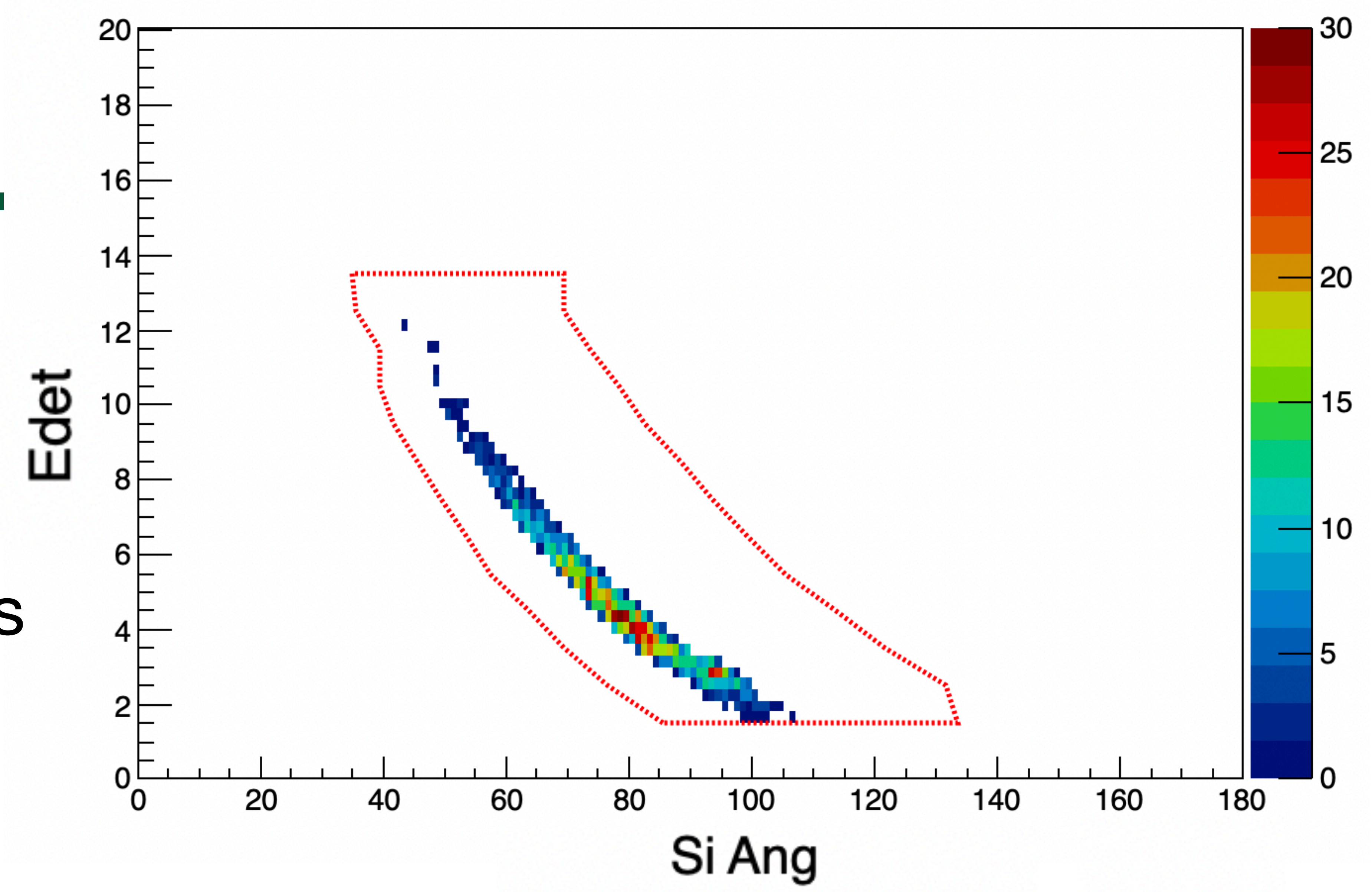

Active target TPC analysis

: Z, θ from track

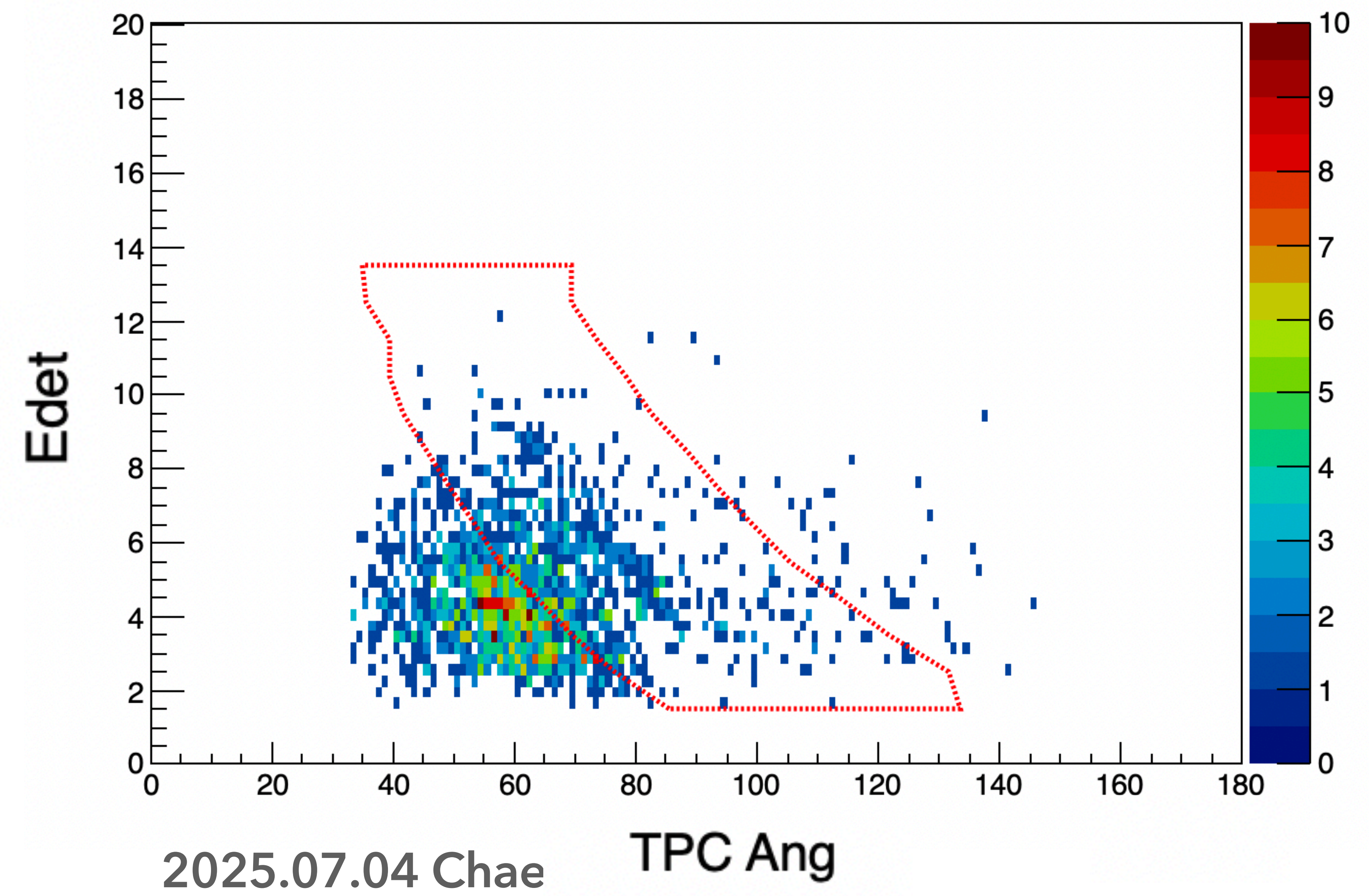

Yield

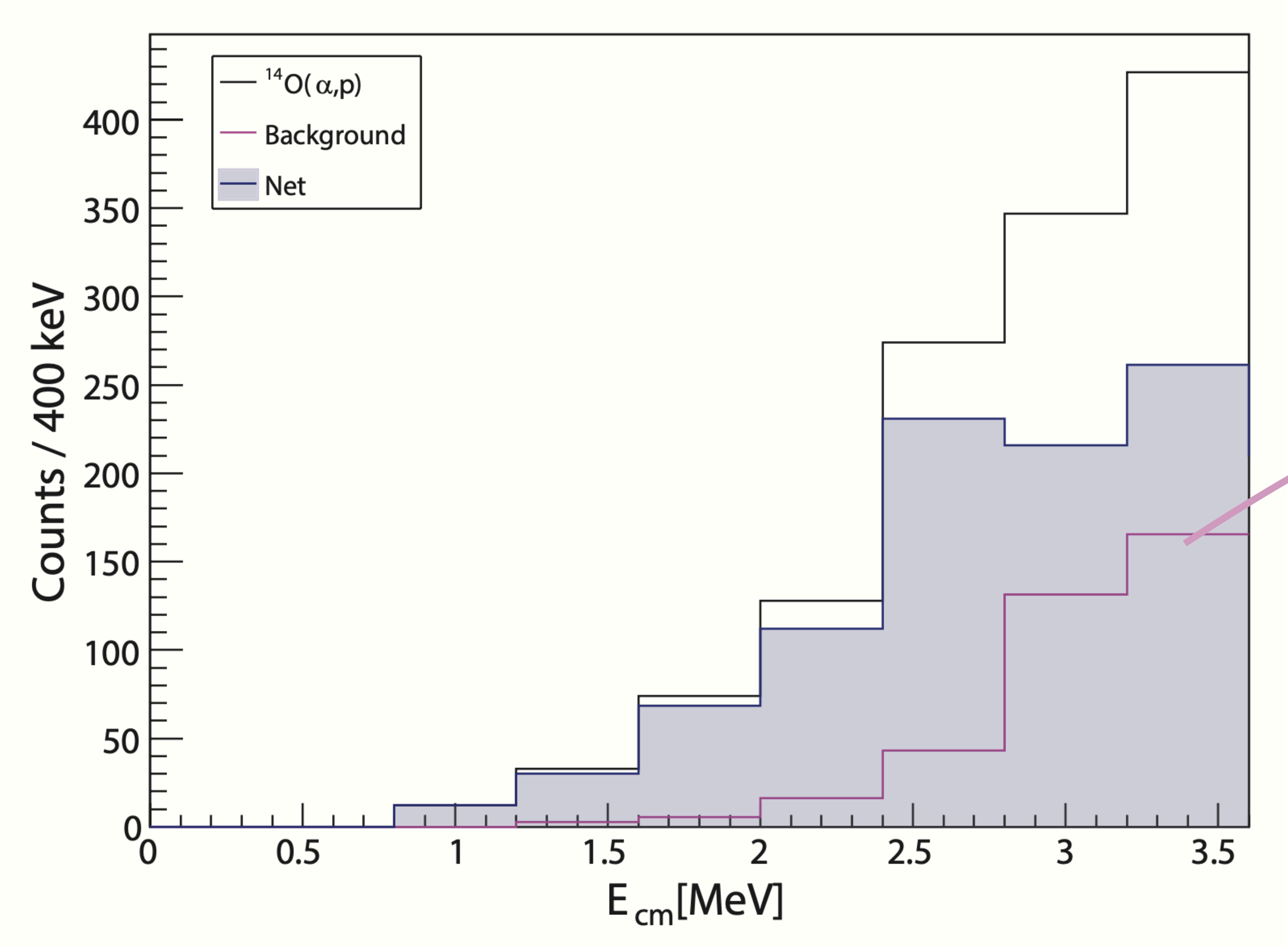

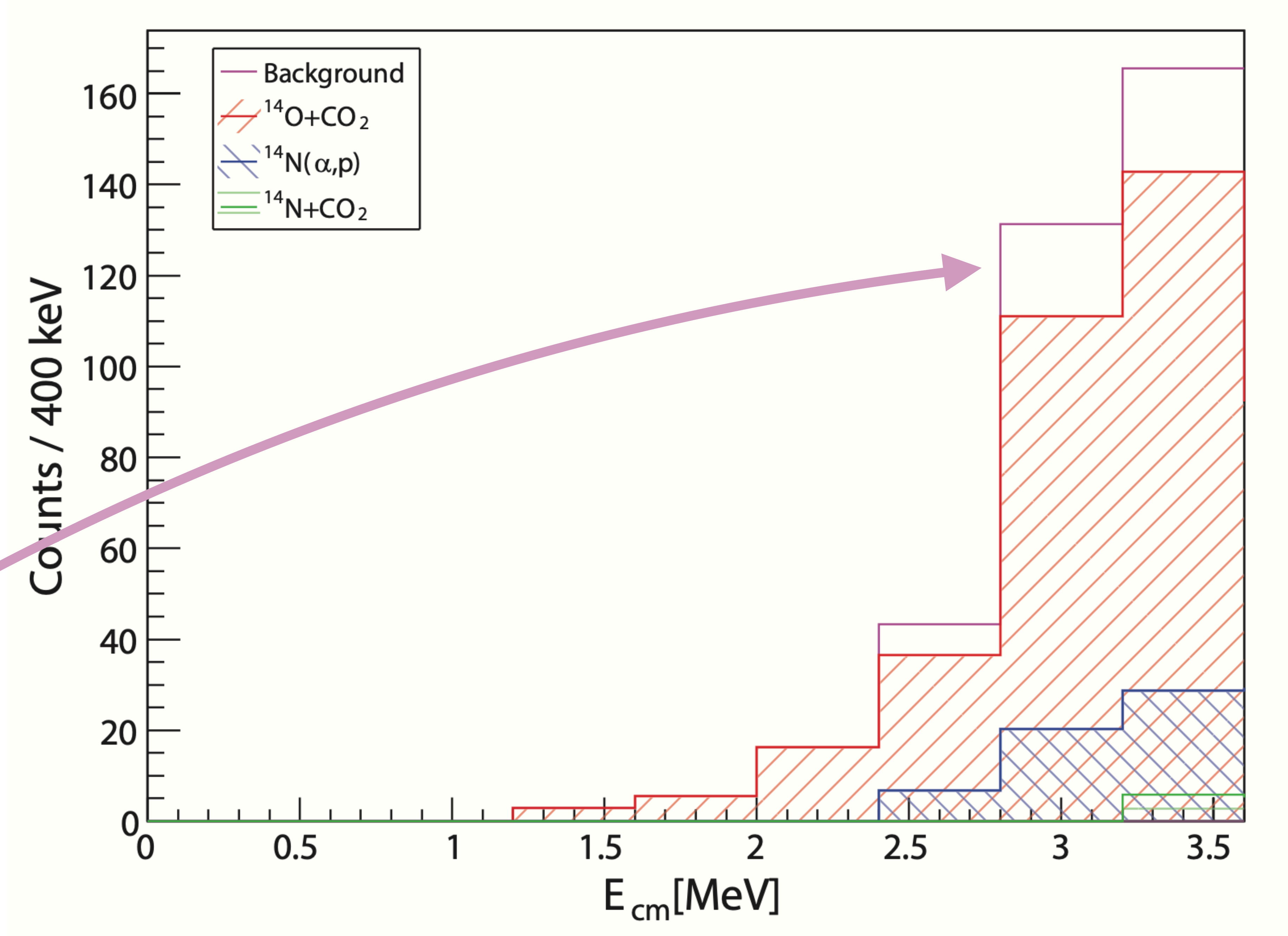

Backgrounds

Excitation Function

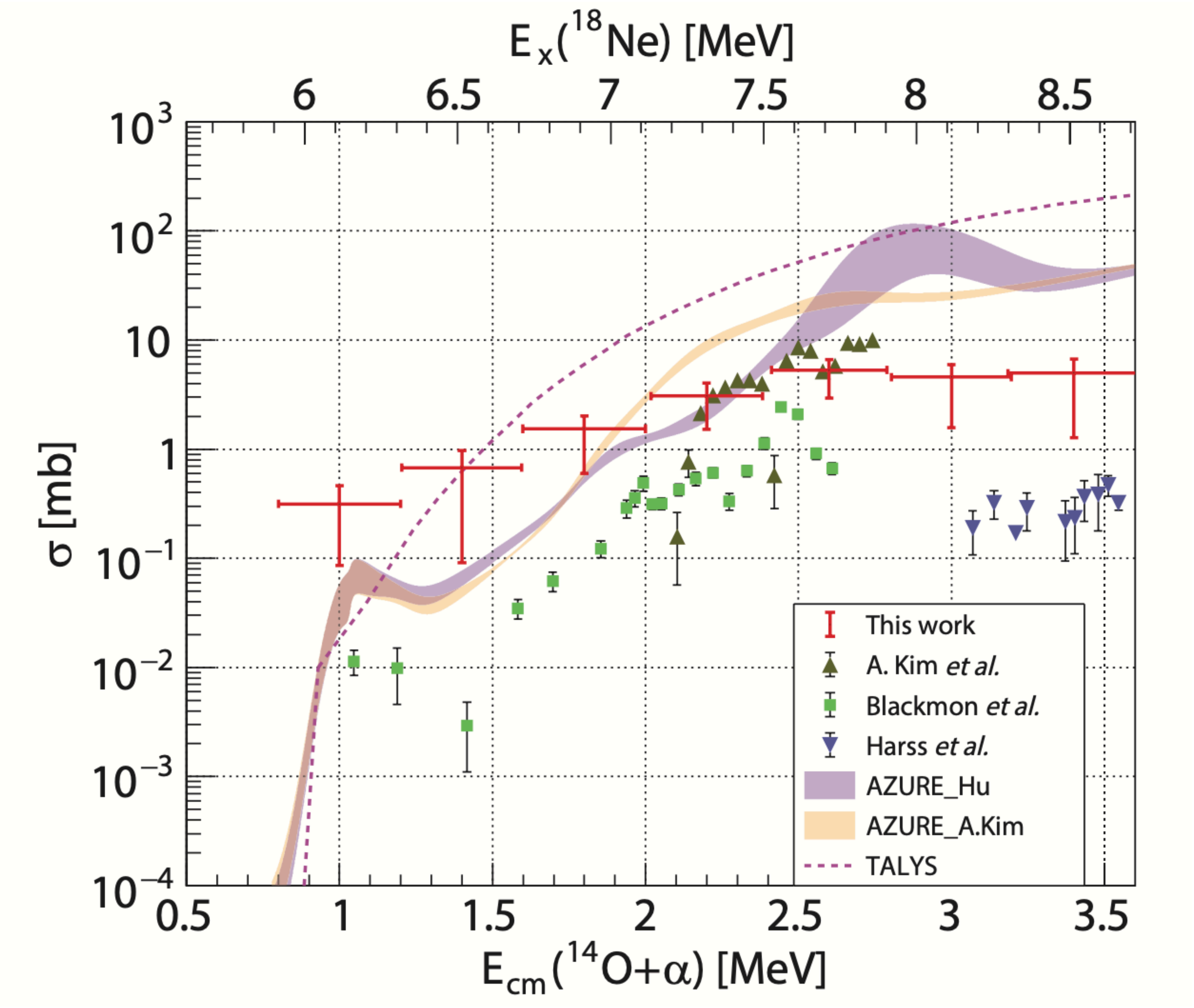

- 2 - 2.4 MeV
  Shows good agreement
- 1 - 1.5 MeV
  Higher cross sections than others
  → contributions from new resonances or the restricted resolution at low energies
- 2.8 MeV -
  Lower cross sections than AZURE

Summary

- A direct measurement of the $^{14}O(\alpha,p)^{17}F$ cross section was performed at CRIB, CNS, due to its significance in Type I X-ray bursts and the current lack of precise data.
- TexAT_v2, a type of active target TPC upgraded from CENS, is utilized.
- A task-based analysis toolkit, LILAK, was developed and implemented.
- Events from $^{14}O(\alpha,p)$ reactions are selected using energy loss and kinematic calculations.
- The cross section is calculated using the yield from each detector and the beam analysis.

- The astrophysical implications of the $^{14}O(\alpha,p)$ reaction, based on the cross section derived from this research, will be studied.

Collaborator List

CENS	S. Ahn, S. Bae, S.M. Cha, K. I. Hahn, D. Kim, Y.H. Kim, J.W. Lee, B. Moon, X. Pereira-López				
CNS	T. W. Chillery, S. Hayakawa, N. Imai, N. Kitamura, K. Okawa, H. Yamaguchi, Q. Zhang				
TAMU	M. Barbui, J. Bishop, E. Koshchiy, C. E. Parker, G. V. Rogachev, M. Roosa				
SKKU	K.Y. Chae, G.M. Gu, M.J. Kim, S.H. Kim, C.H. Kim			**Ewha Womans University**	C. Kim
Korea University	S. Do, B. Hong, A. Kim			**TITech**	H. Lee, T. Nakamura
RIKEN Nishina Center	S. Kubono, M. Sasano	**ANL**	M. L. Avila	**Université Libre de Bruxelles**	M. Sferrazza
University of Notre Dame	D. W. Bardayan	**McMaster University**	A. Chen	**Tohoku University**	N. Iwasa
INFN	M. La Cognata	**Van Lang University**	N. N. Duy	**TUNL**	A. Psaltis

Thank you

Back up

A. Kim

Direct measurement @ CRIB

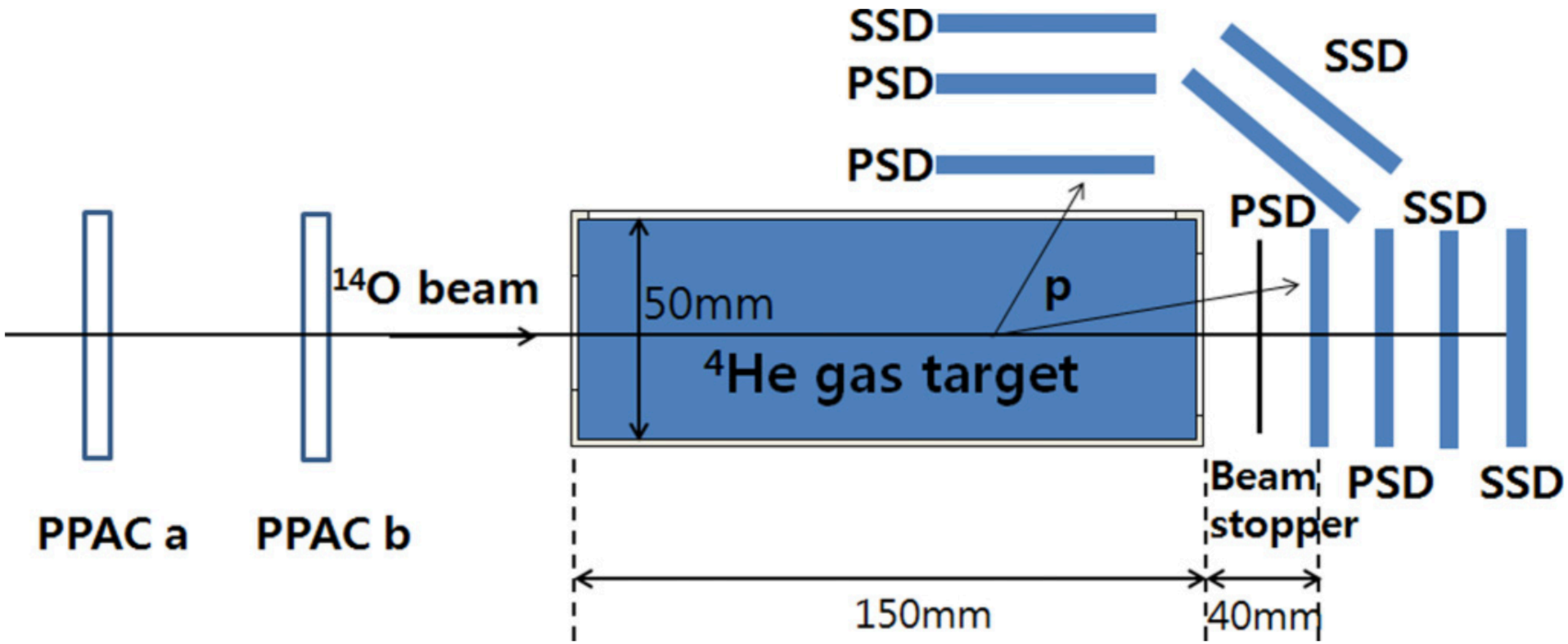

Blackmon

Time-reversal reaction measurement @ HRIBF

17F beam → polypropylene (H) target
Measure alphas in coincidence with 14O recoil

Hu

Proton eleastic scattering @ CRIB

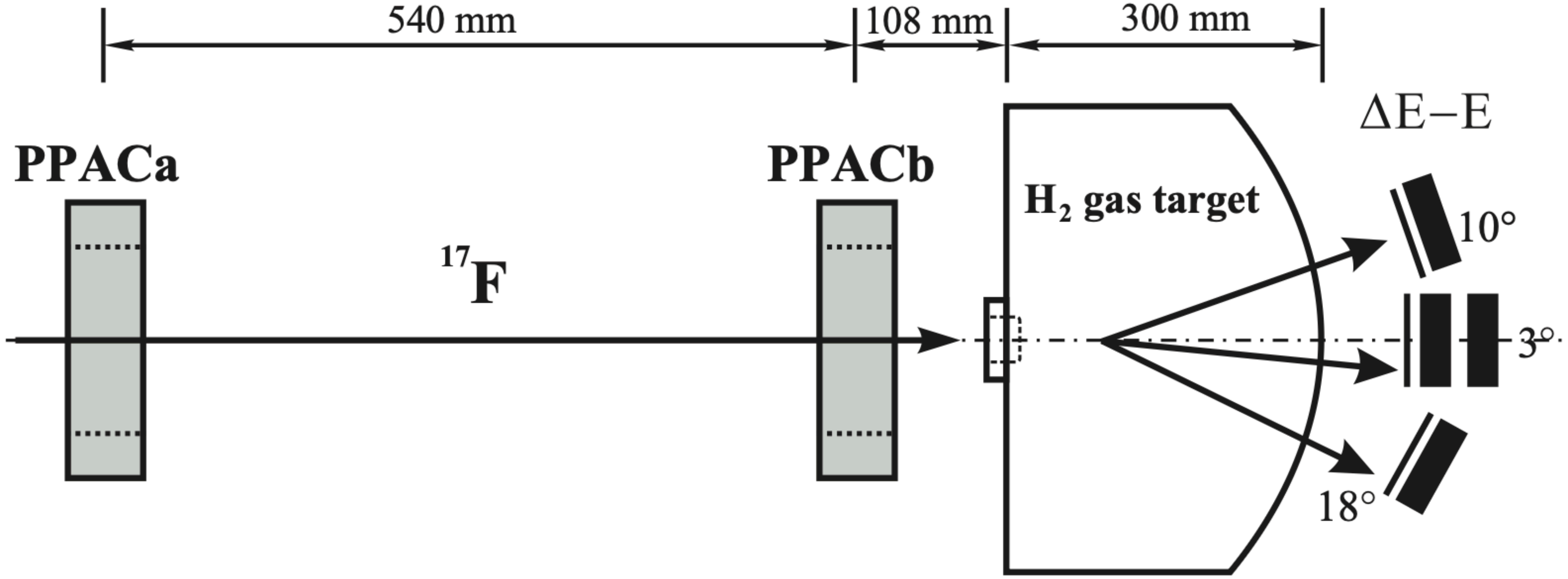

AZURE Calculation

TABLE II. Resonance parameters adopted in the calculation of the $^{14}O(\alpha,p)^{17}F$ reaction rate.

Hu *et al.* (2014)

E_x (MeV)[a]	E_{res} (MeV)[a]	J^π	Γ_α (eV)	Γ_p (keV)	$\Gamma_{p'}$ (keV)	Γ (keV)	$\omega\gamma$ (MeV)
5.153 ± 0.01	0.039	3^-	4.3×10^{-52}[a]	1.7[a]		$\leqslant 15$[a]	3.0×10^{-57}
6.150 ± 0.01	1.036	1^-	3.9 ± 1.0[b]	37.8 ± 1.9[c]	15.9 ± 0.7[c]	53.7 ± 2.0[c]	1.2×10^{-5}
6.286 ± 0.01	1.172	3^-	0.34[a]	20 ± 15[d]		20 ± 15[d]	2.4×10^{-6}
7.05 ± 0.03	1.936	4^+	22.6 ± 3.2[e]	90 ± 40[f]		90 ± 40[f]	2.0×10^{-4}
7.35 ± 0.02	2.236	2^+	40 ± 30[f]	70 ± 60[f]		70 ± 60[f]	2.0×10^{-4}
7.62 ± 0.02	2.506	1^-	1000 ± 120[f]	72 ± 20[f]	<2[f]	75 ± 20[f]	3.0×10^{-3}
7.94 ± 0.01	2.826	3^-	$(11 \pm 6.6) \times 10^3$[g]	35 ± 15[g]	9.0 ± 5.6[g]	55 ± 20[g]	6.2×10^{-2}
8.11 ± 0.01	2.996	3^-	$(6.3 \pm 3.9) \times 10^3$[g]	20 ± 4[g]	4 ± 3[g]	30[a]	3.5×10^{-2}

[a]From Hahn *et al.* [25]. $^{16}O(^3He,n)\,^{18}Ne$, $^{12}C(^{12}C,^6He)\,^{18}Ne$, and $^{20}Ne(p,t)\,^{18}Ne$ reactions

[b]From Fortune [68]. $^{14}C(^6Li,d)^{18}O$

[c]From Bardayan *et al.* [37]. $^{17}F(p,p')^{17}F^*$

[d]From present work. elastic scattering of $^{17}F+p$

[e]From Fortune [40]. Reexamine Almaraz-Calderon

[f]From Harss *et al.* [35]. $p(^{17}F,\alpha)^{14}O$

[g]From Almaraz-Calderon *et al.* [39]. $^{16}O(^3He,n)$

Wiescher *et al.* [1] assigned $J^\pi = 5^-$ to this level on the basis of mirror states in ^{18}O. Hahn *et al.* [2] observed such a level at $E_x = 8.11 \pm 0.10$ with $\Gamma \leqslant 30$ keV. We measured

Wiescher *et al.* [1] adopted a state at $E_x = 7.915$ MeV as $J^\pi = 1^-$. Hahn *et al.* [2] reported this level at $E_x = 7.92 \pm 0.02$ MeV with $\Gamma = 70 \pm 20$ keV via the $^{20}Ne(p,t)$ reaction and at $E_x = 7.94 \pm 0.01$ MeV with $\Gamma = 40 \pm 10$ keV via the $^{16}O(^3He,n)$ reaction. We adopted the average of their

E_{cm} Calculation

$$M_1c^2 + E_1 + M_2c^2 = M_3c^2 + E_3 + M_4c^2 + E_4$$ (Energy conservation)

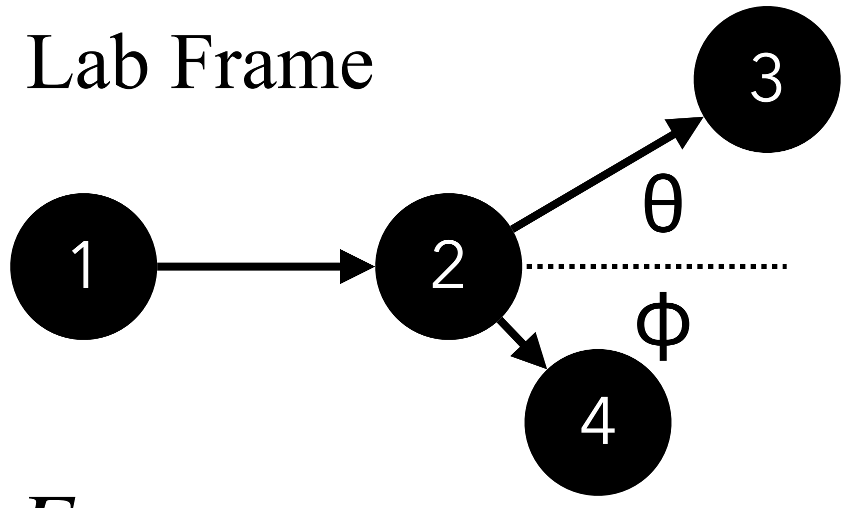

$$\sqrt{2M_1E_1} = \sqrt{2M_3E_3}\ cos\theta + \sqrt{2M_4E_4}\ cos\phi$$
$$0 = \sqrt{2M_3E_3}\ sin\theta - \sqrt{2M_4E_4}\ sin\phi$$

(Momentum conservation)

$$\rightarrow M_1E_1 + M_3E_3 - 2\sqrt{M_1M_3E_1E_3}\ cos\theta = M_4E_4$$

$$Q = E_3 - E_1 + \frac{1}{M_4}\ [M_1E_1 + M_3E_3 - 2\sqrt{M_1M_3E_1E_3}\ cos\theta]$$

$$\underbrace{(M_4 - M_1)}_{a}E_1 + 2\ \underbrace{cos\theta\sqrt{M_1M_3E_3}}_{b'}\sqrt{E_1} + \underbrace{[M_4Q - (M_3 + M_4)\ E_3]}_{c} = 0$$

$$\sqrt{E_1} = \frac{-b' + \sqrt{b'^2 - ac}}{a}$$ (∵ Positive, Real)

$$E_{CM} = E_1\ \frac{M_2}{M_1 + M_2}$$

Forward Detector Array

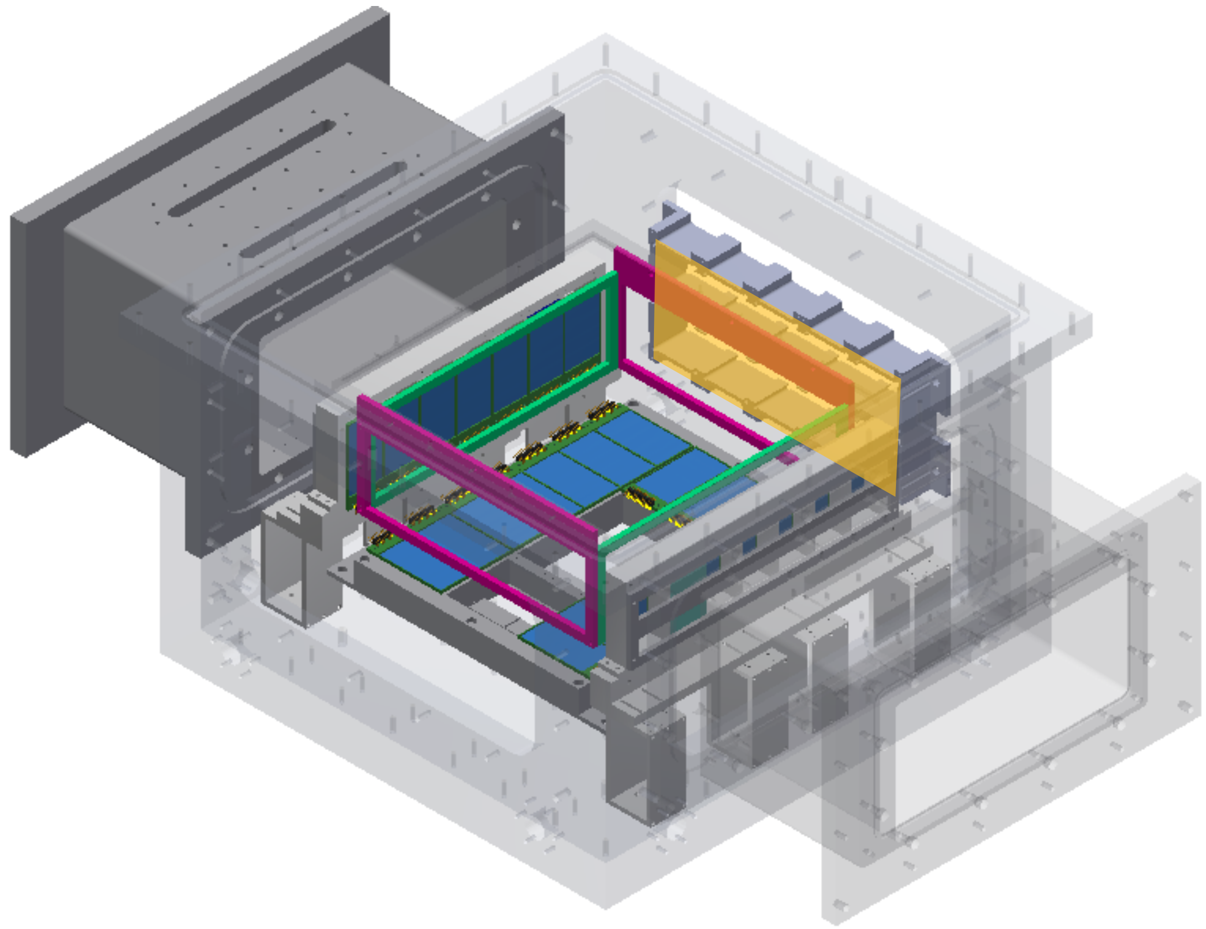

- Measuring charged particles (i.e. proton, α, …)
- Si (50 × 50 mm^2) + CsI(Tl) (50 × 50 × 40 mm^3) with PIN diode

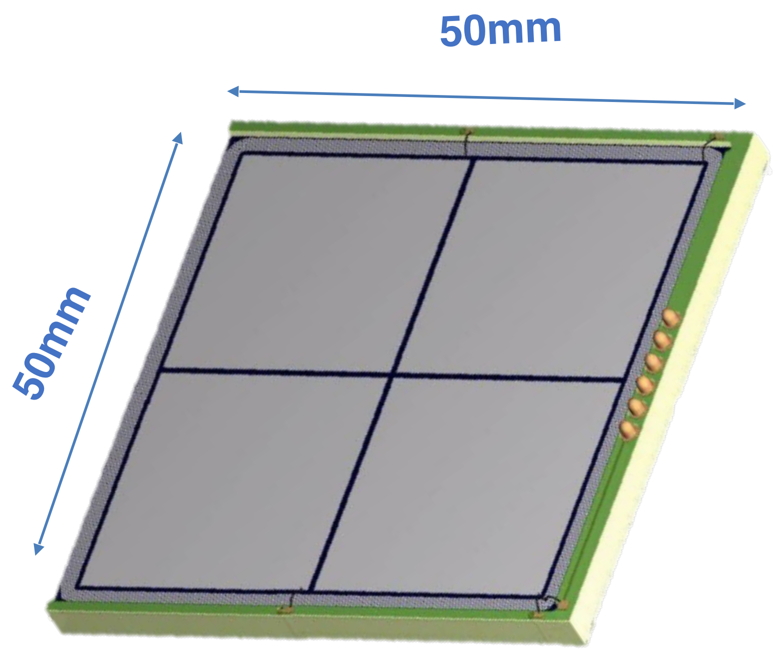

MSQ-25 (TexAT)
forward angle coverage

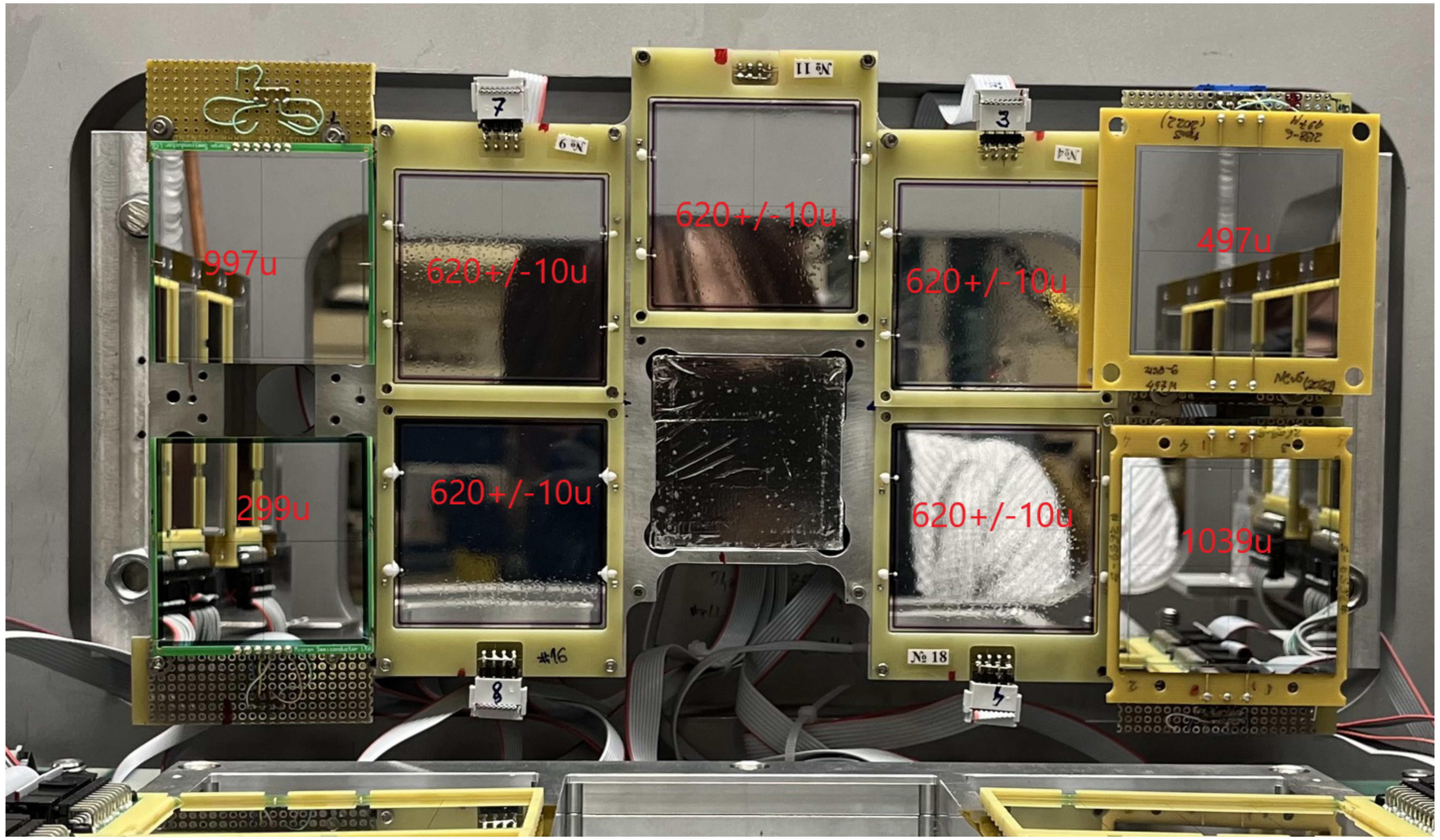

* Punch-through energy
- 300um: 6.109 MeV
- 500um: 8.239 MeV
- 625um: 9.383 MeV
- 1000um: 12.325 MeV

New Detector Arrays

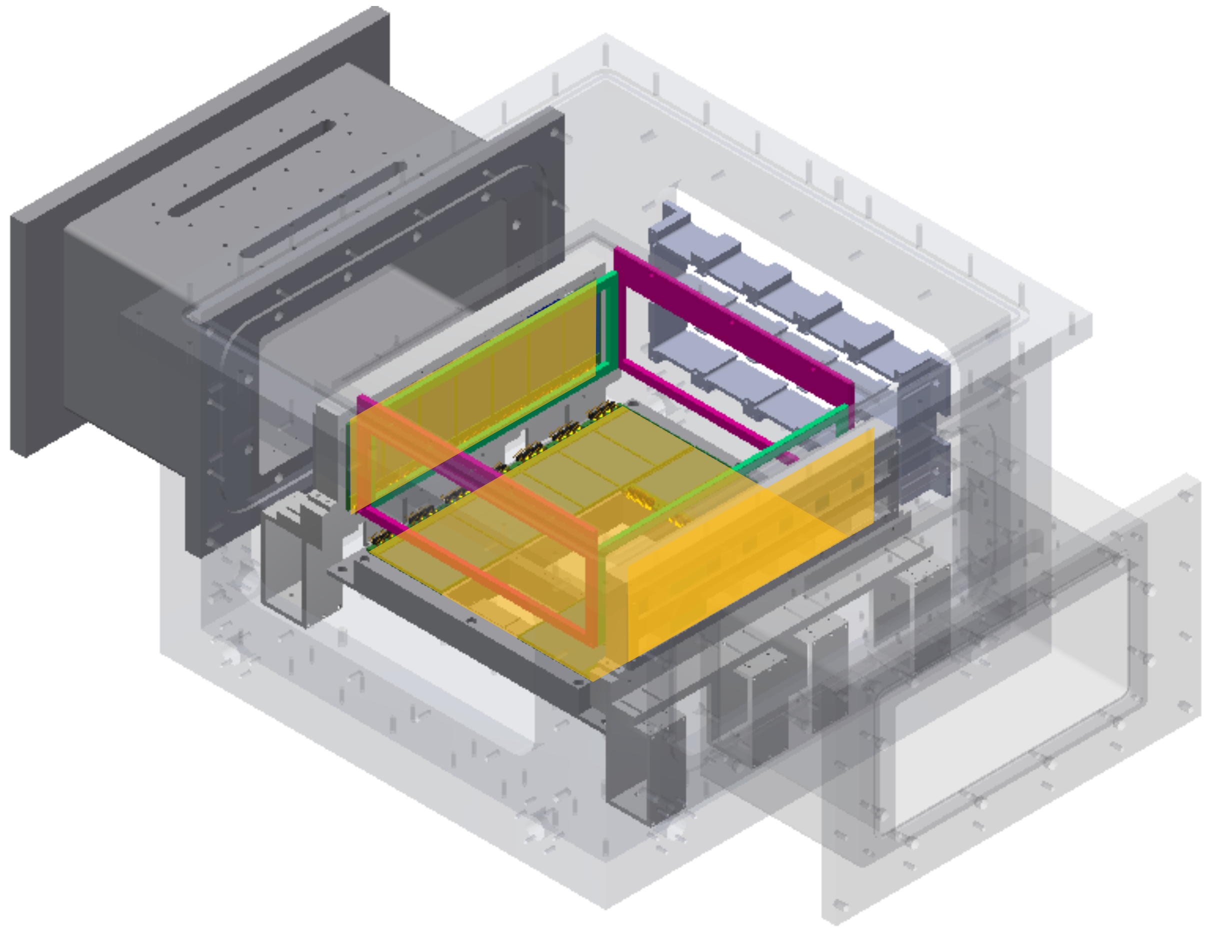

CsI(Tl) + SiPM

X6 detector

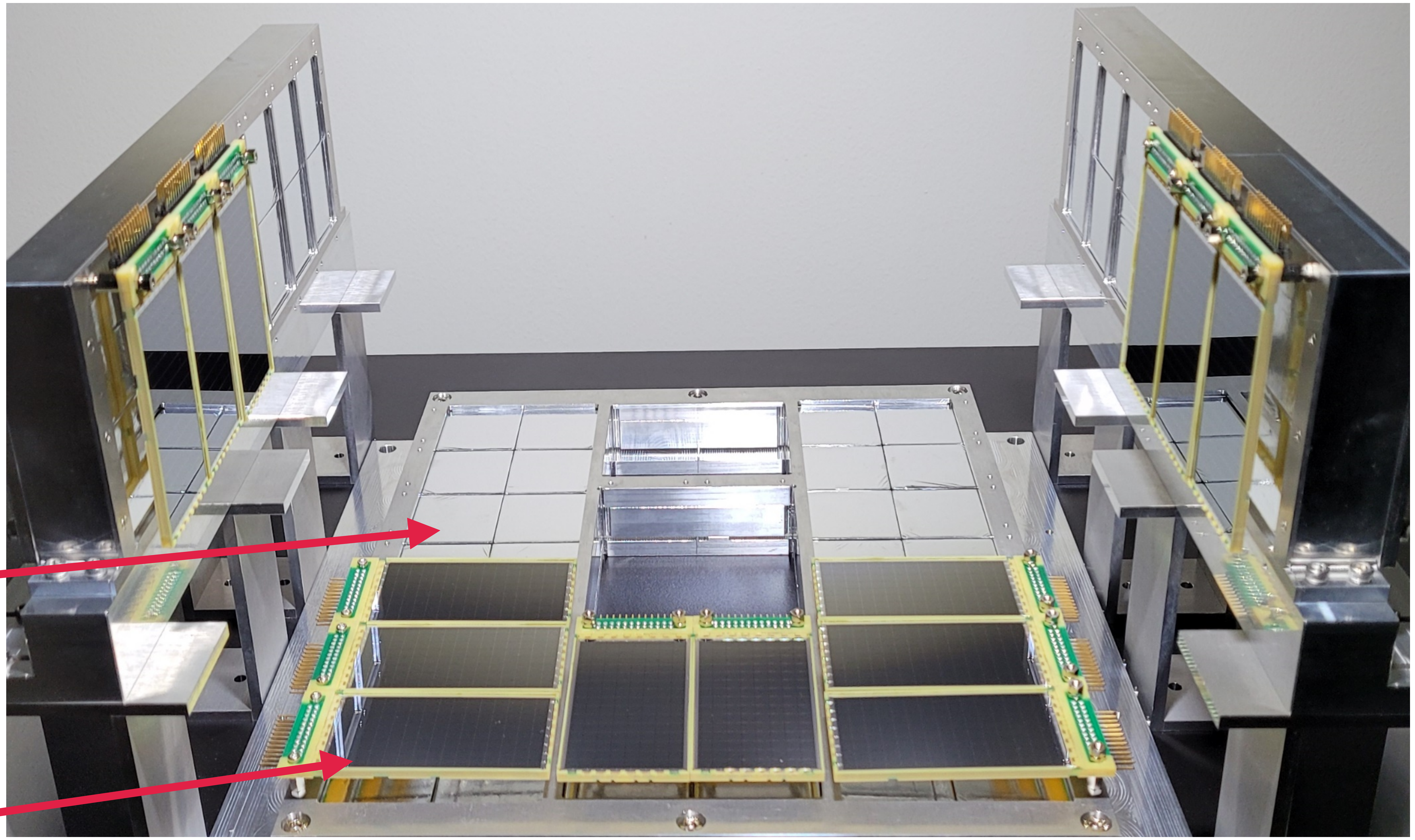

New Detector Arrays: X6

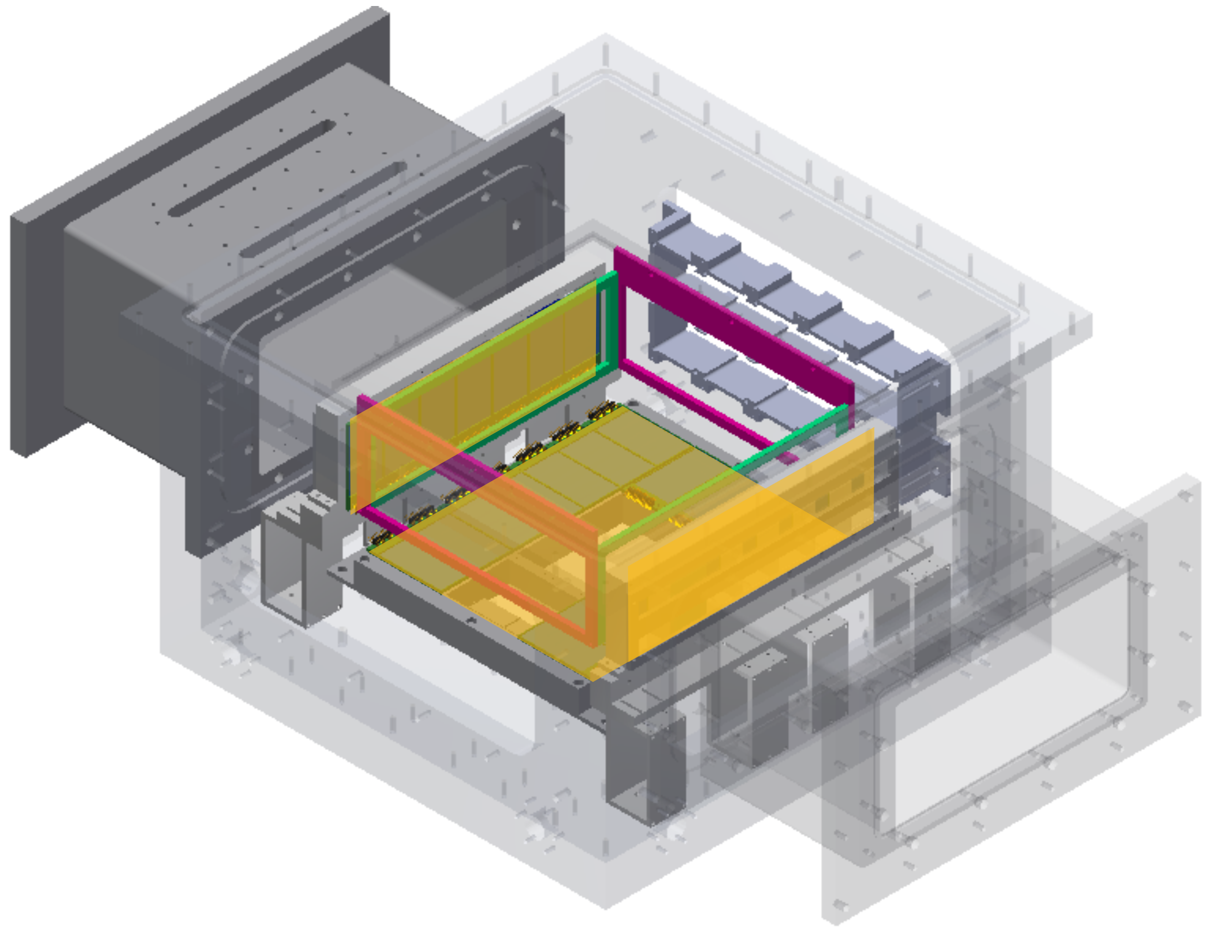

- 8 resistive strips (junction) + 4 non-resistive strips (ohmic)
  → improved position and energy resolution

- Leakage current, depletion voltage and energy & position resolution test
  - ^{241}Am is used as radiation source (5.5 MeV α particle) for position resolution, and Δp < 1 mm are identified
  - Energy recorded with a 4-alpha source , and resolution was measured < 70 keV ΔE/E ~ 1% (FWHM, junction)

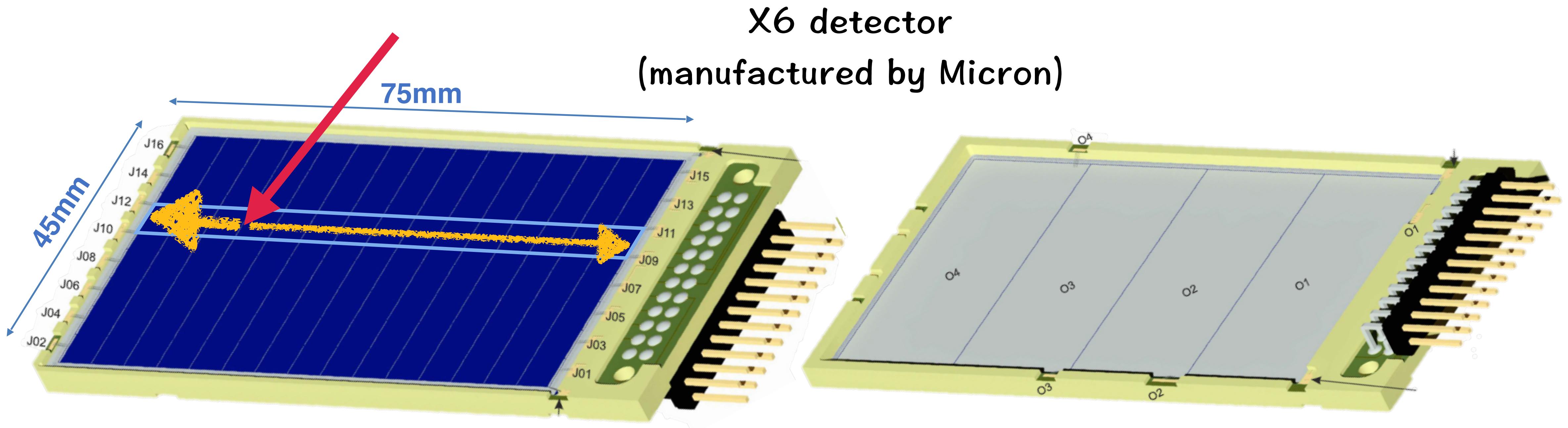

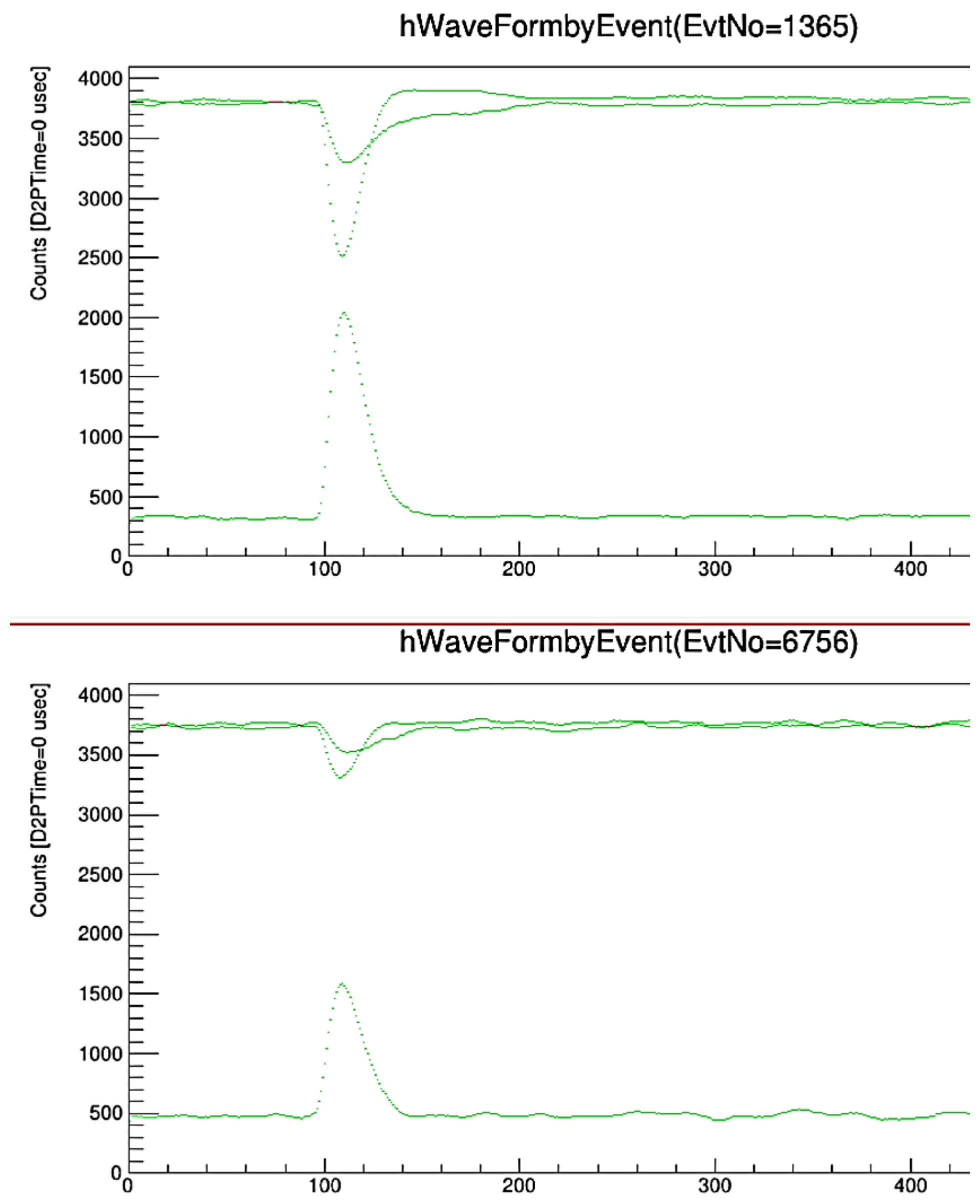

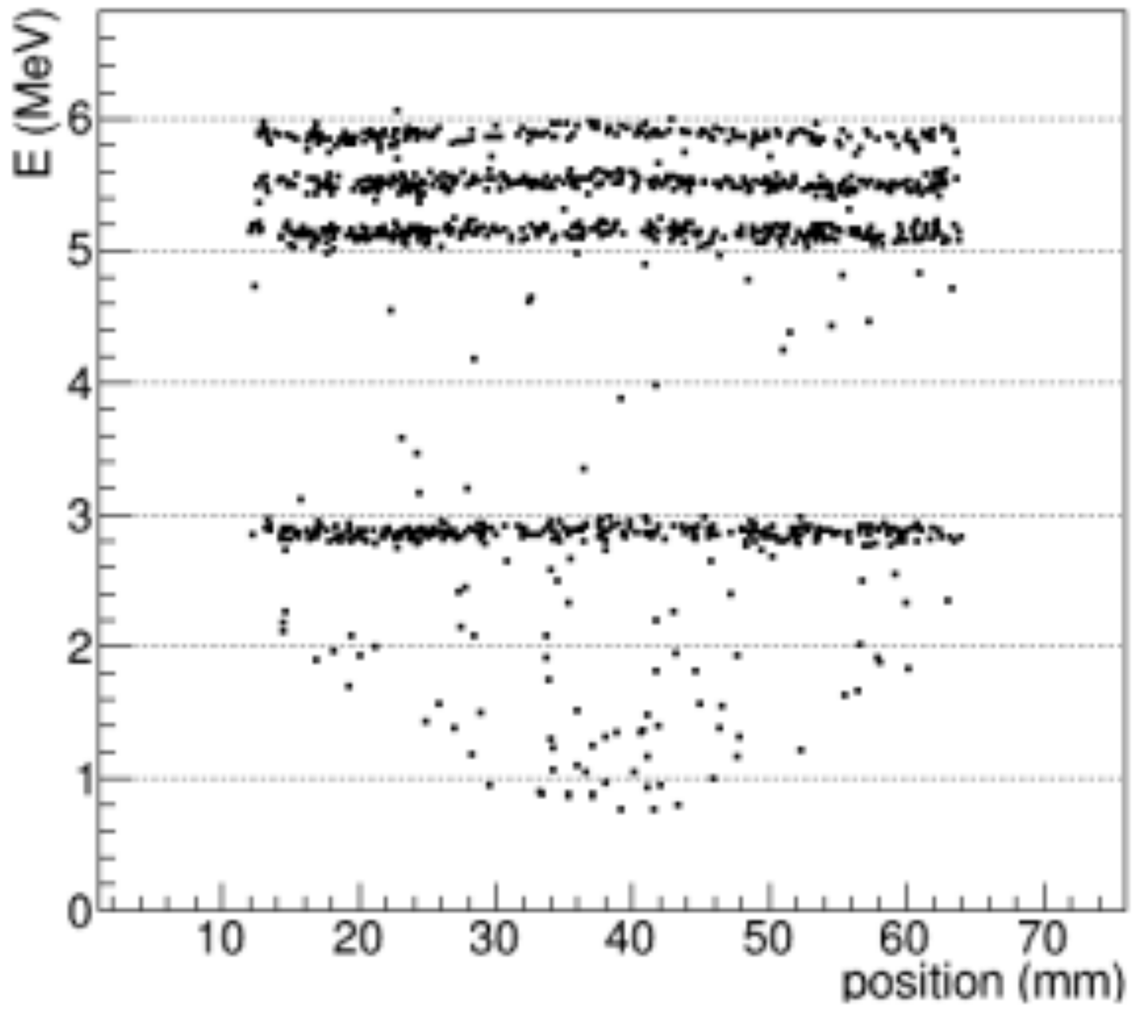

New Detector Arrays: CsI(Tl) + SiPM

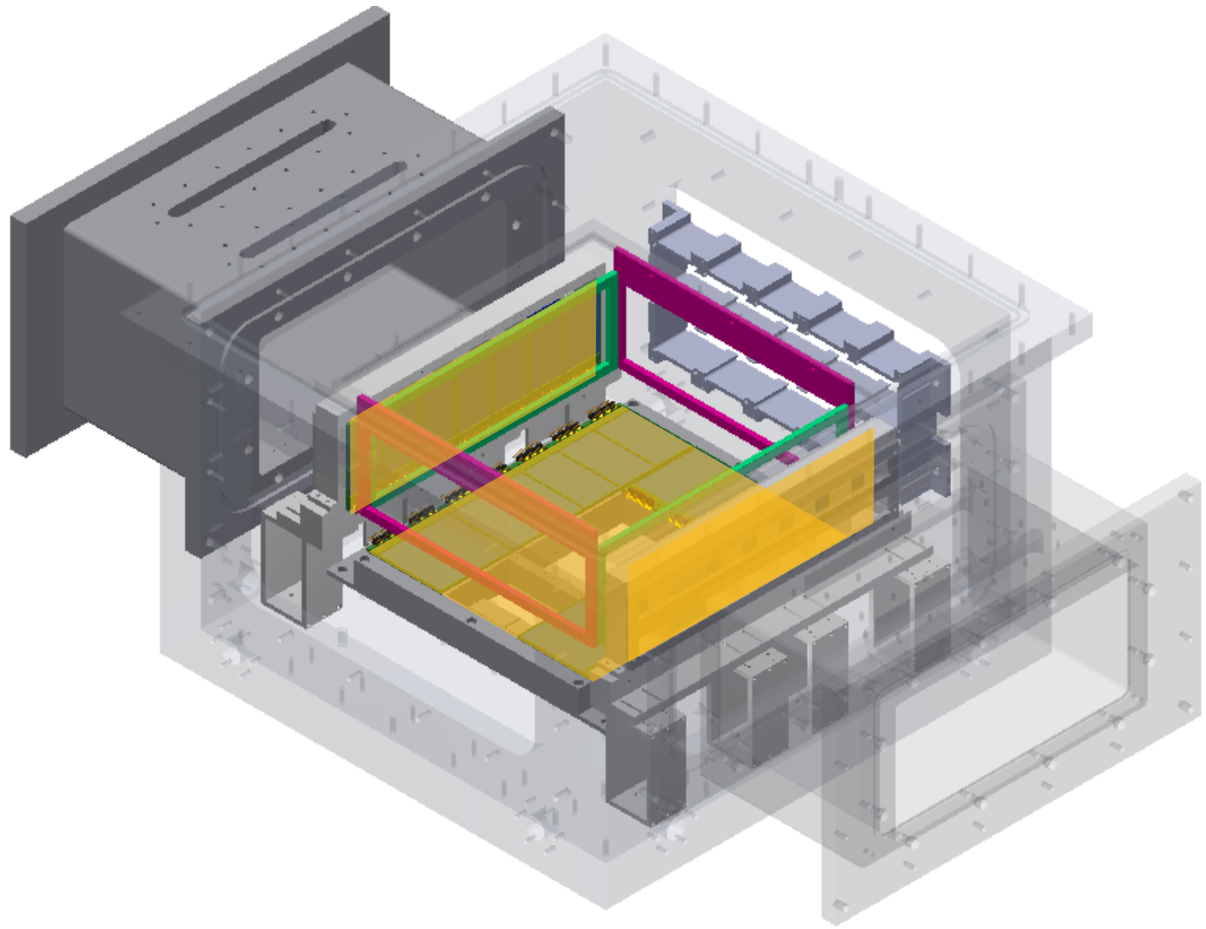

- CsI(Tl) + Silicon photomultiplier (SiPM)
  - short rise time (~0.5μs)
  - large signal height → no preamp for GET
  - sample test done (^{241}Am, ^{137}Cs sources)
  - enhanced energy resolution (6%)

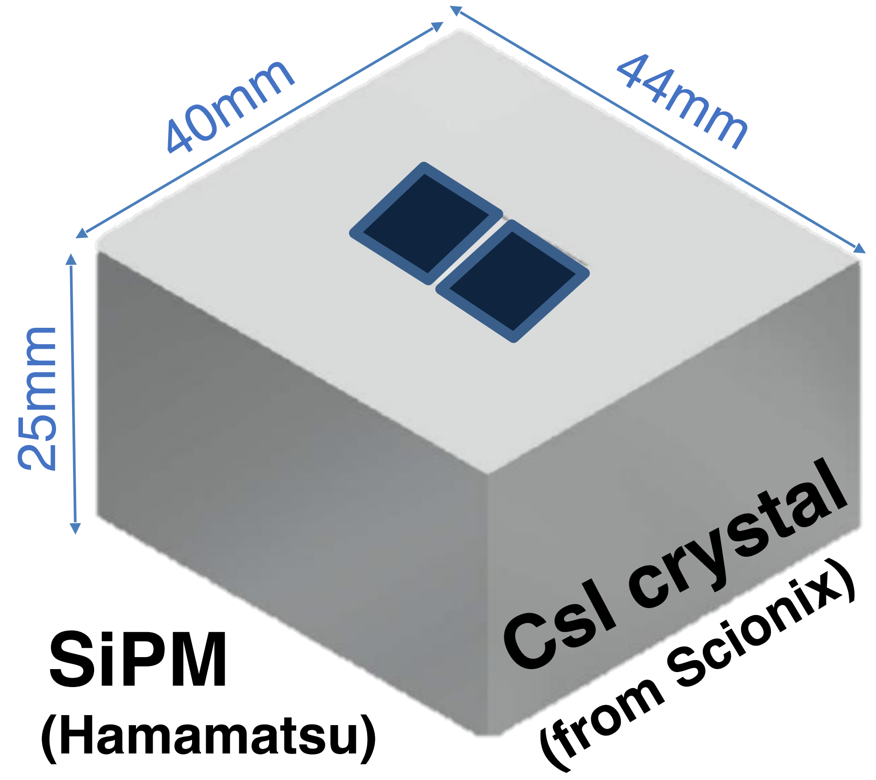

S13360-6050PE
6.0x6.0mm^2 sensitive area
14400 pixels (50um pitch)

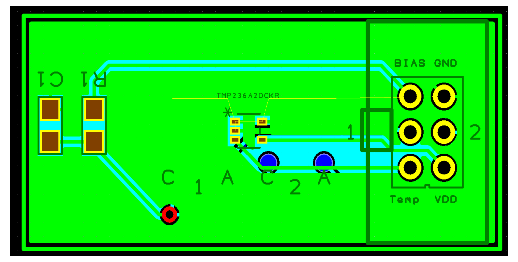

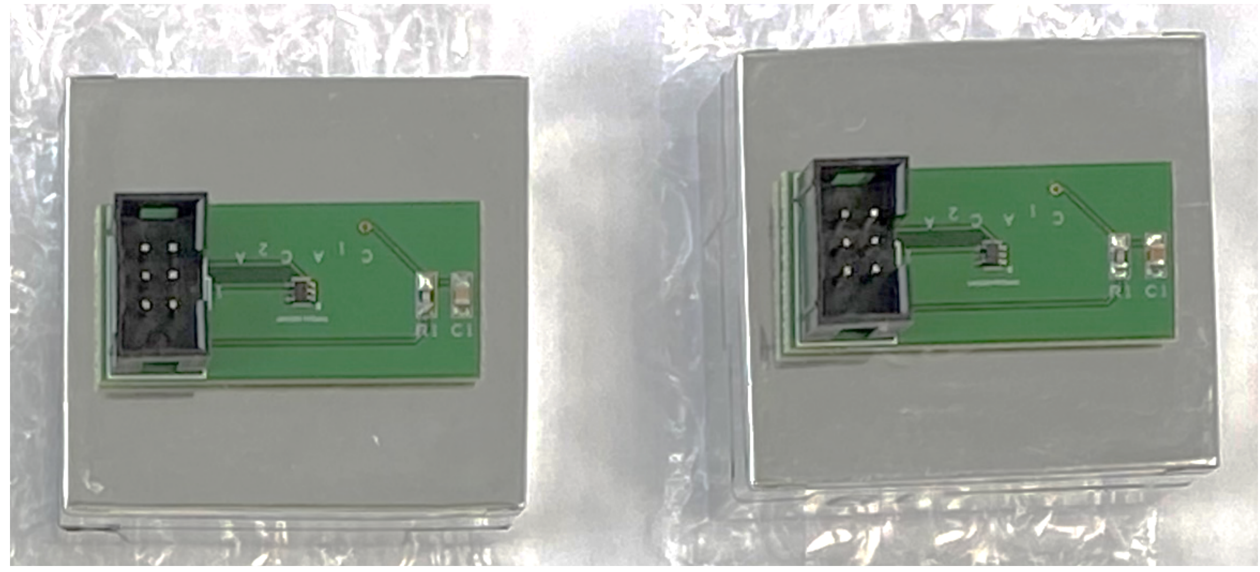

Charge terminator PCB

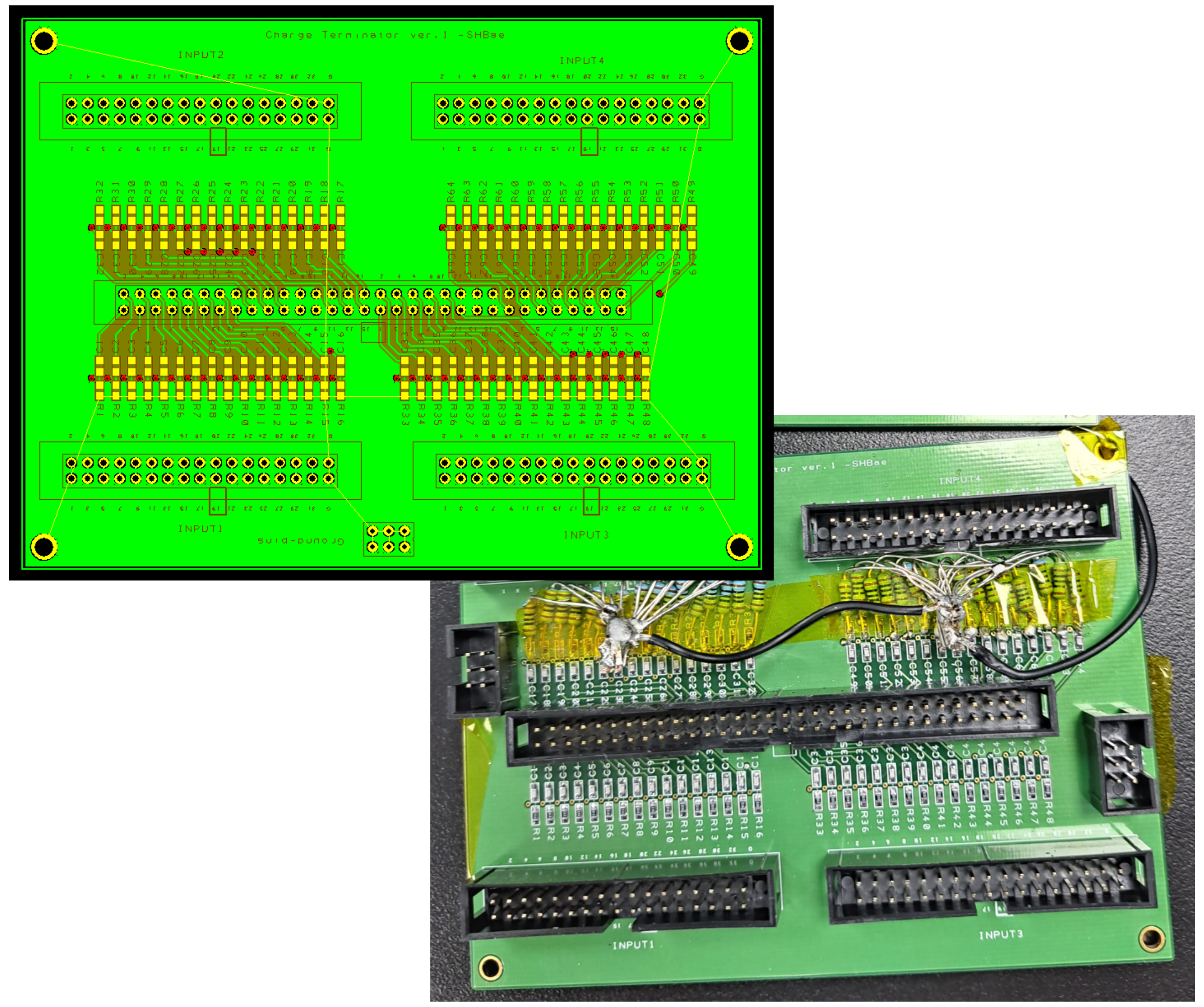

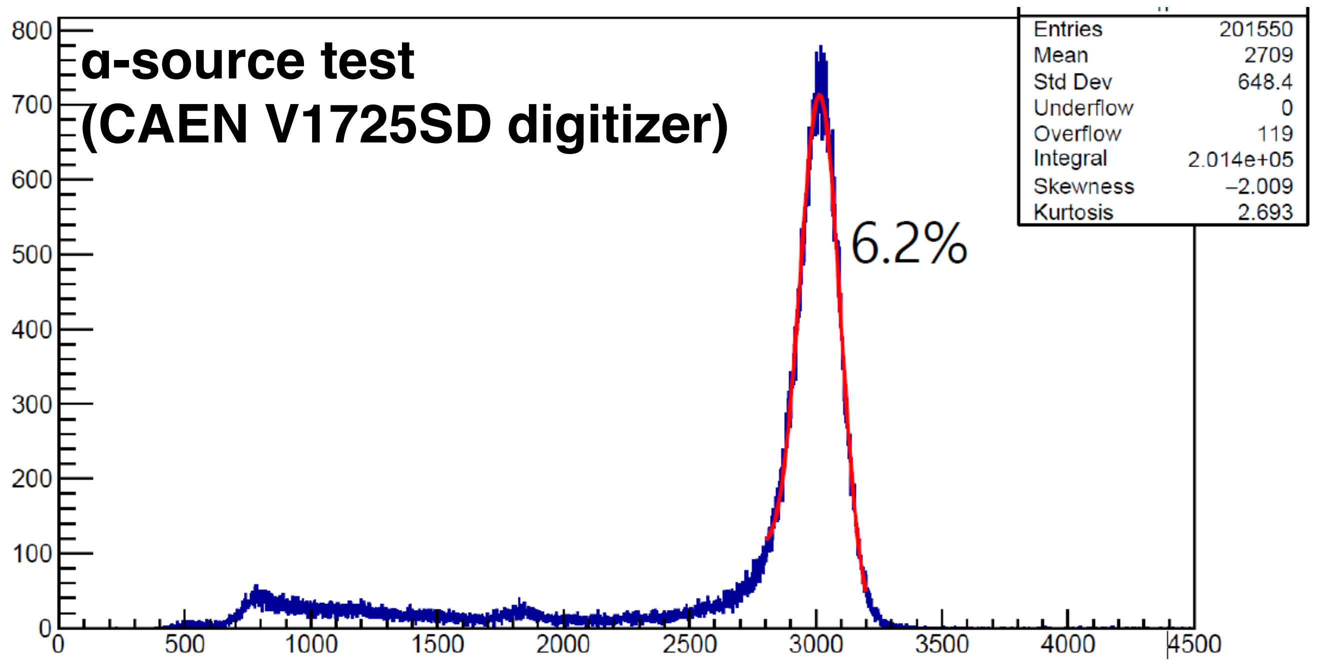

Micromegas

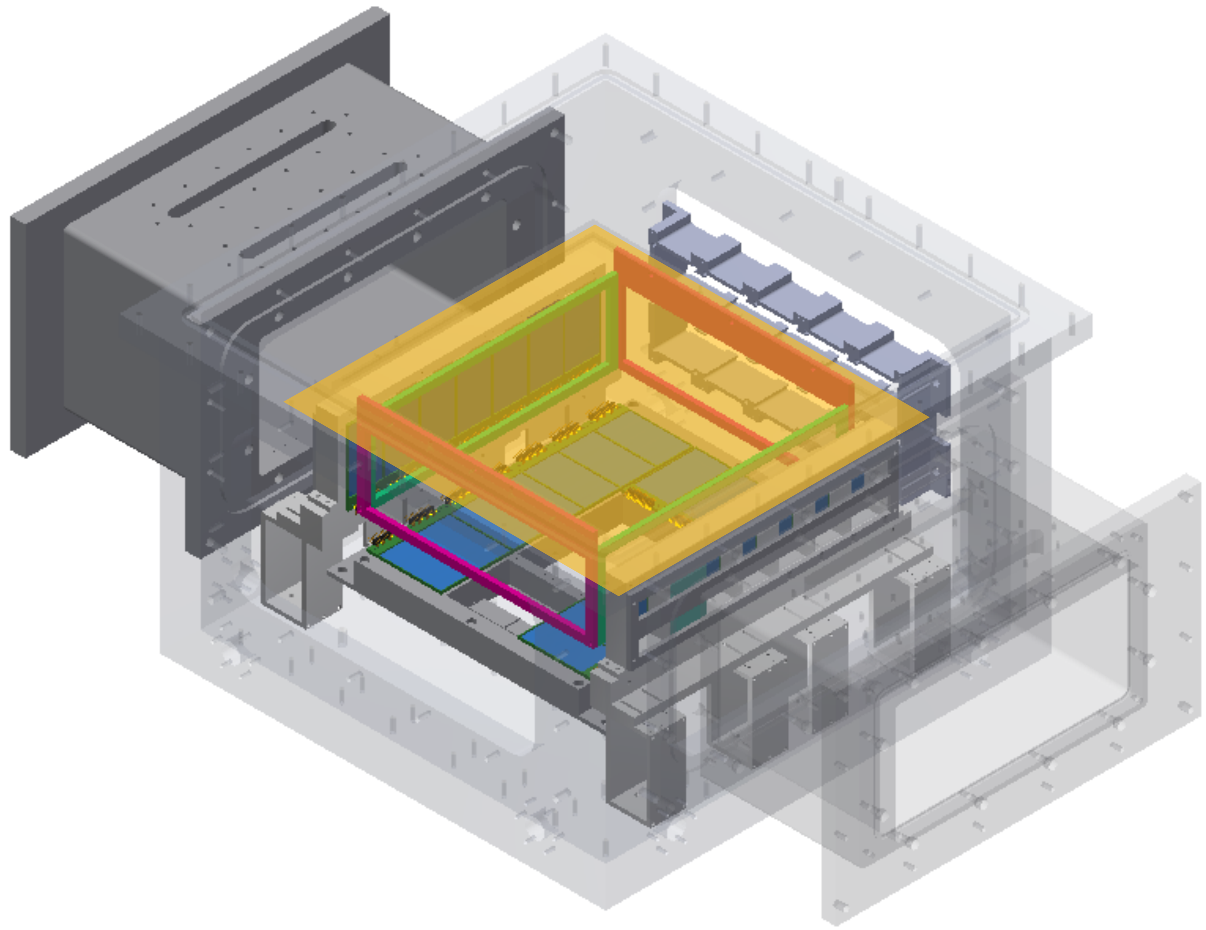

- <u>Mi</u>cro-<u>Me</u>sh <u>Ga</u>seous <u>S</u>tructures
  - Use multiplexing technique for reducing the number of total channels
  - Central region (pixel) + Side region (strip & chain)

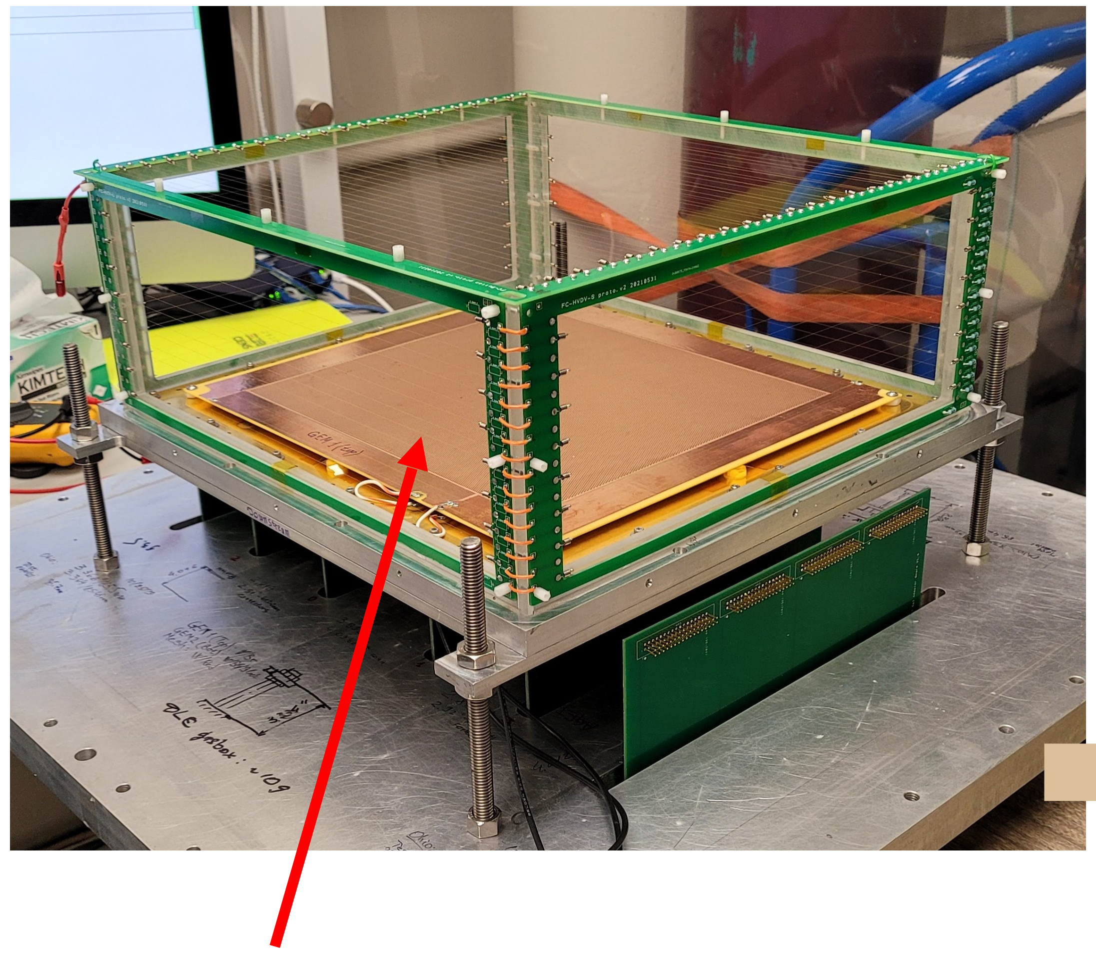

Micromegas +GEM foil

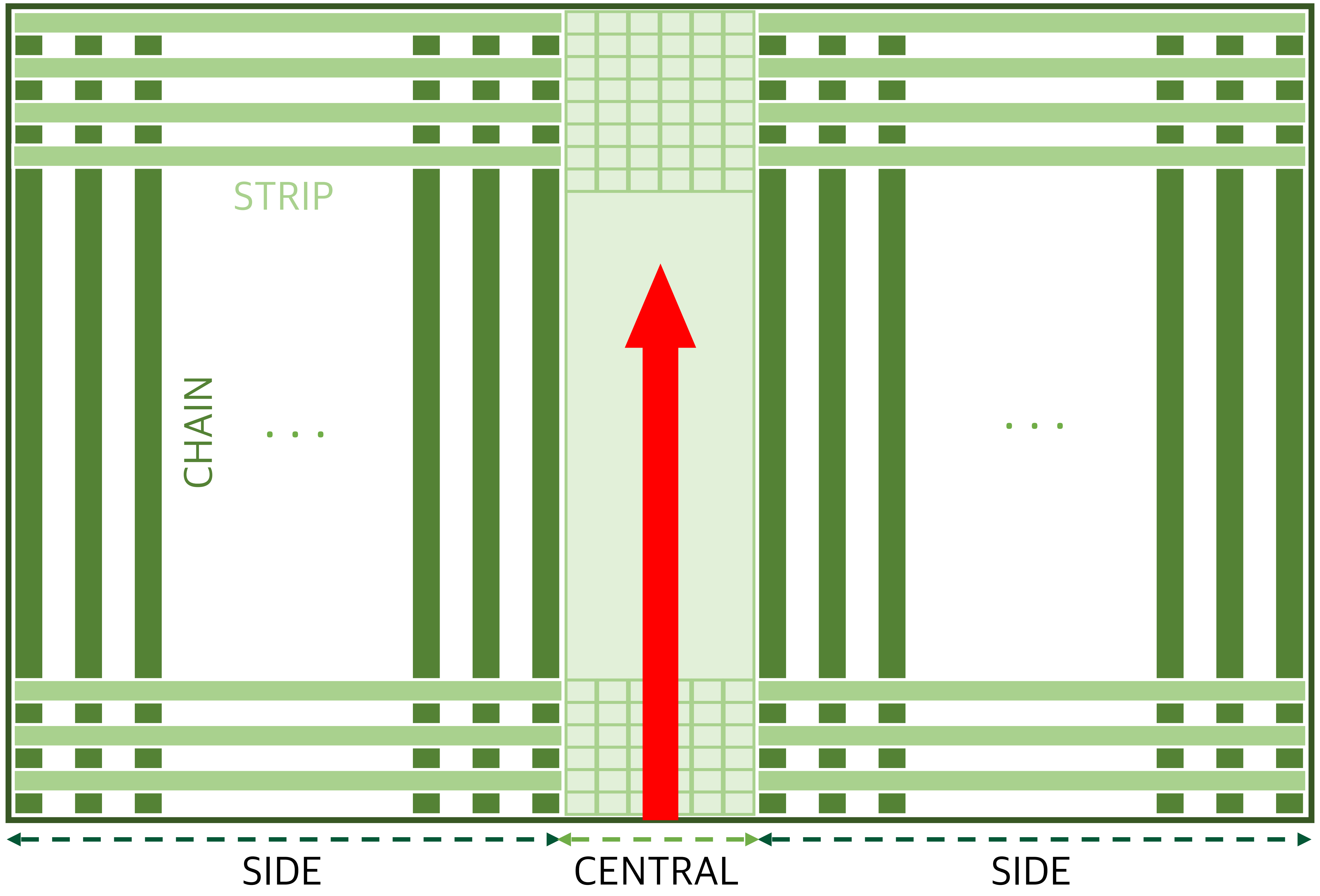

Effect of Gating Grid

Accumulated waveforms from…

The first quarter of Micromegas   The second quarter of Micromegas

Entire: - 260 V
Grid: - 260 V

Entire: - 260 V
Grid: - 230 V

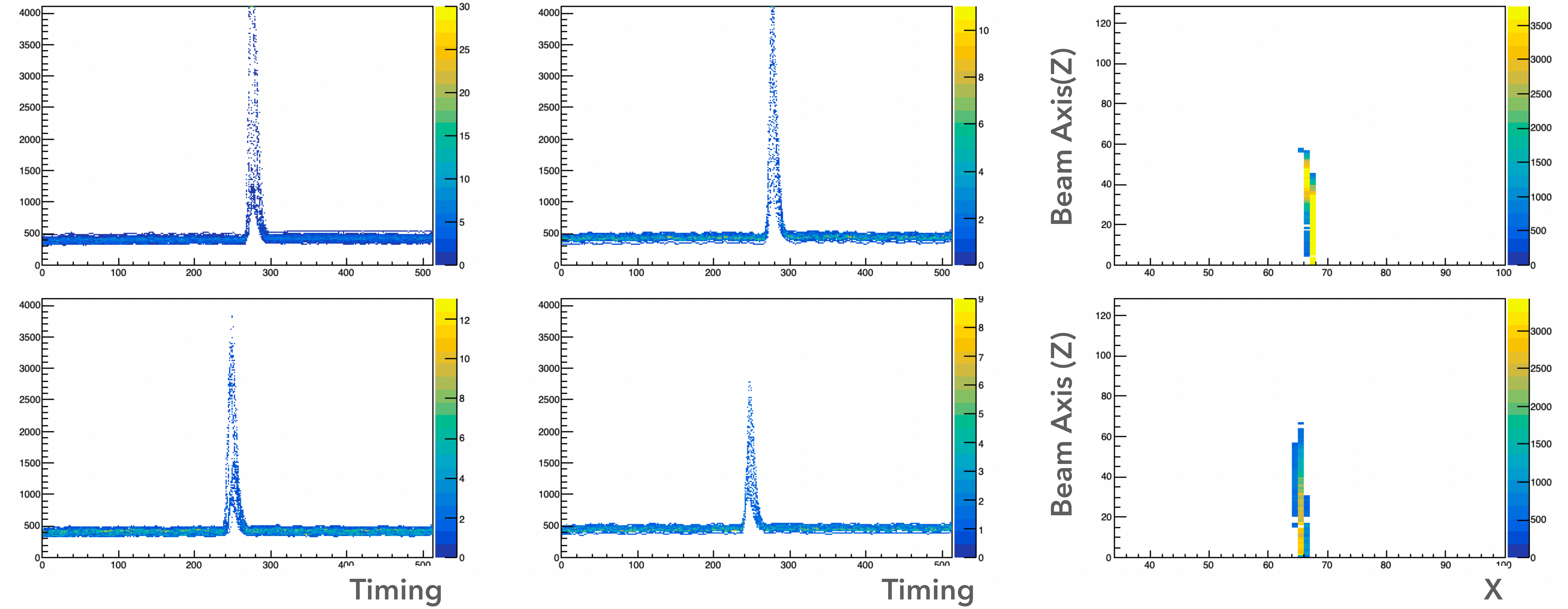

→ Reduce amplitude of beam region signal

PID on Focal Planes

$$\frac{mv^2}{q} = qvB \quad \Rightarrow \quad B\rho = \frac{p}{q} \quad \Rightarrow \quad B\rho = \frac{mv}{q} \propto \frac{A}{q} \cdot \frac{1}{\Delta t}$$

$$\overrightarrow{F} = q(\overrightarrow{E} + \vec{v} \times \overrightarrow{B}) \quad \xrightarrow{\overrightarrow{F} = 0} \quad v = \frac{E}{B}$$

Hough Transformation

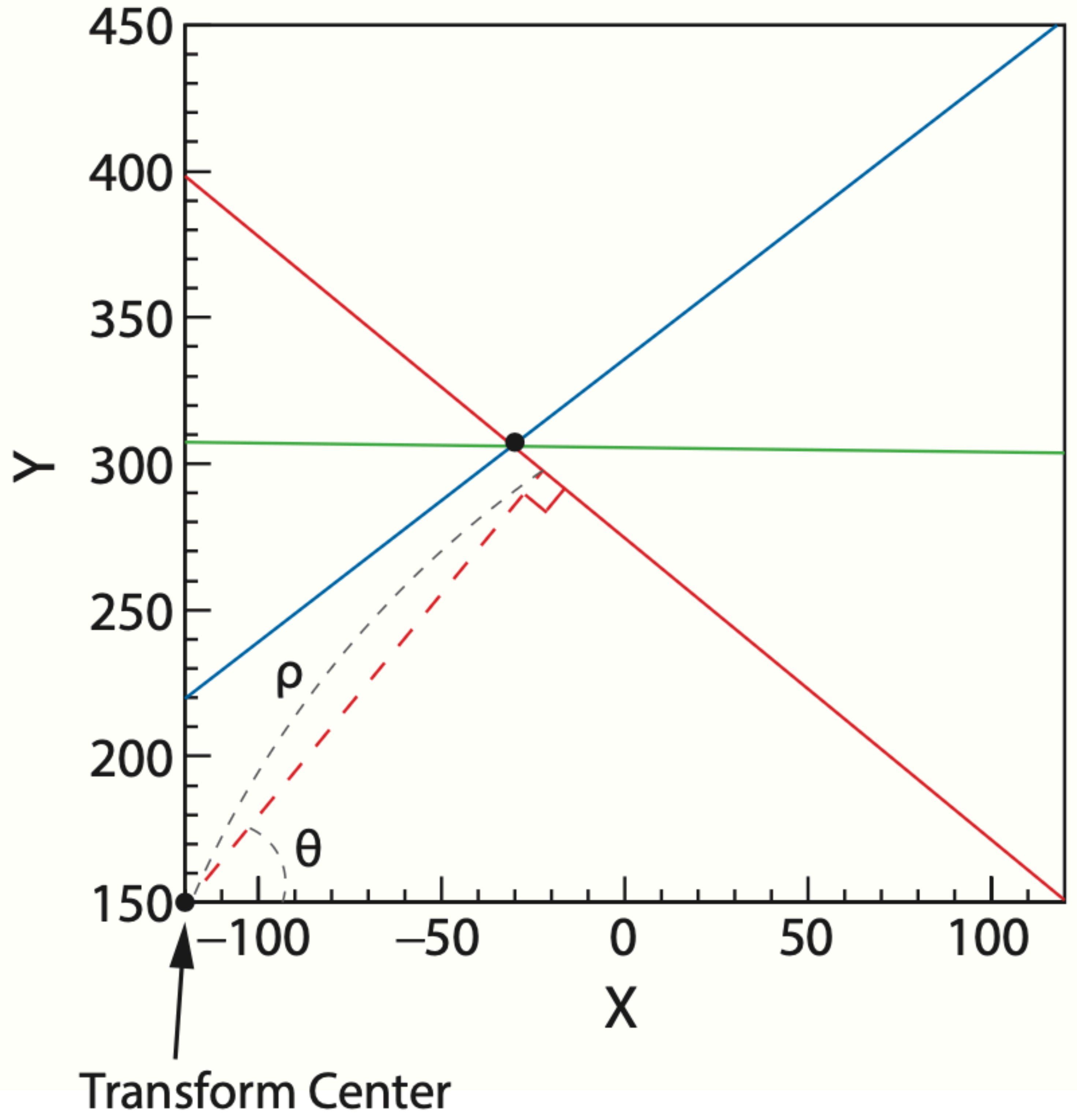

Image space

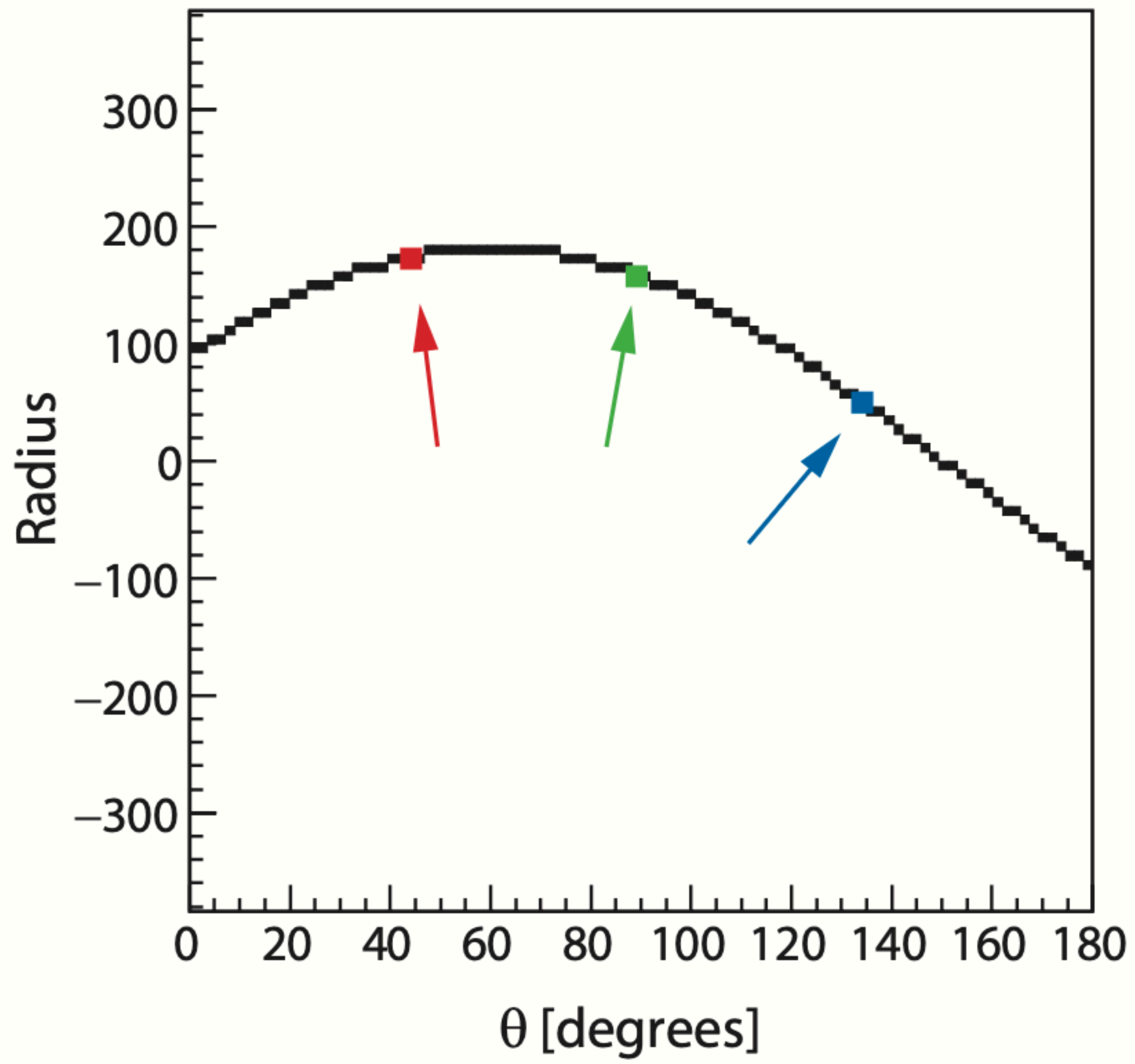

Parameter space

Line-fitting with Typical Events

Strip (X axis)

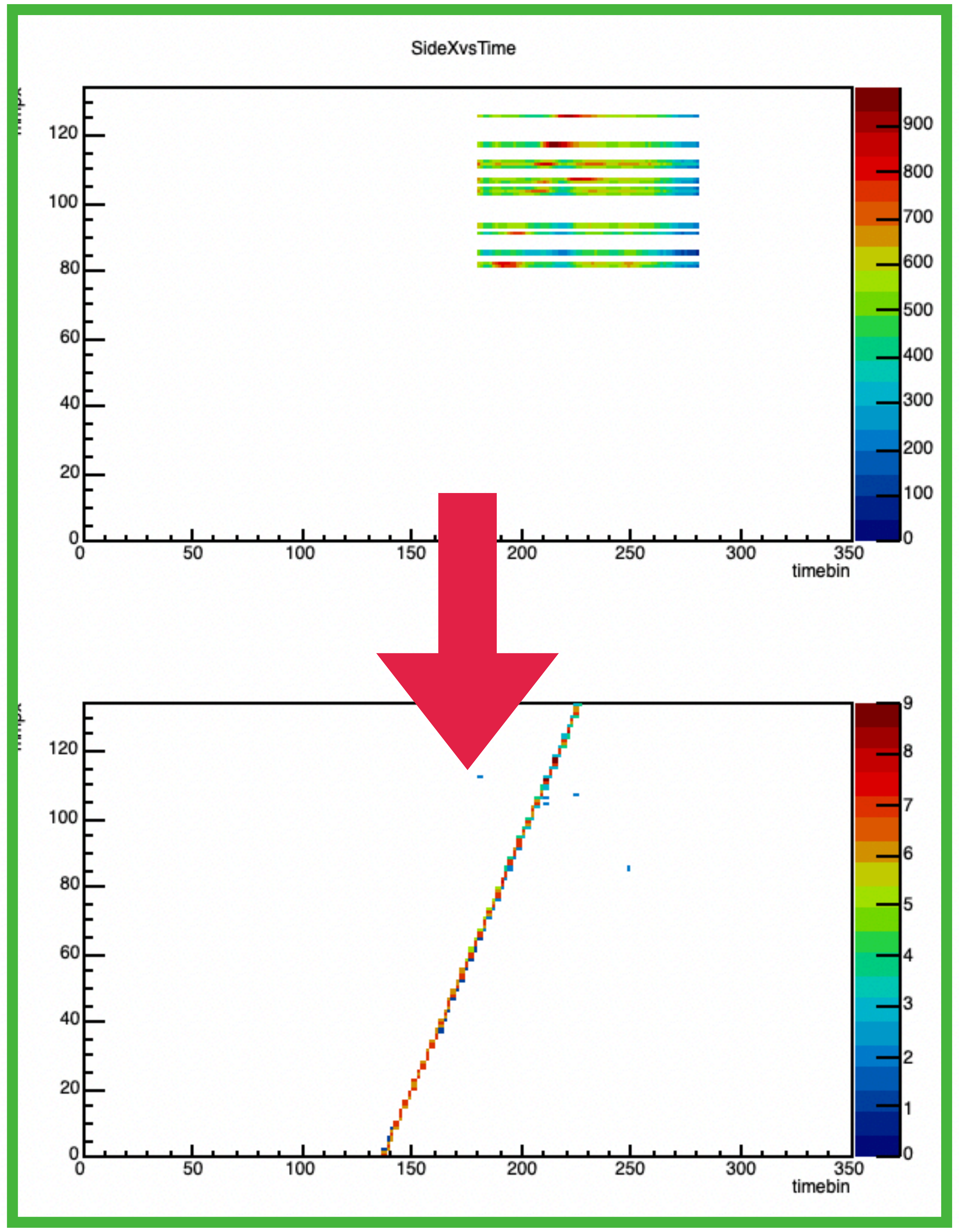

Timing

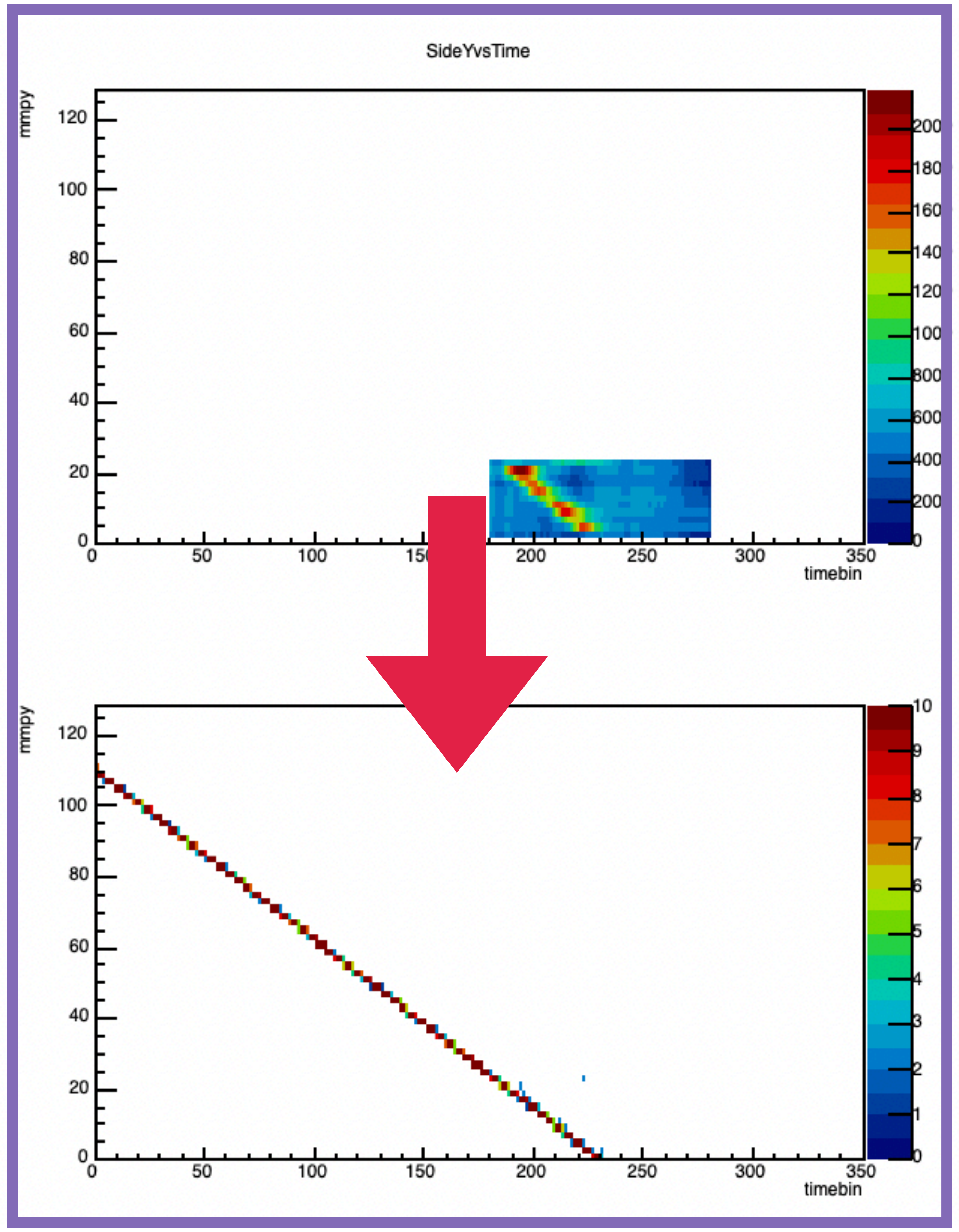

Chain (Z axis)

Timing

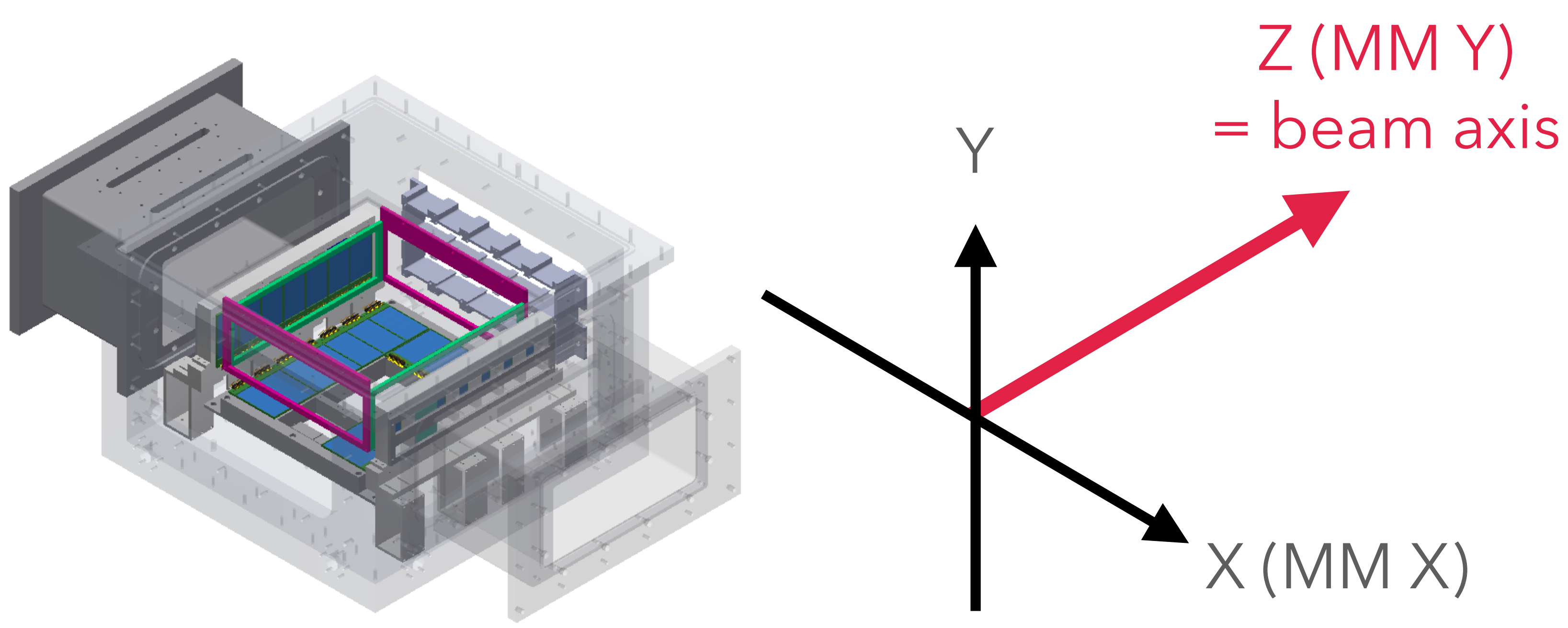

MM Y

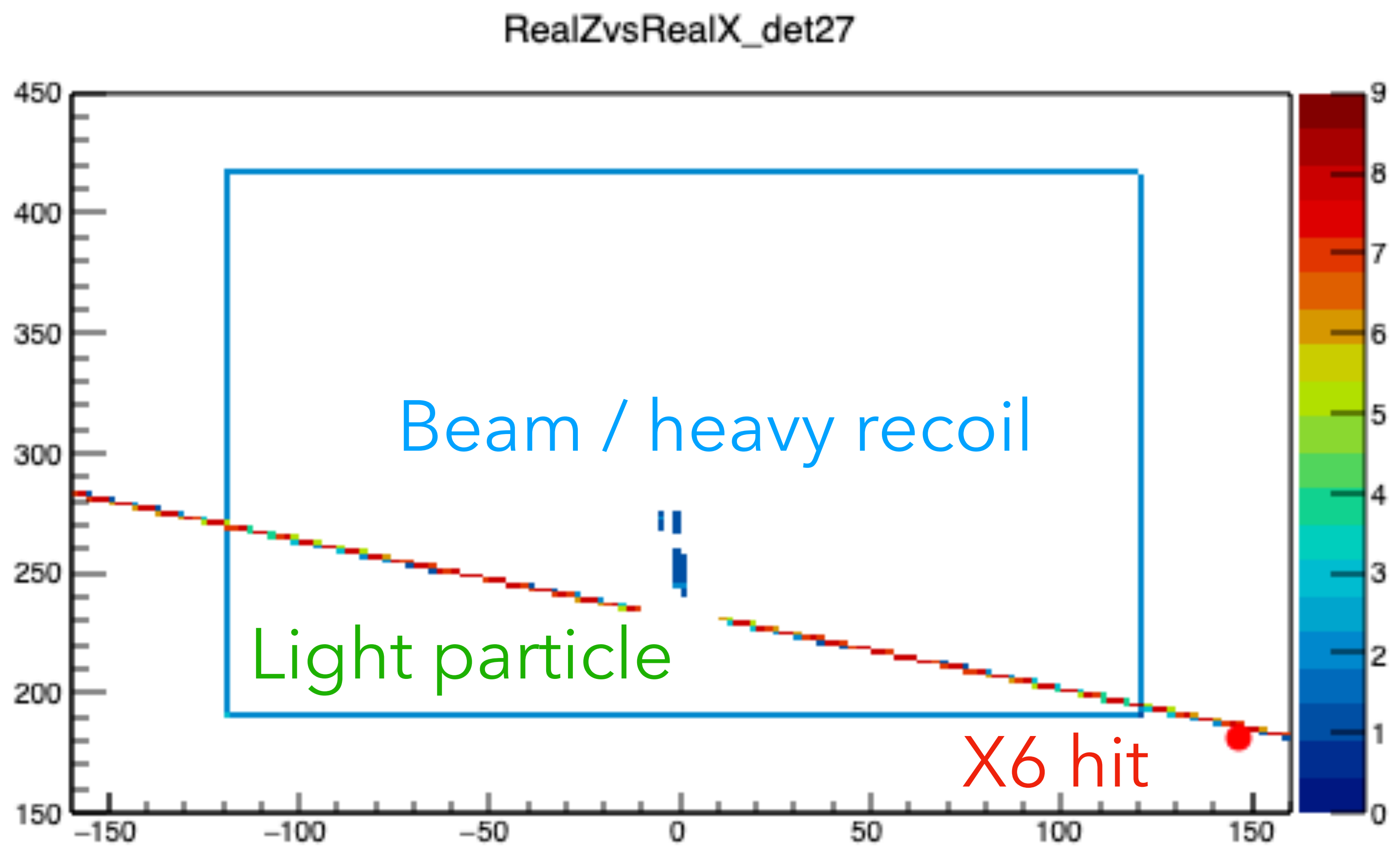

MM X

Reaction Idendification

(a,p) / (a,a)

$$\frac{dE}{dx} = \sum_{fired\ MM\ channel} \frac{ADC\ value}{Distance\ traveled\ on\ the\ channel\ [mm]}$$

cf) Energy loss calculation

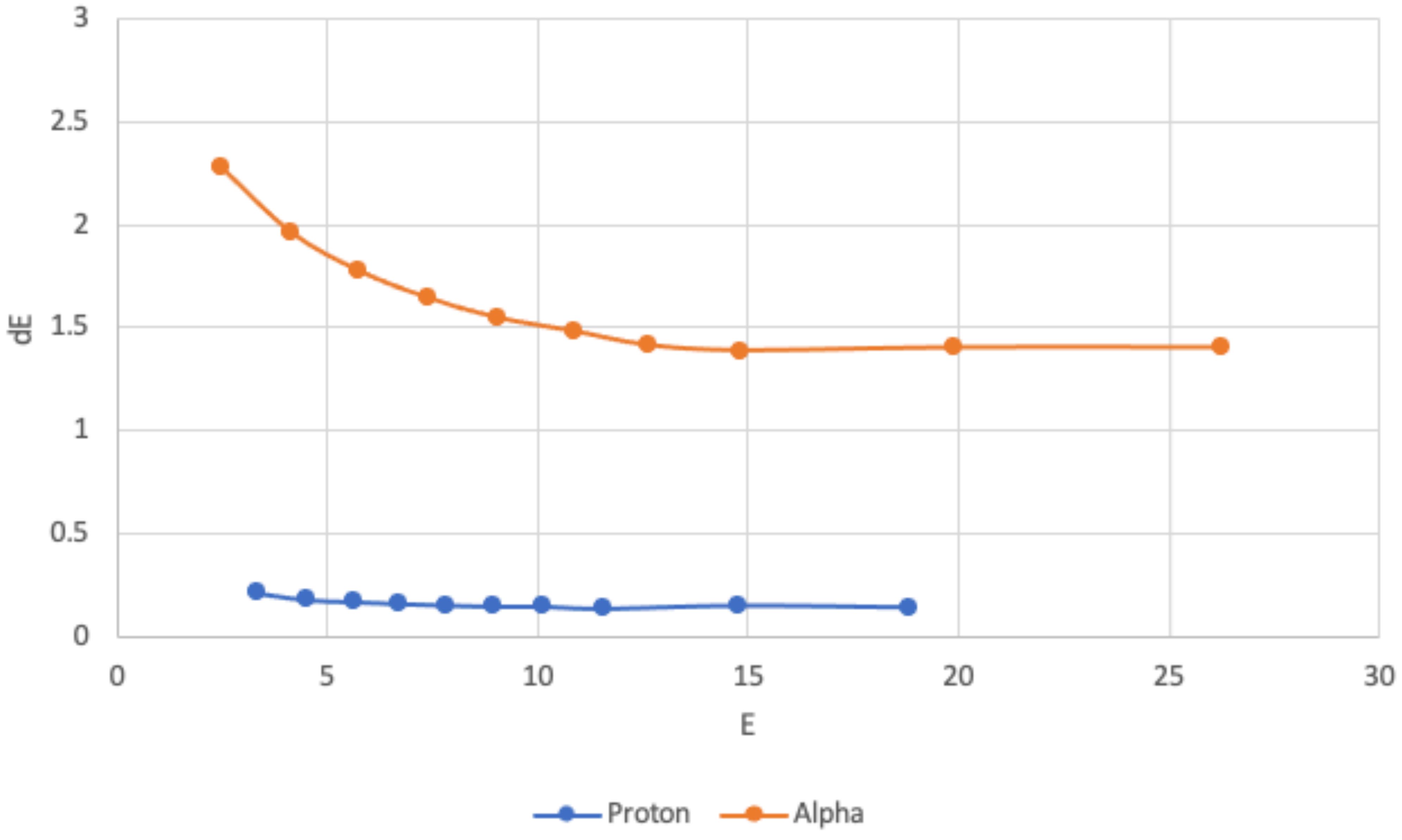

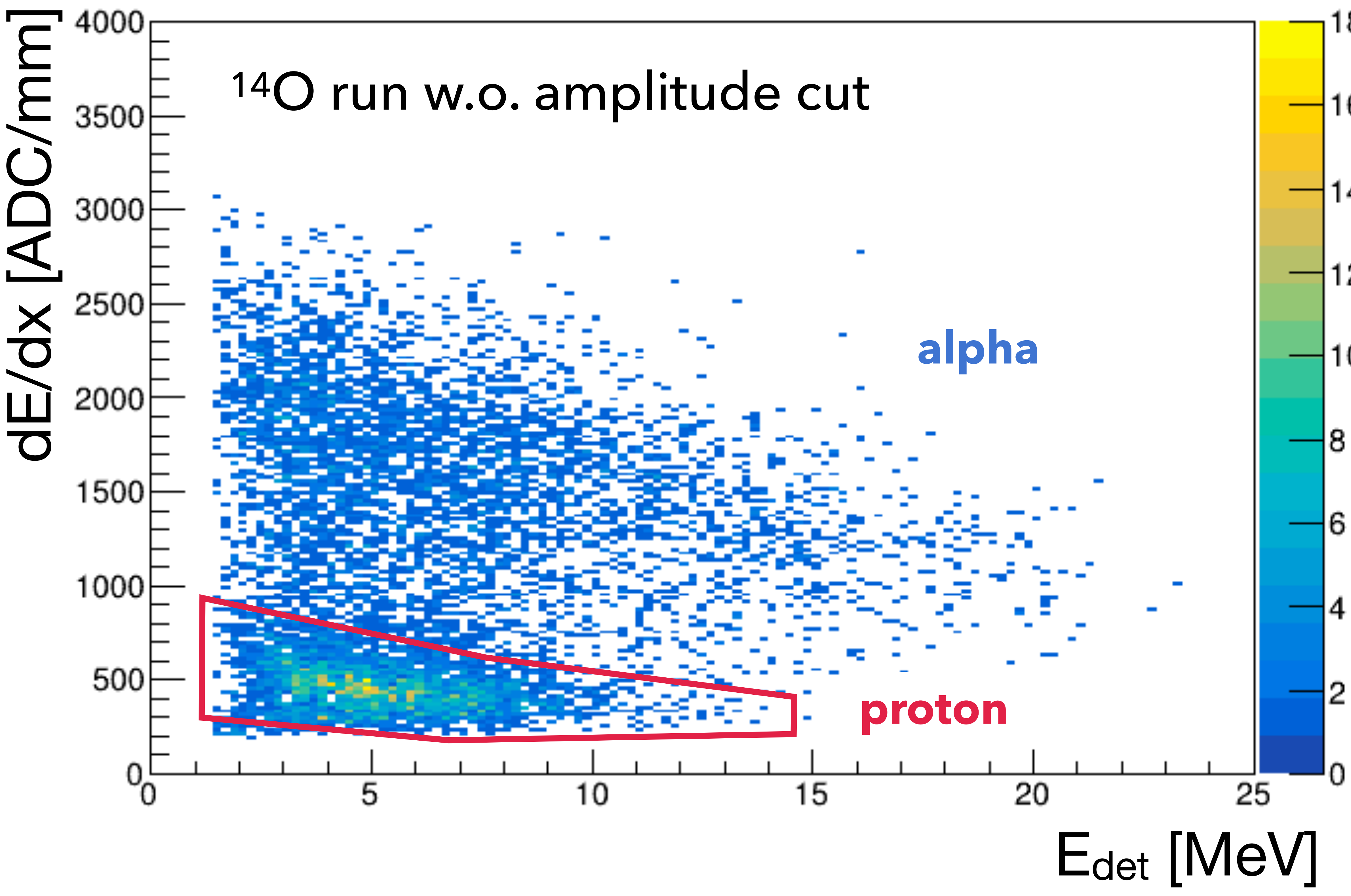

Reaction Idendification

^{14}O / ^{14}N

- Red: ^{14}O kineamtics calculation
- Orange: ^{14}N kinematics calculation <u>if ^{14}O</u>

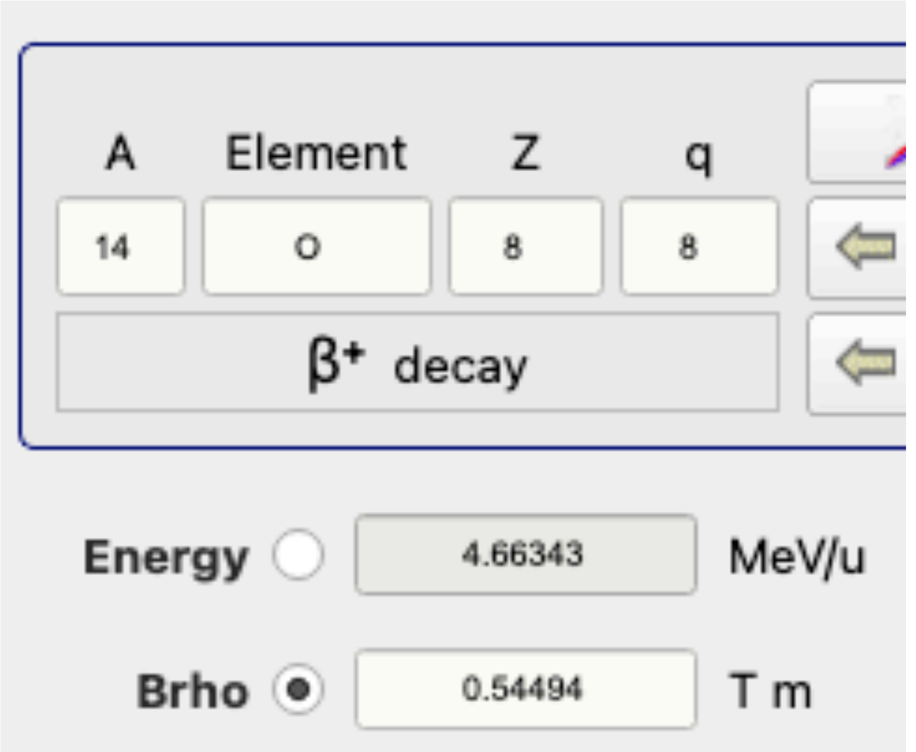

Find E_{lab}, θ_{lab} of $^{14}N(\alpha,p)$ with the same $B\rho$
→ Calculate E_{cm} as it is $^{14}O(\alpha,p)$

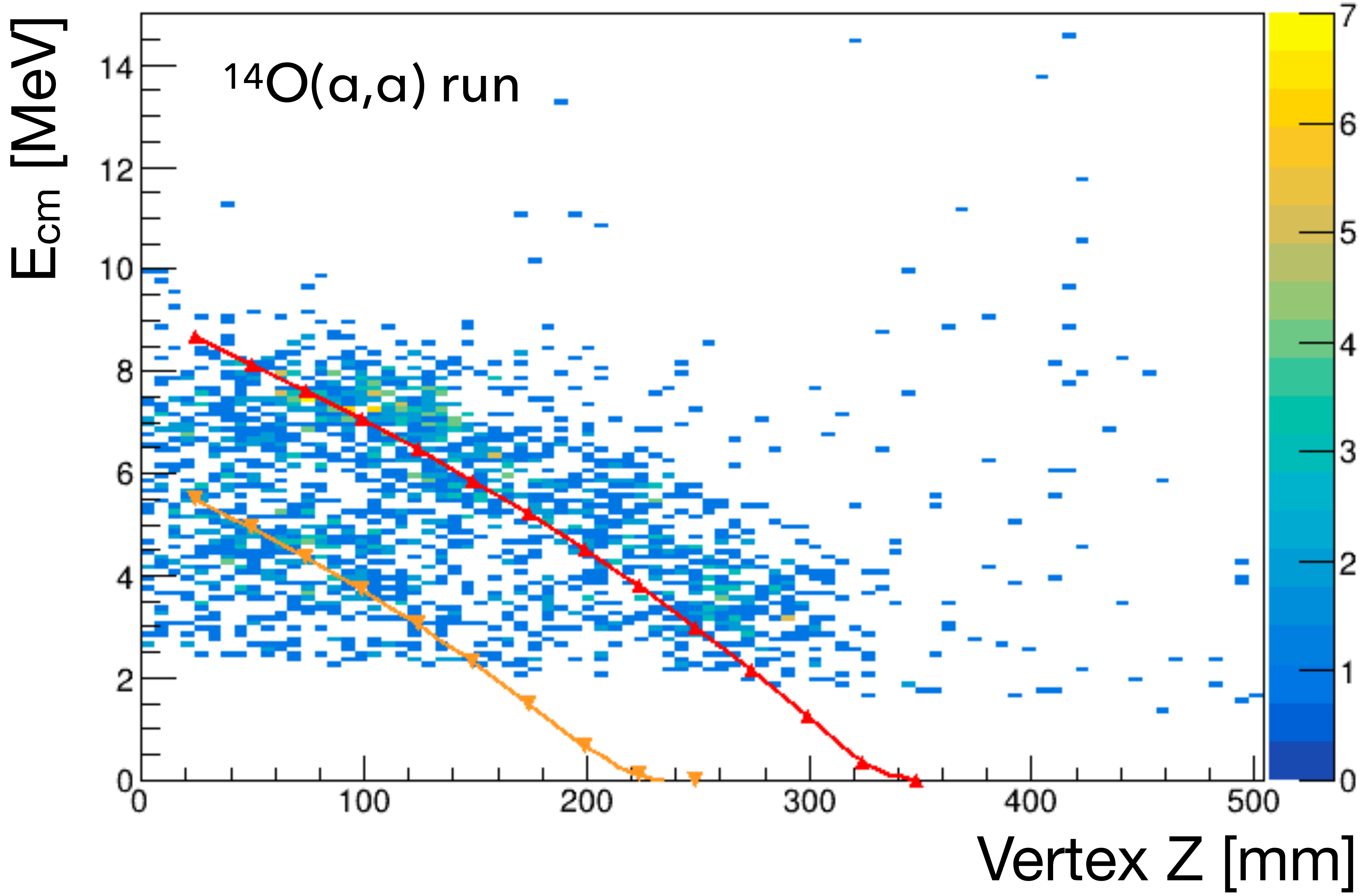

Reaction Idendification

Kinematic subtraction

- Use kinematics between detected energy and ejection angle of light particle.

^{14}O(α,α) run

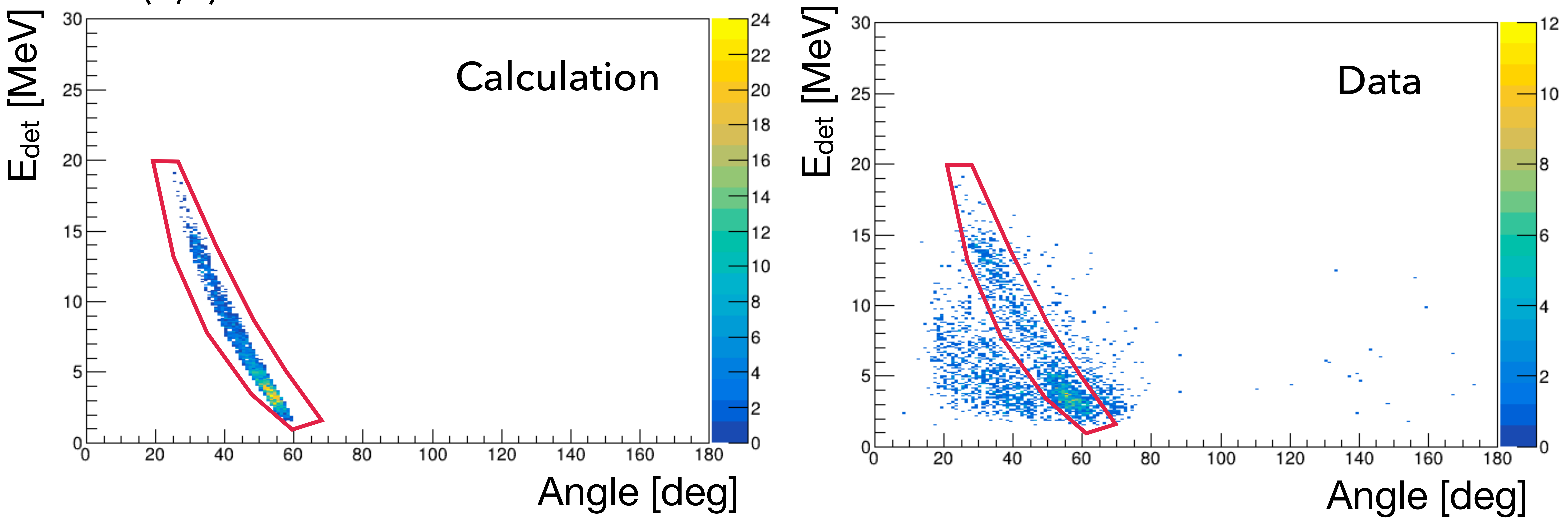

Center-of-Mass Energy Determination

- Conversional TTIK

  $Z \rightarrow E_{cm}$

- Active target TPC

  E_{det} & $\theta \rightarrow E_{cm}$

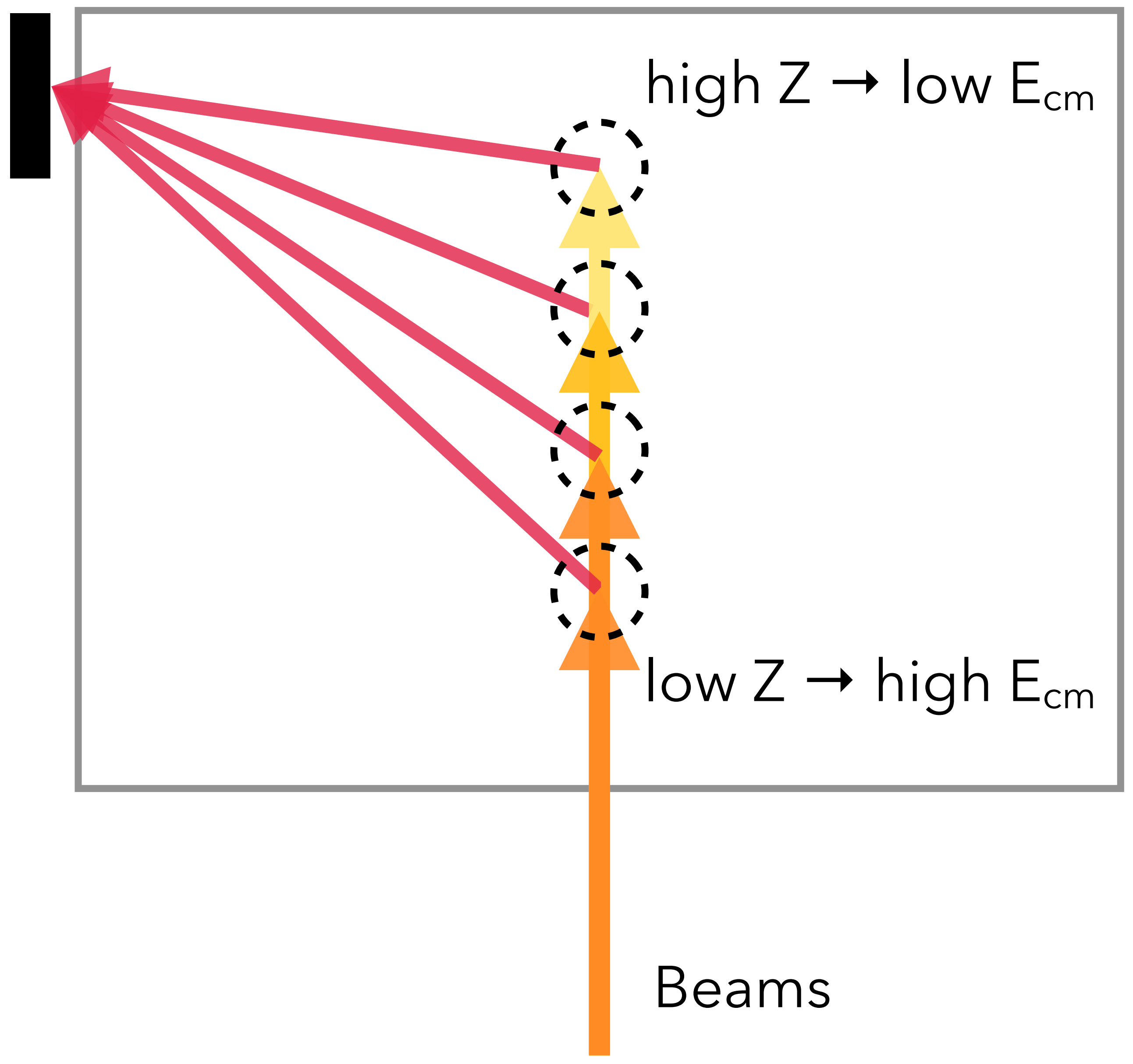

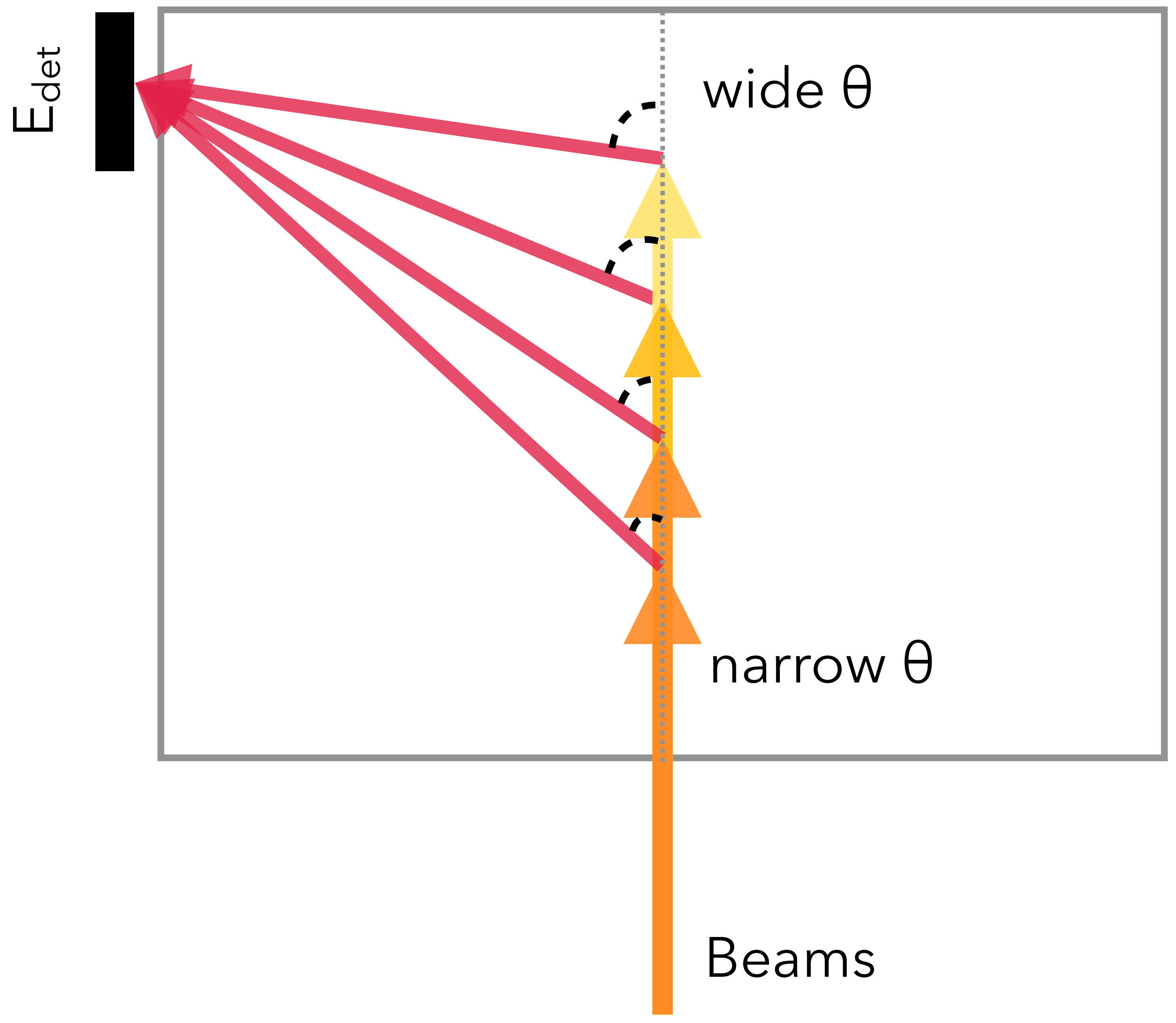

Calculated E_{cm} vs Vertex Z

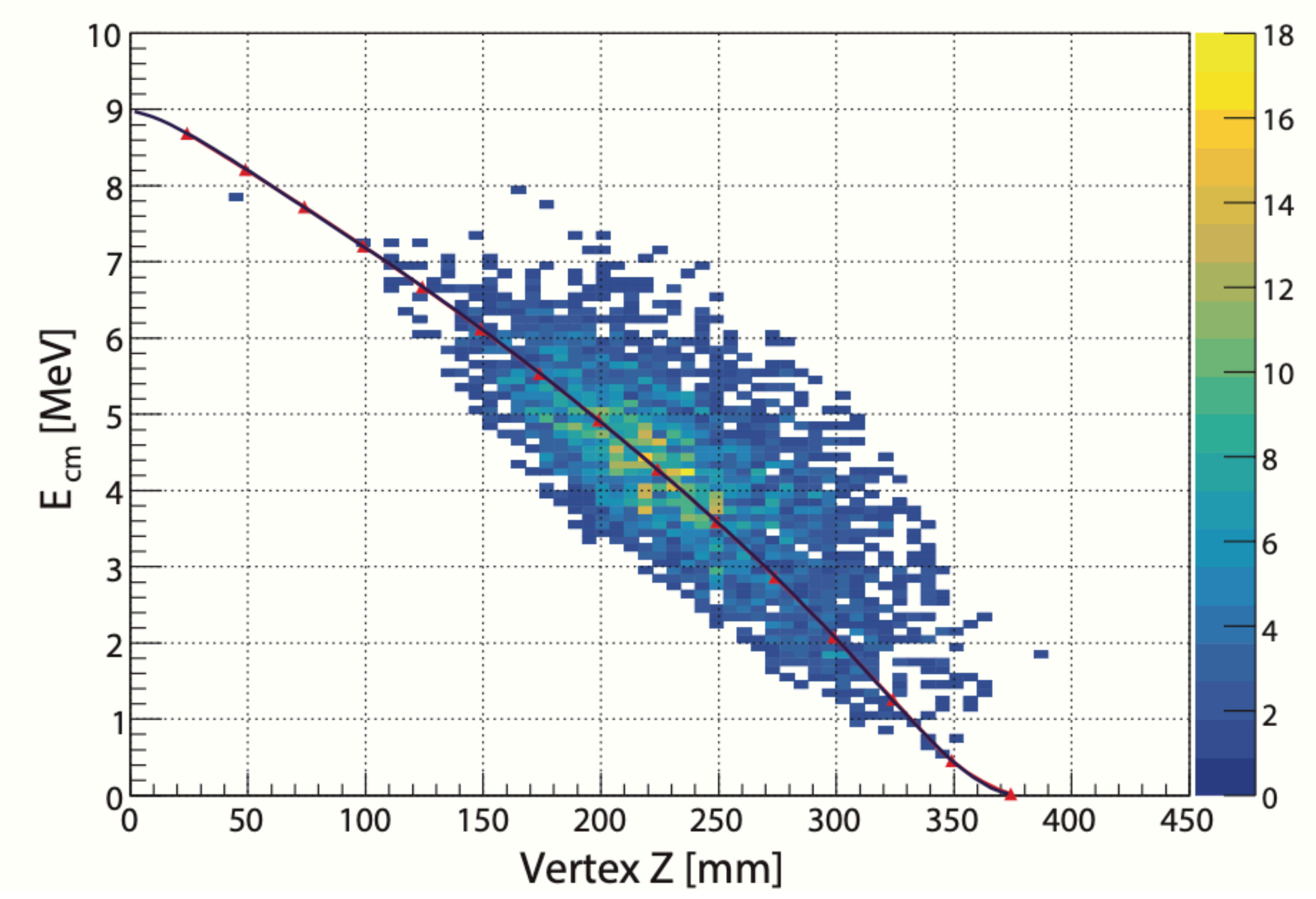

→ Beam energy straggling is treated as an uncertainty.

p0 vs p1 vs p2

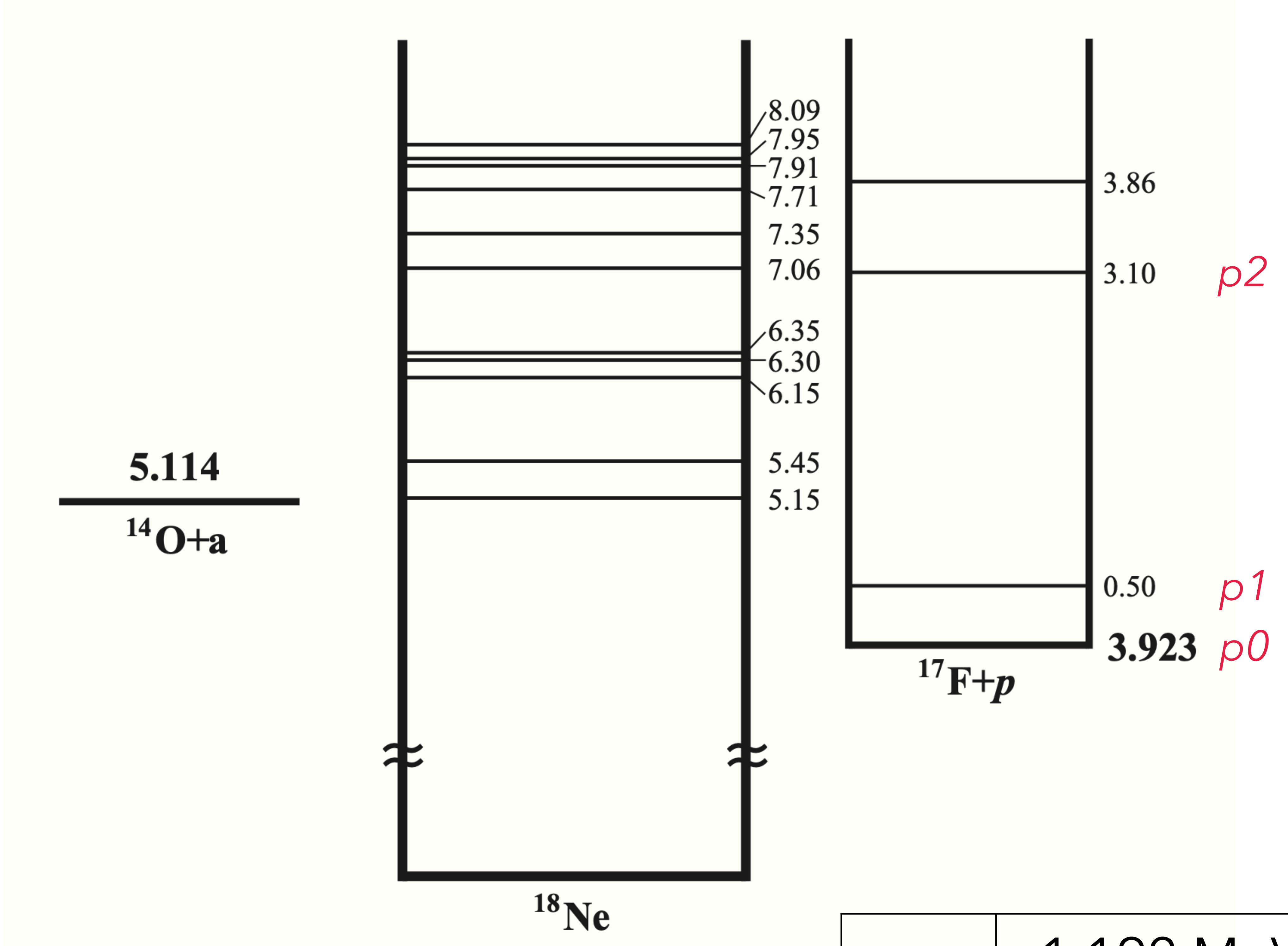

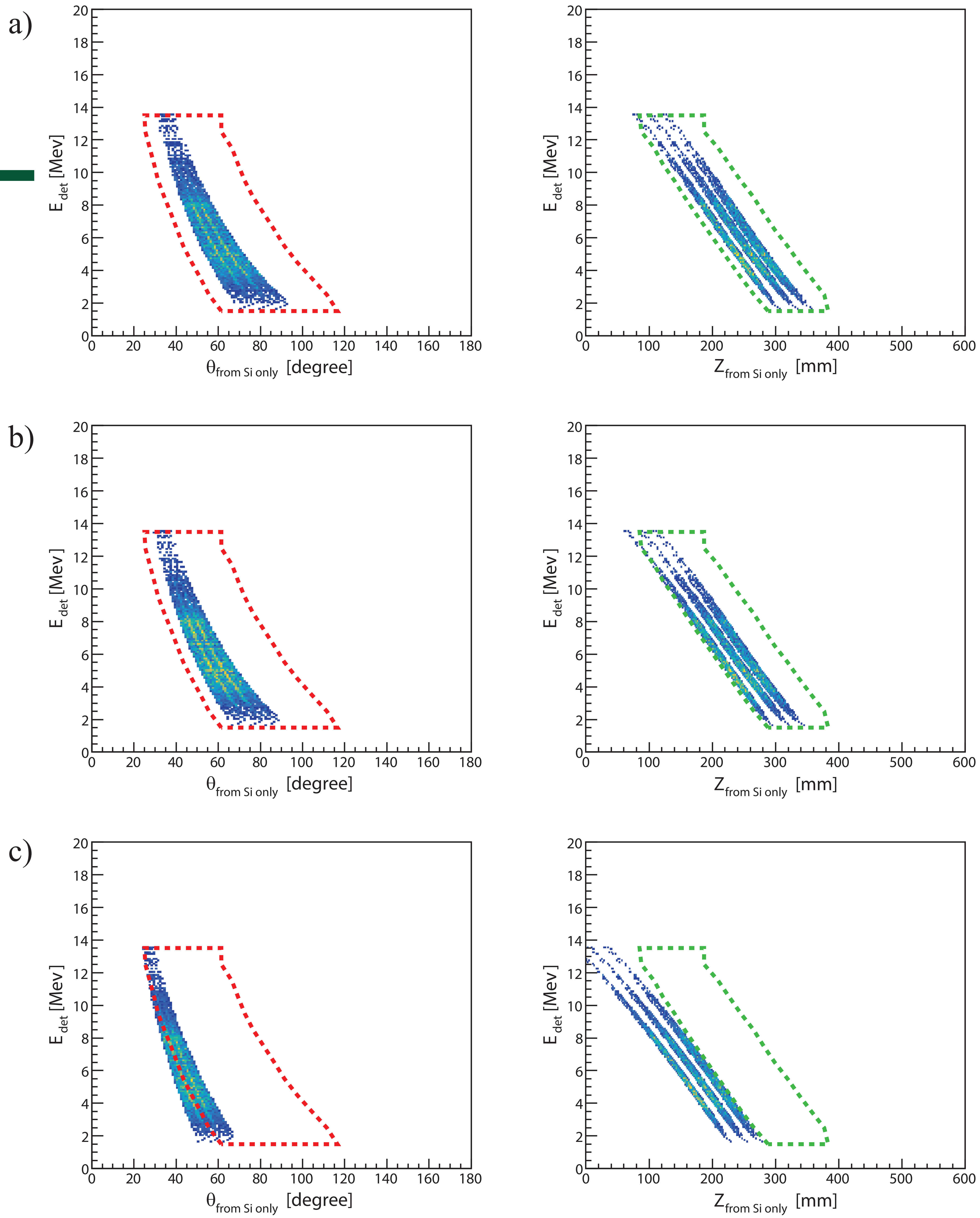

p	1.192 MeV
d	-13.383 MeV
t	-21.084 MeV
^{3}He	-7.354 MeV

* Q-values

Tracking Efficiency

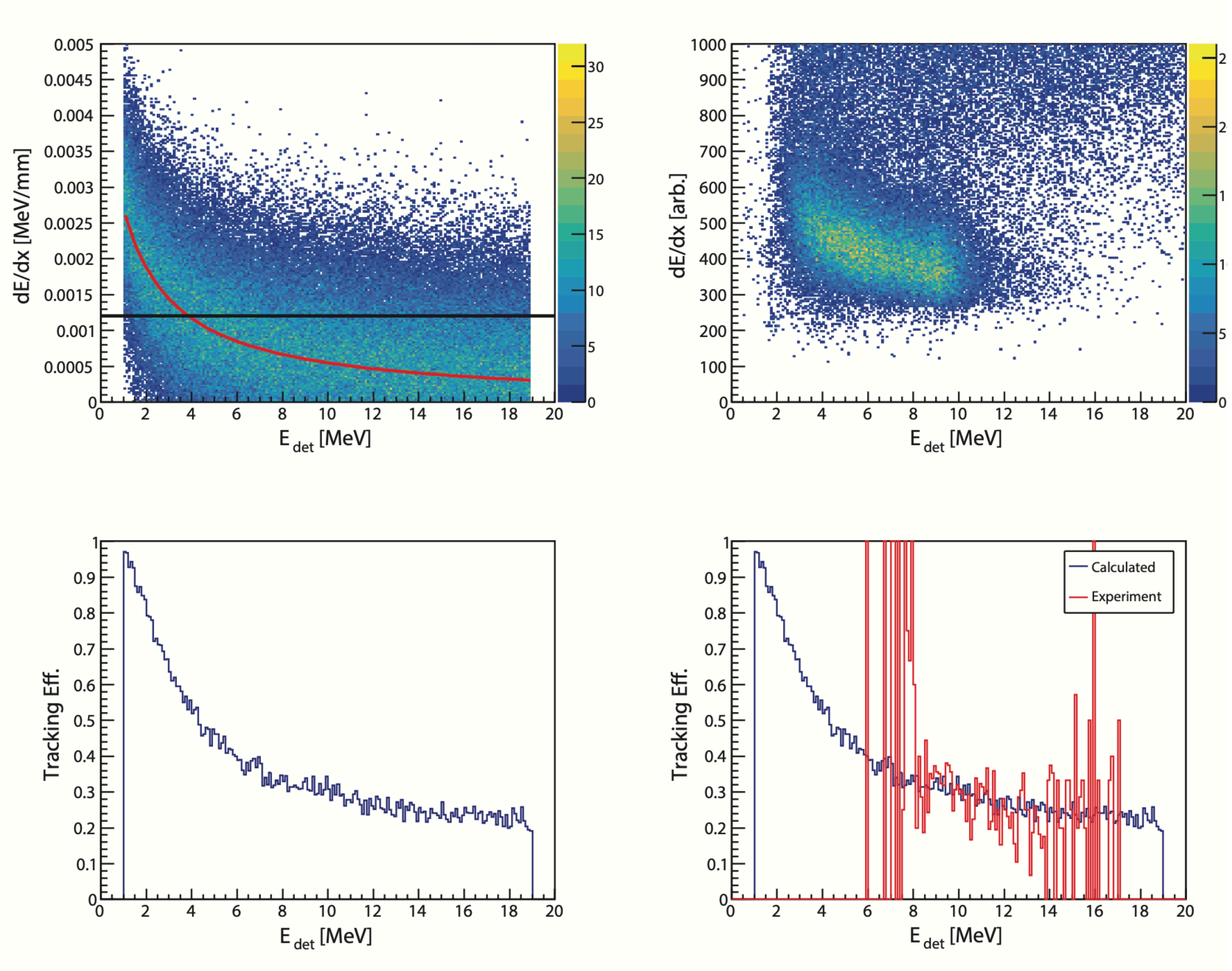

Excitation Function

$$\sigma = \frac{\text{Yield}}{I_{\text{beam}} \times n_{\text{target}} \times \epsilon}$$

$$n_{\text{target}} = \rho\,\Delta x$$

$$\rho = \frac{d_{\text{He}}}{M_{\text{He}}} \times N_A$$

$$\Delta x = x_{E_n} - x_{E_{n-1}}$$

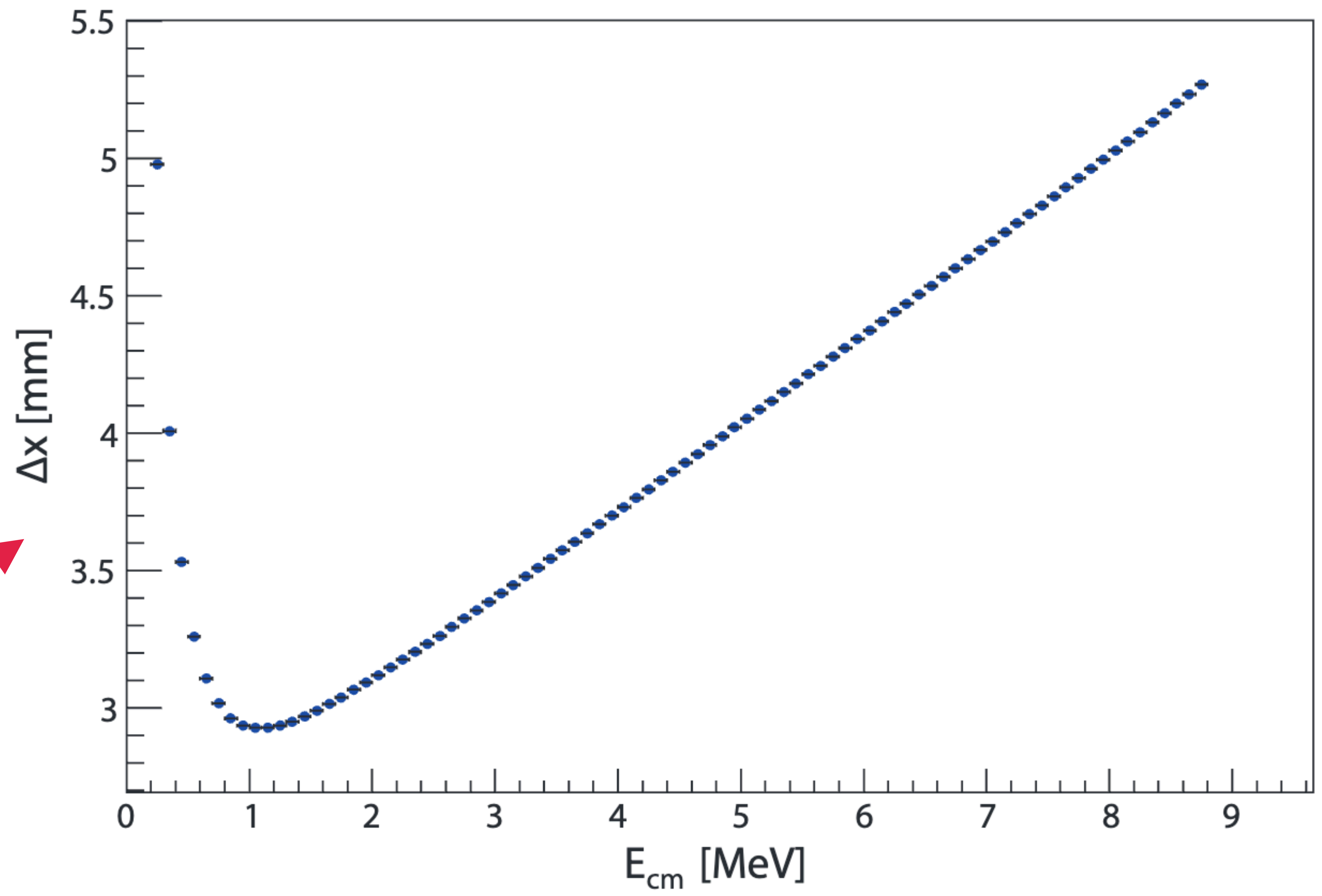

Error Propagation

Statistical Uncertainty

$$\left[\Delta\sigma_{stat.} = \sigma\frac{\Delta Y}{Y},\ \Delta Y = \frac{\sqrt{Y}}{\epsilon_{dead}\ \epsilon_{track}}\right]_{Det}$$

$$\Delta\sigma_{stat.} = Avg(\ [\Delta\sigma_{stat.}]_{Det}\ )$$

Combine *p0* + *p1*

$$\sigma = \frac{\sigma_{p0} + \sigma_{p1}}{2}$$

$$\Delta\sigma_{stat.} = \frac{\sqrt{\Delta\sigma^2_{stat.\ p0} + \Delta\sigma^2_{stat.\ p1}}}{2}$$

$$\Delta\sigma_{sys.} = \frac{|\sigma_{p0} - \sigma_{p1}|}{2}$$

$$\Delta\sigma = \sqrt{\Delta\sigma^2_{stat.} + \Delta\sigma^2_{sys.}}$$

AZURE + Direct Reaction

$$S_{\mathrm{DR}}^{J^\pi=1^-} = \begin{cases} 9.19\cdot 10^4 \exp(1.28E - 0.43E^2) & E \leqslant 1.5\ \mathrm{MeV} \\ 2.45\cdot 10^5 & 1.5 \leqslant E \leqslant 3.5\ \mathrm{MeV} \\ 12.39 \exp(8.27E - 2.23E^2 + 0.22E^3 - 0.79\cdot 10^{-2}E^4) & E \geqslant 3.5\ \mathrm{MeV} \end{cases}$$

MeV * barn

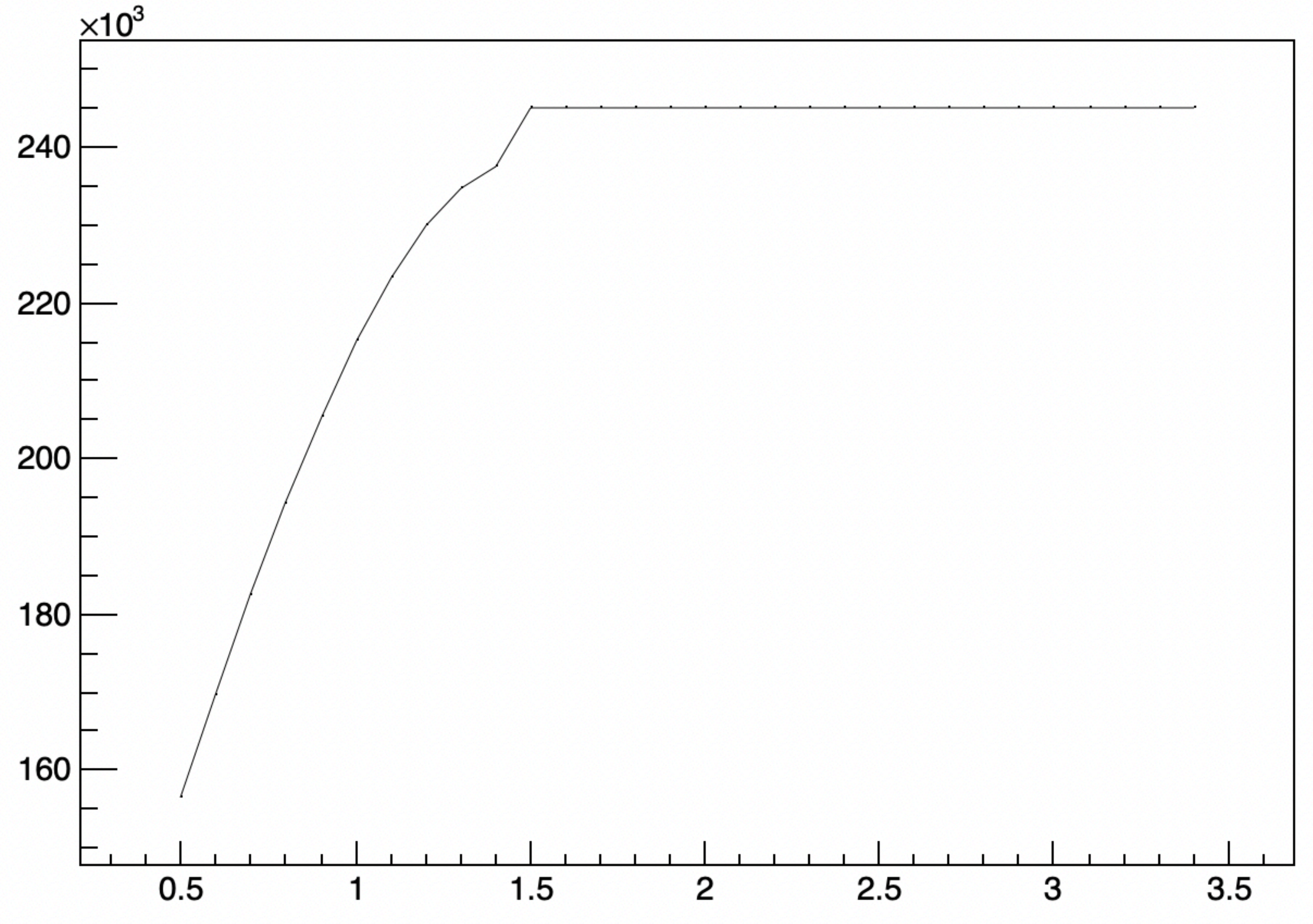

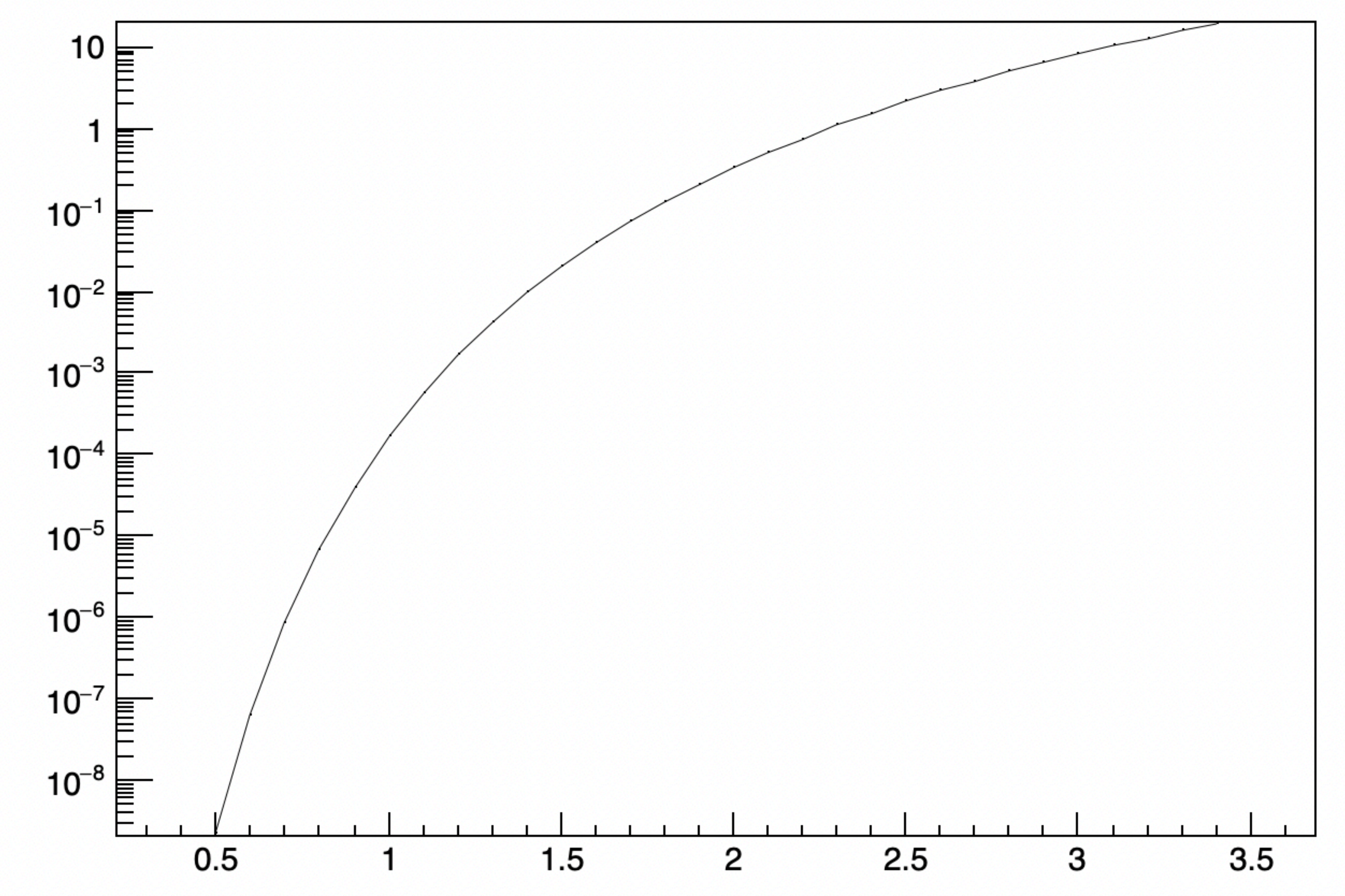

Low Ecm new resonance (Hu)

(b) State at 6.85 MeV. It is very interesting that a shoulder-like structure around $E_{\text{c.m.}} = 2.93$ MeV was observed by both telescopes as shown in Figs. 3(a) and 3(b). This is possibly a new state at $E_x = 6.85 \pm 0.10$ MeV. Both $J^\pi = 0^-$ and 0^+ resonances can reproduce the observed shape as shown in Fig. 3(d). Because of the small energy shift for the negative-parity states in this excitation energy region [59], such a state is possibly the analog state of ^{18}O at $E_x = 6.880$ MeV (0^-) [64]. In fact, Wiescher *et al.* [19] predicted a $J^\pi = 0^-$ state in ^{18}Ne, analog to the 6.88 MeV state in ^{18}O, at 6.85 MeV with a proton spectroscopic factor of $C^2S_p = 0.01$. However, another possibility still exists.

from Harss *et al.* [35]. Based on the suggestion of Fortune, Almaraz-Calderon *et al.* thought that their large number might be attributed to an unknown state at $E_x \sim 6.7$ MeV in ^{18}Ne. In fact, a hint of a weak state is observed at $E_x \sim 6.8$ MeV (see Fig. 6 in Ref. [39]). As discussed above, such a state at $E_x = 6.85 \pm 0.10$ MeV was also observed in the present work. Therefore, we conclude that very likely a new state around 6.8 MeV exists in ^{18}Ne. Since this state was populated in the direct ^{14}O$(\alpha,p)^{17}$F reaction, it should have a natural parity. Thus, it is also possibly a candidate for the $J^\pi = 0^+$ state, a bandhead

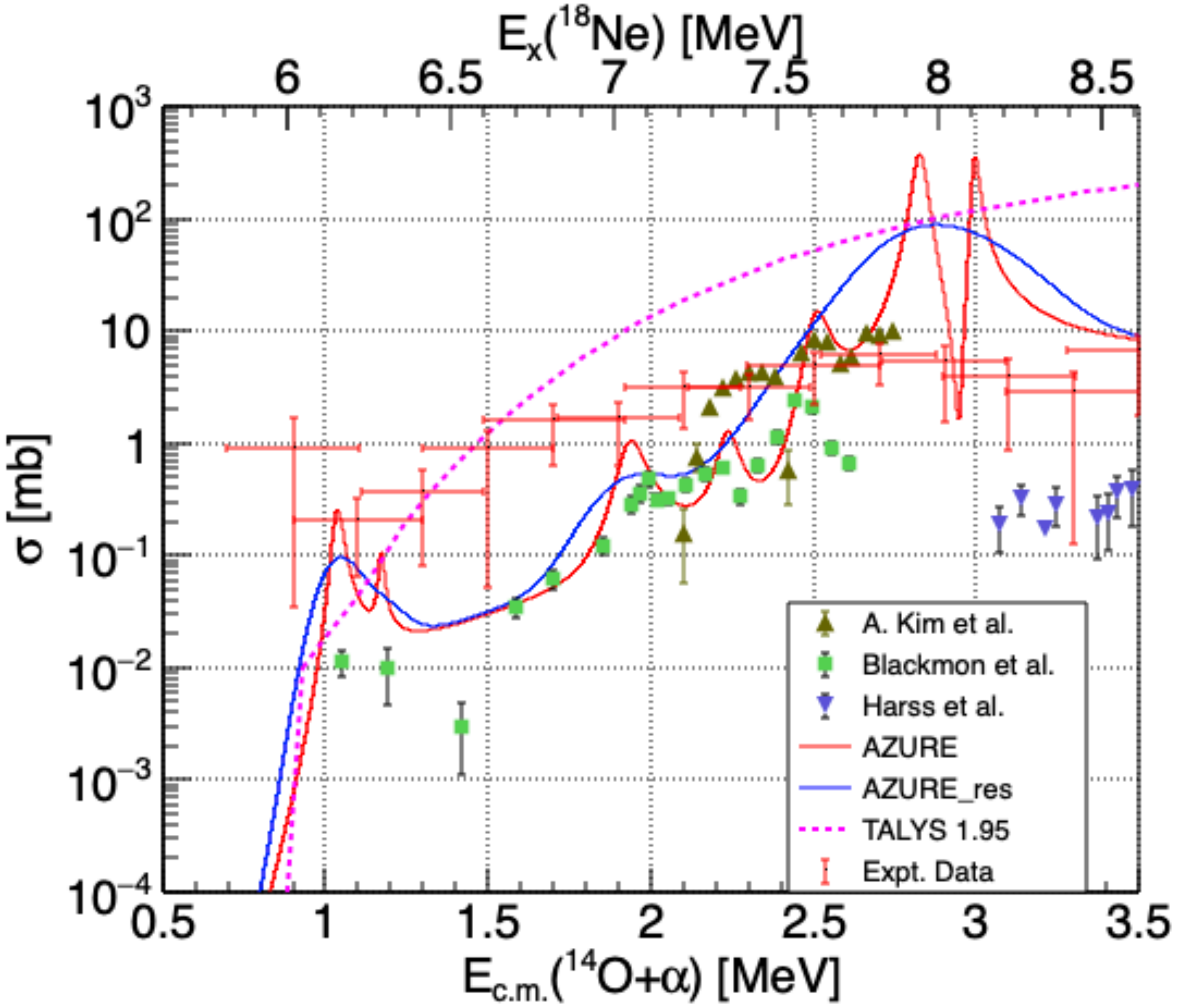

슬라이드 3장 + 백업 16:9

Low Ecm new resonance (Wiescher)

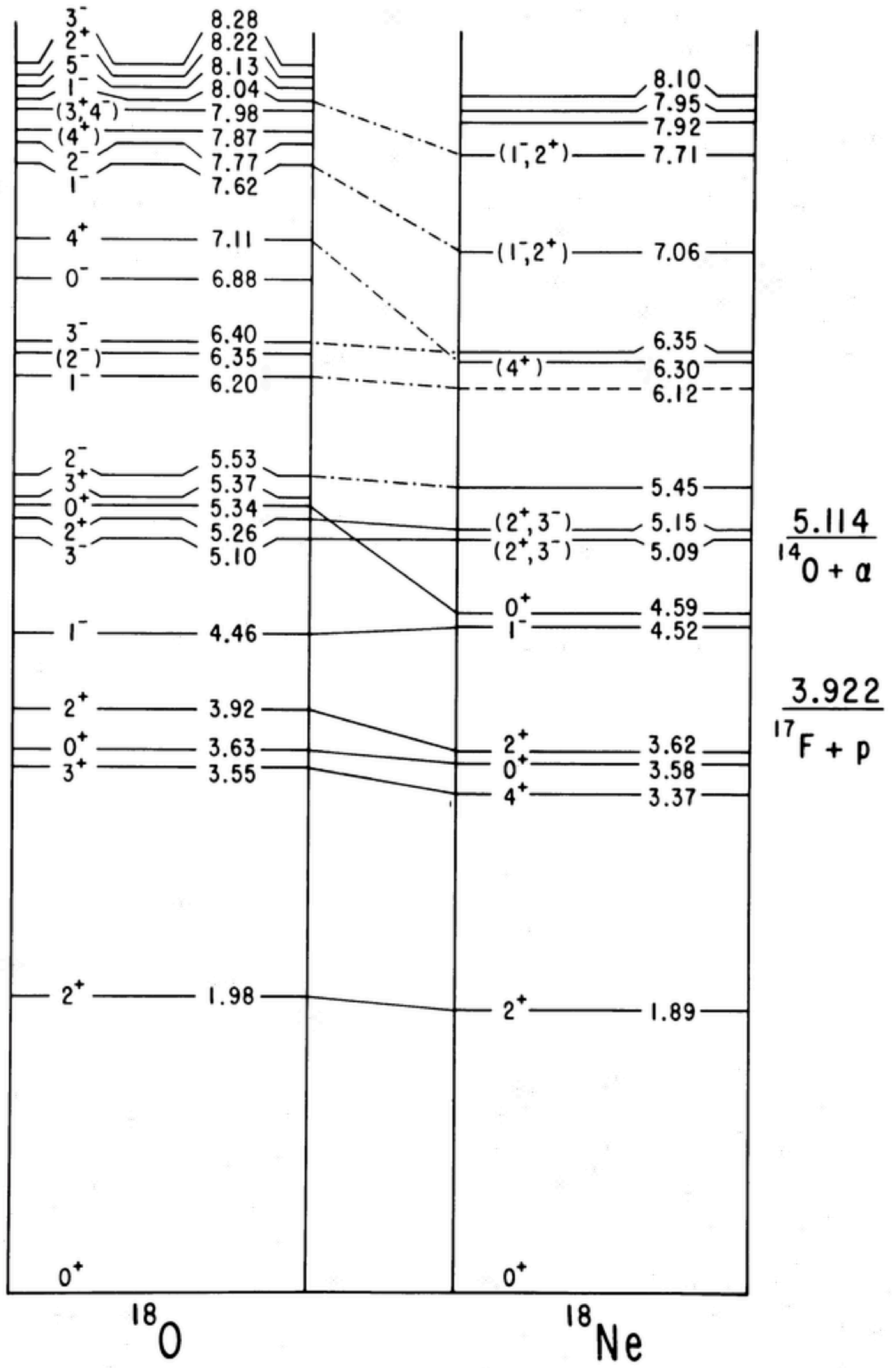

TABLE 1

$T = 1$ ANALOG STRUCTURE OF ^{18}O AND ^{18}Ne

$J^{\pi}(^{18}O)$	$E_x(^{18}O)$ EXPERIMENTAL	C^2S Experimental	C^2S Theoretical	$E_x(^{18}Ne)$ Calculated	$E_x(^{18}Ne)$ Experimental	$J^{\pi}(^{18}Ne)$
3^-	5.098	0.03[a]	0.02[b]	5.037	5.075	$2^+, 3^-$
					5.099	
2^+	5.260	0.35[a]	0.05[b]	4.308	5.141	$2^+, 3^-$
			0.13[c]		5.151	...
		0.04[d]	...	5.154	...	...
				5.055[e]		
0^+	5.336	0.16[a]	0.14[b]	4.526[f]	4.590	0^+
			0.18[c]	4.550[e]		
1^-	6.198	0.03[a]	...	6.125	...	...
3^-	6.404	<0.04[d]	...	>6.306	6.353	...
		0.02[b]		6.356		
4^+	7.114	0.13[a]	0.17[b]	6.860	6.294	(4^+)
		0.15[d]	0.44[c]	6.820		
1^-	7.618	0.05[d]	...	7.526	7.062	$1^-, 2^+$
		0.30		7.069		
4^+	7.866	0.01[g]	...	7.840	...	...
1^-	8.038	0.01[g]	...	7.995	7.915	$1^-, 2^+$
		0.1		7.915		
5^-	8.126	0.01[g]	...	8.086	...	...
2^+	8.216	0.01[g]	...	8.209	...	...
3^-	8.287	0.01[g]	...	8.269	...	...

[a] From ^{17}O(d, p)^{18}O; Li *et al.* 1976.
[b] Engeland and Ellis 1972.
[c] Sakuda *et al.* 1979.
[d] Calculated from the experimental observed level width.
[e] Nero and Adelberger 1981.
[f] Double Thomas-Ehrman shift $\Delta E(^{17}O - ^{17}F) = 370$ keV (Adelberger and McDonald 1970; Rolfs *et al.* 1973).
[g] Adopted value.

p0 / p1 Simulation

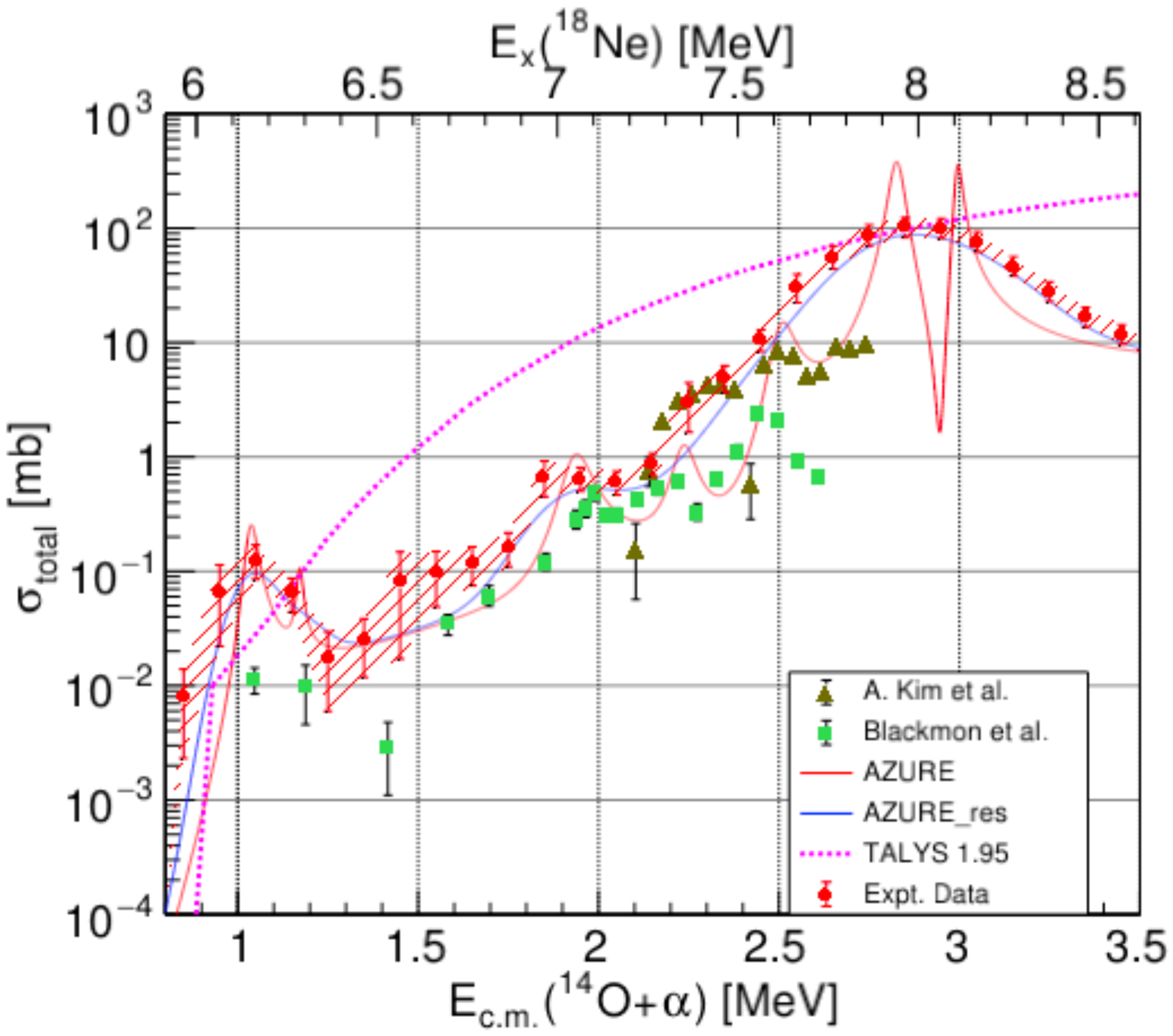

p0 simulation w. resolution

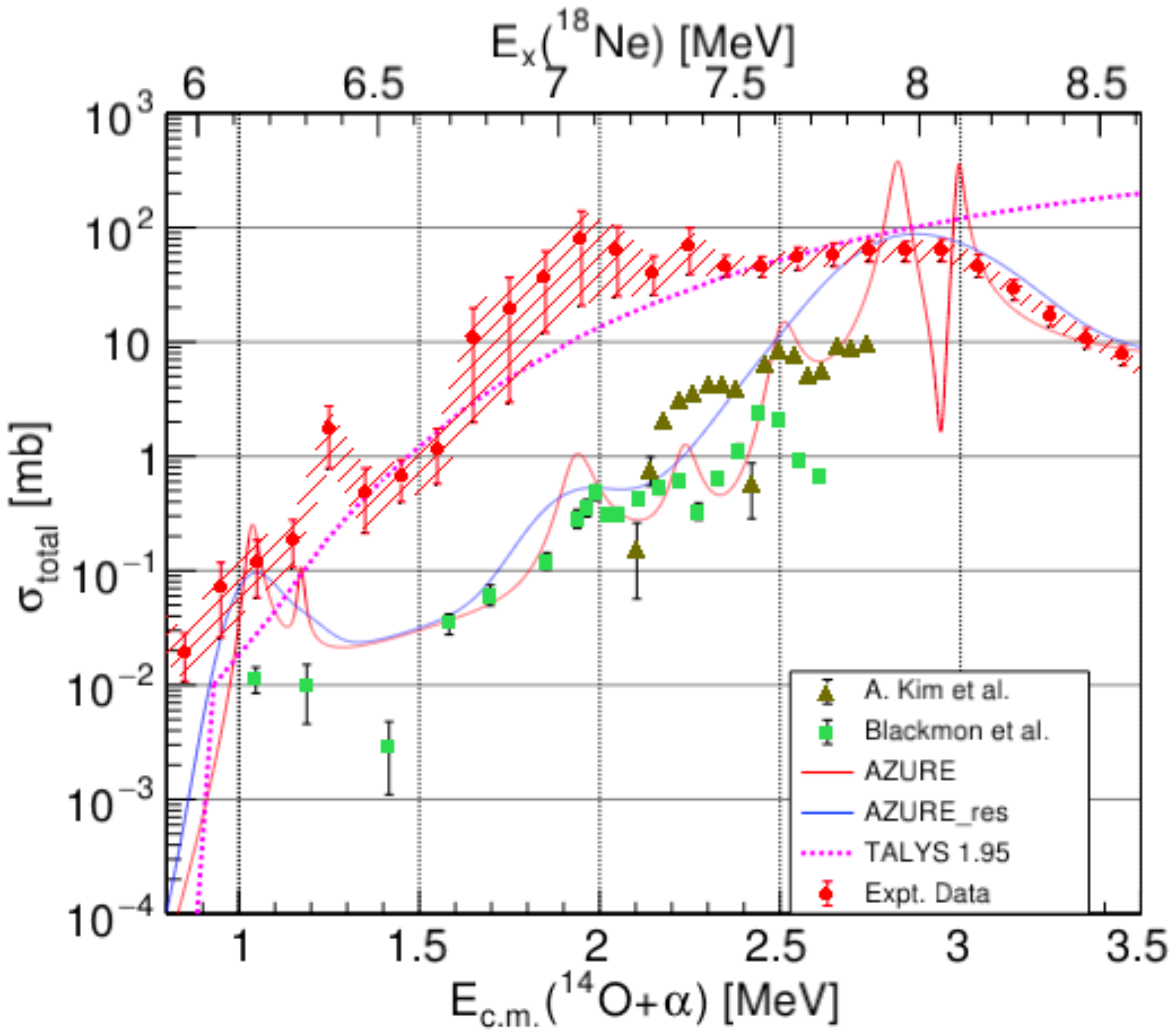

p0 + p1 (calculated from angle as *p0*)

$^{14}O + \alpha$ Channels

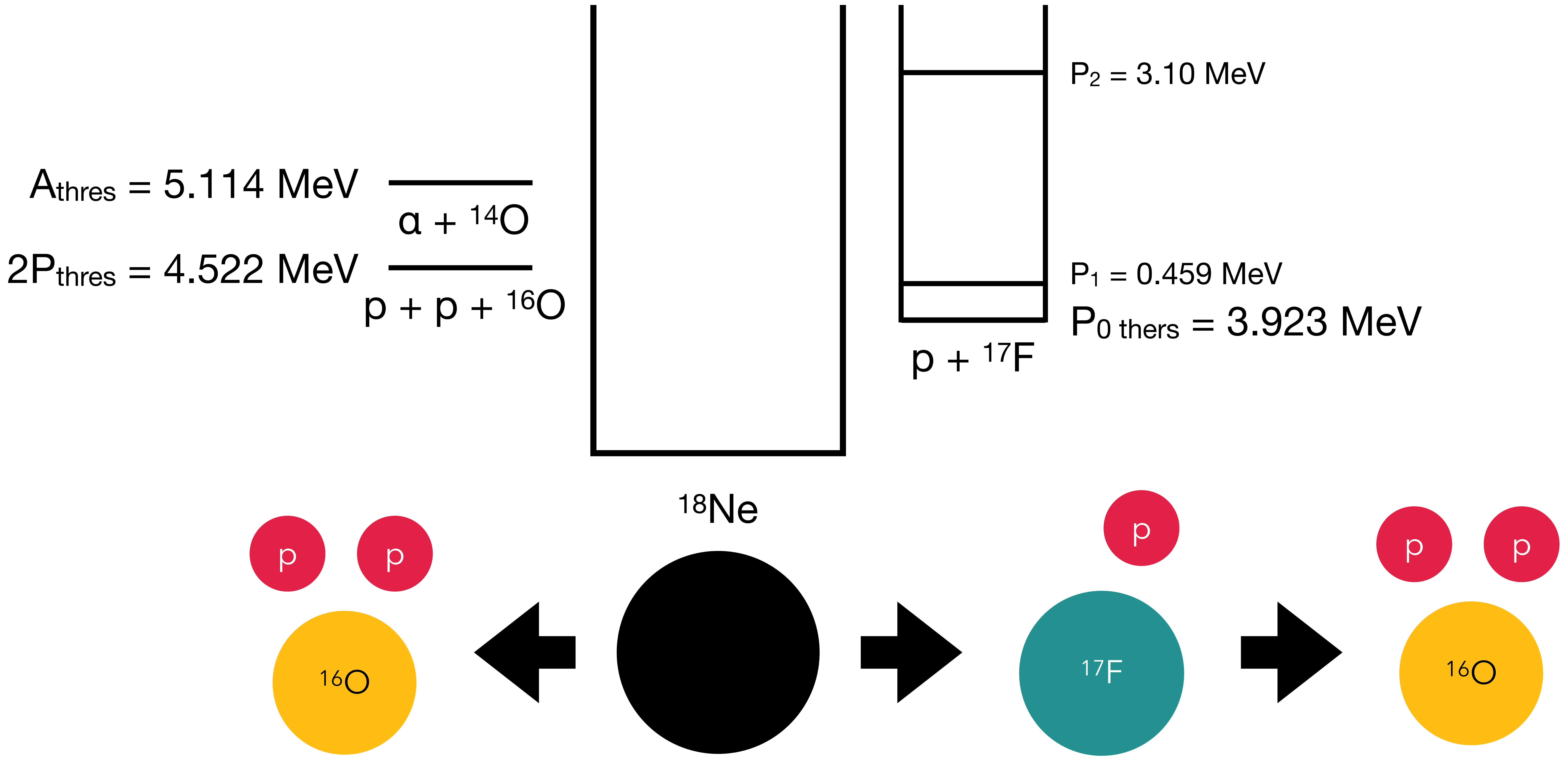

(a,a) Yield

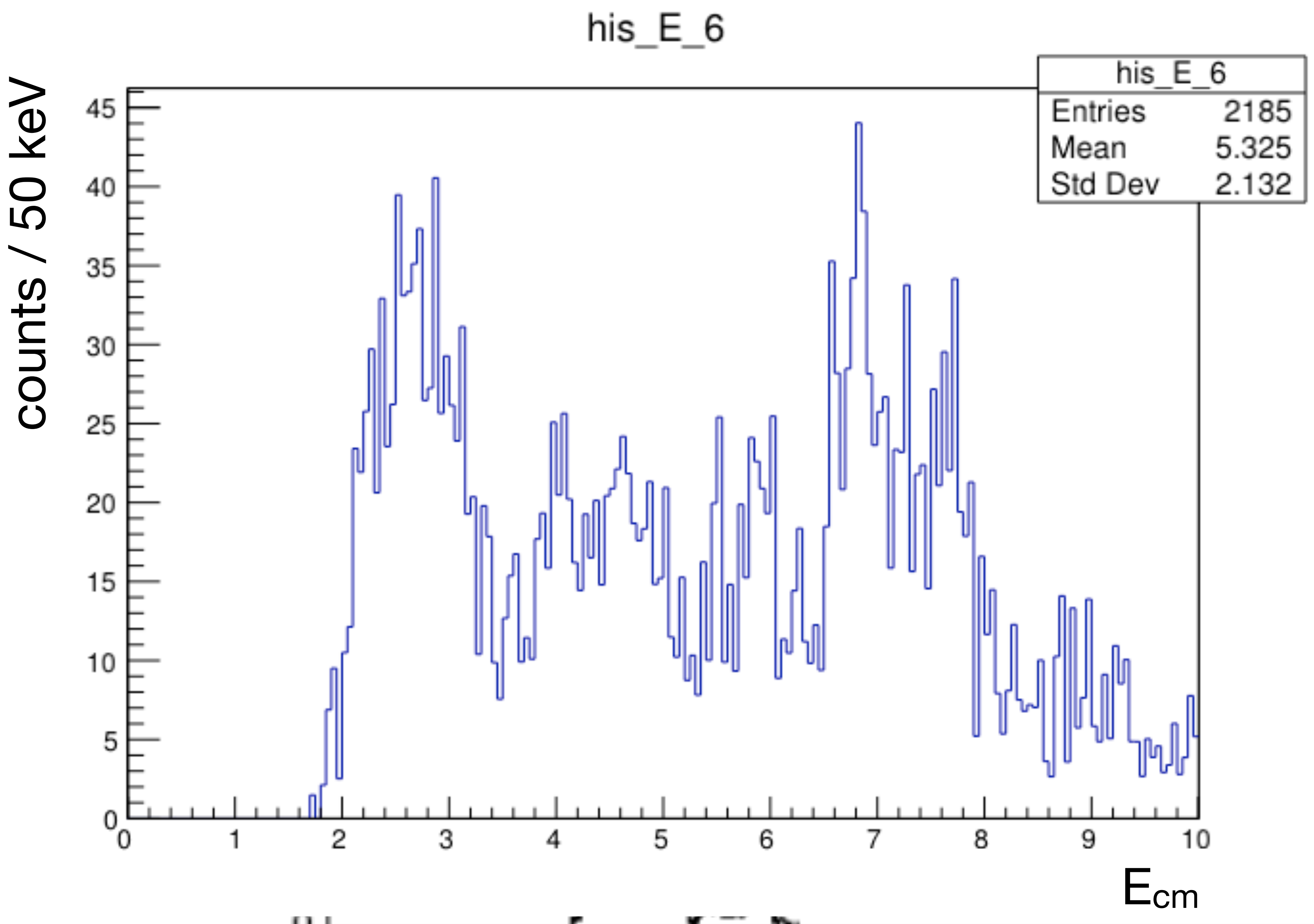

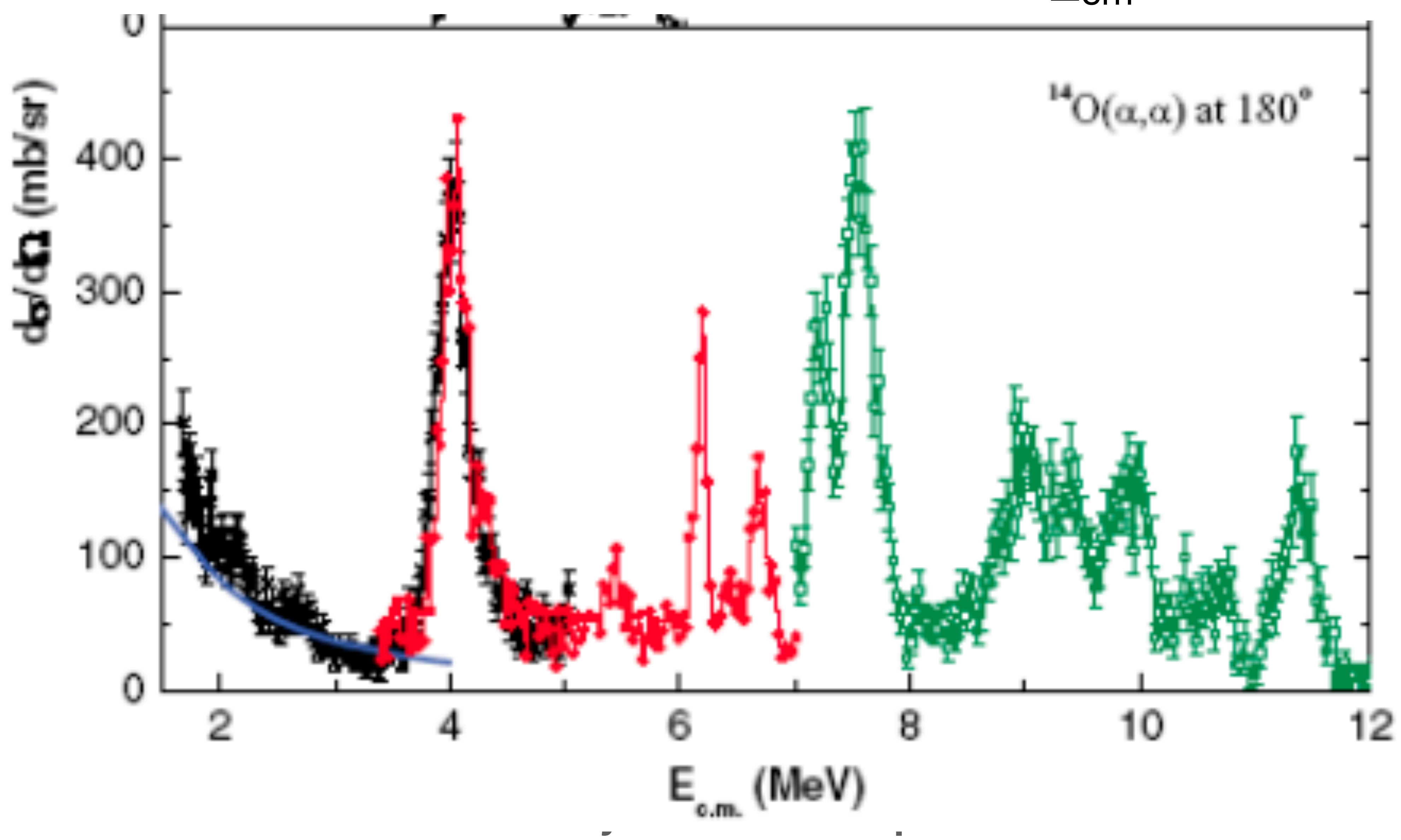

A. Kim Dissertation

(a,a) Yield

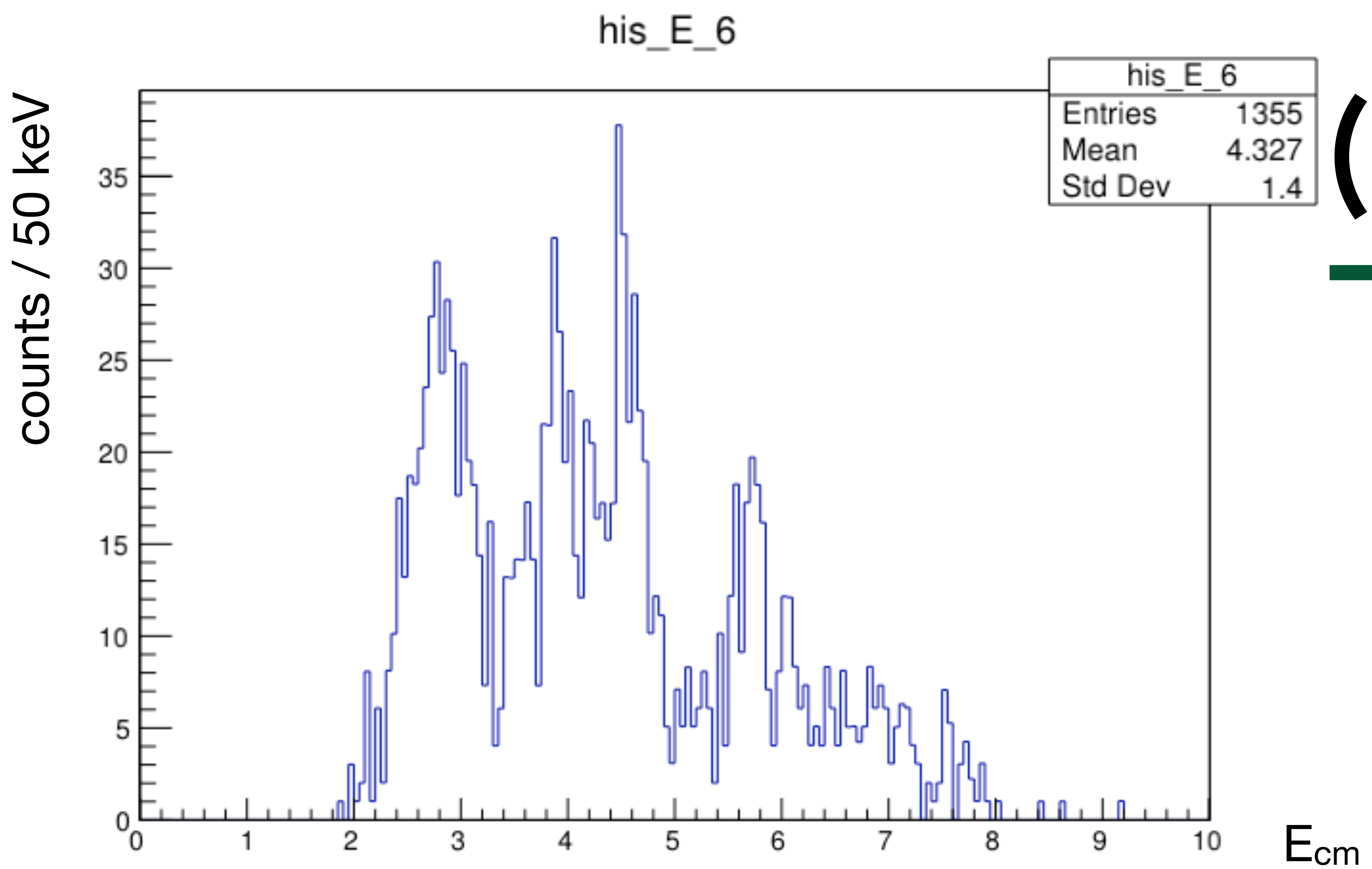

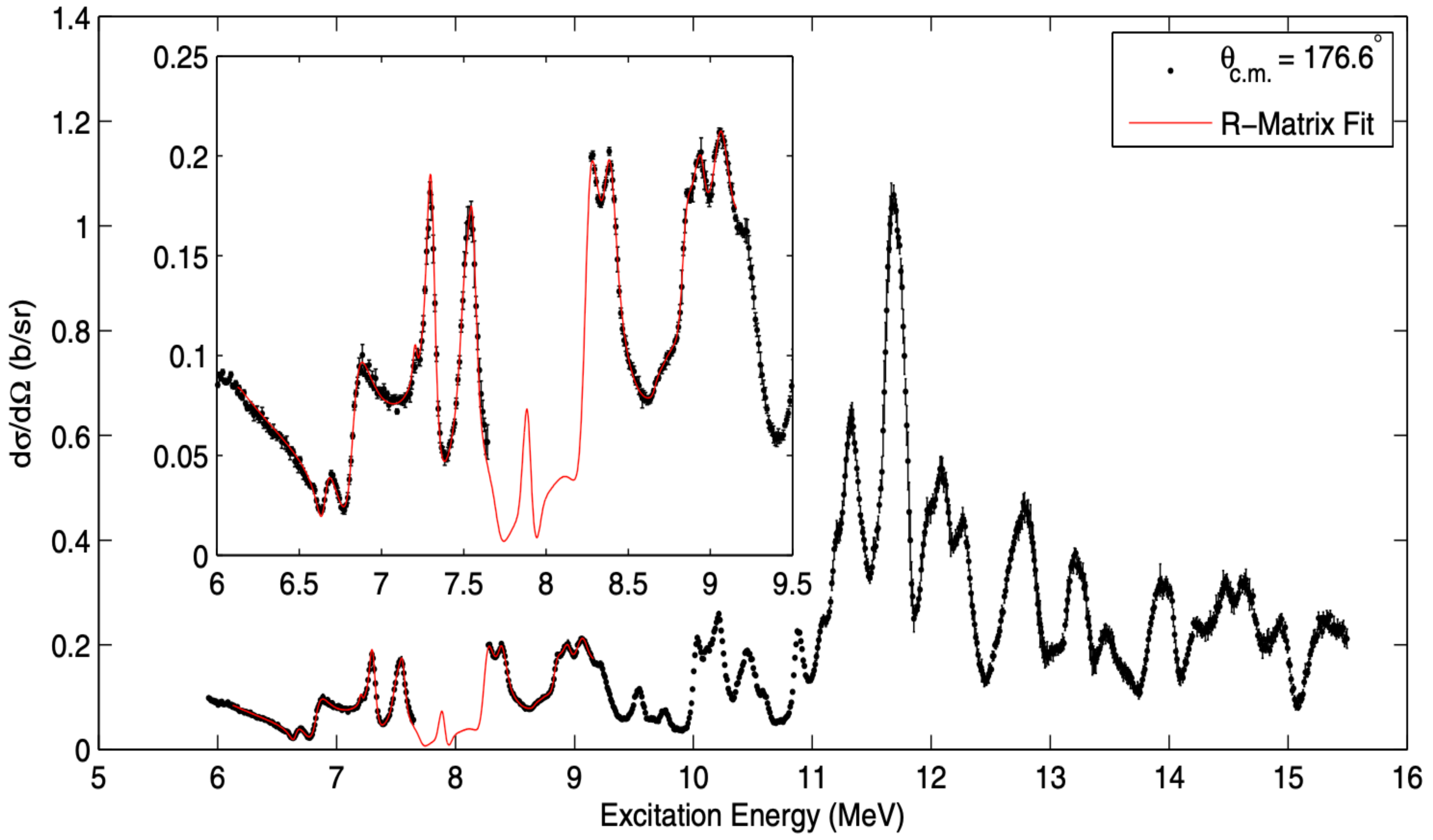

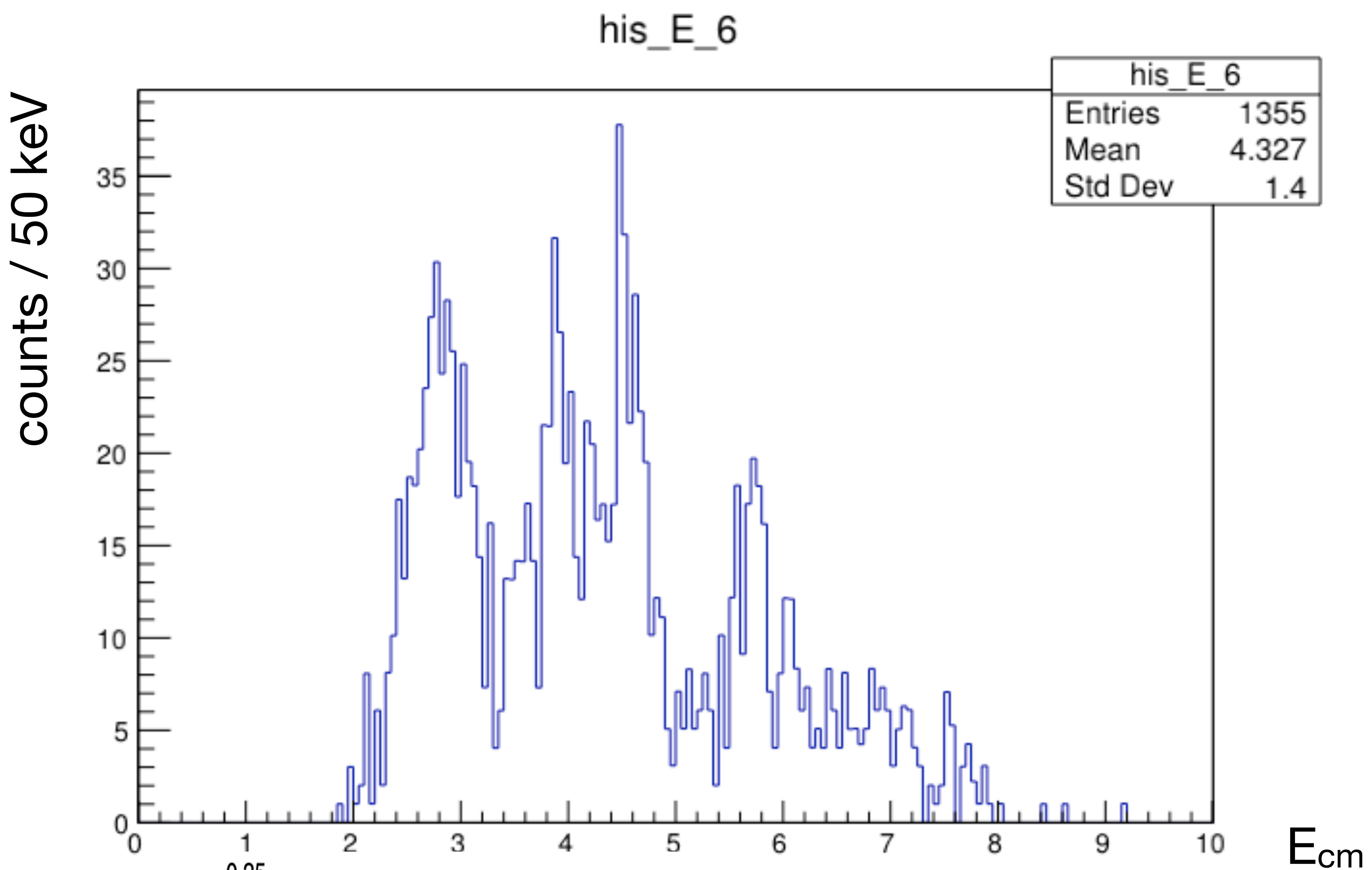

S. Bailey *et al.*

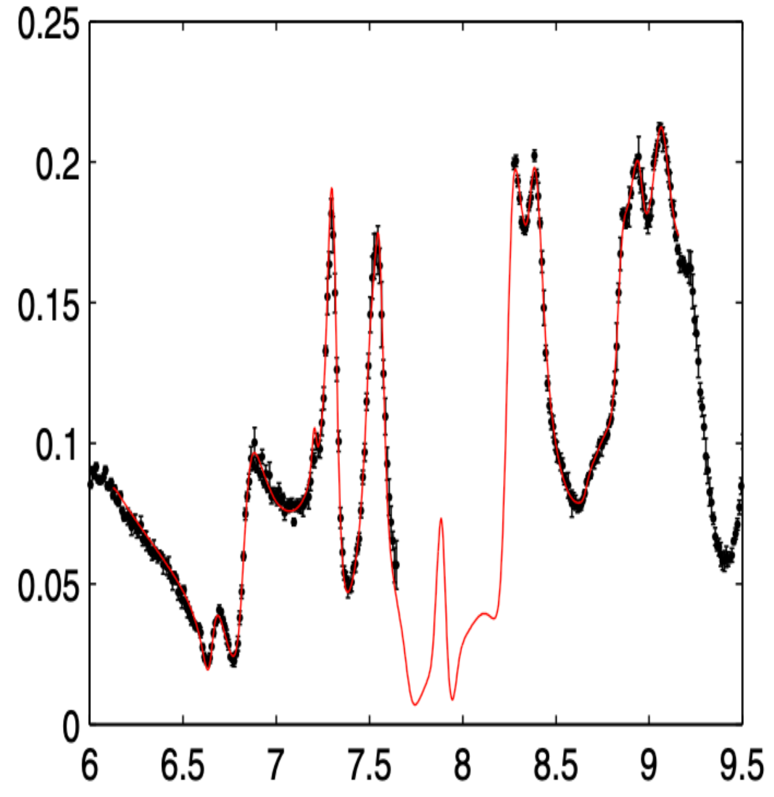

* $E_x = E_{cm} + 4.415$